Technische Universität München
Lehrstuhl für Wassergüte- und Abfallwirtschaft

On-site Infiltration of Roof Runoff by Using Clinoptilolite as an Artificial Barrier Material

Konstantinos Athanasiadis

Vollständiger Abdruck der von der Fakultät für Bauingenieur- und Vermessungswesen der Technische Universität München zur Erlangung des akademischen Grades eines

Doktor-Ingenieurs

genehmigten Dissertation.

Vorsitzender: **Univ.-Prof. Dr.-Ing. Martin Faulstich**

Prüfer der Dissertation:

1. **Univ.-Prof. Dr.-Ing., Dr. h. c. Peter A. Wilderer, i. R.**

2. **Univ.-Prof. Dr.-Ing. Michael Manhart**

3. **Prof. Saburo Matsui, Ph. D., Kyoto Univ./Japan (schriftliche Beurteilung)**

Die Dissertation wurde 16.06.2005 bei der Technischen Universität München eingereicht und durch die Fakultät für Bauingenieur- und Vermessungswesen am 27.10.2005 angenommen.

Zusammenfassung

Die Vor-Ort-Versickerung ist eine viel versprechende Lösung, Niederschläge in urbanen Gebieten zu bewirtschaften. Grundvoraussetzung ist jedoch, dass mögliche Schadstoffe aus Niederschlagsabflüssen vor einer Versickerung vollständig entfernt werden, um eine Kontamination von Boden und Grundwasser zu verhindern.

Ziel der vorliegenden Arbeit war, die Einsetzbarkeit von Klinoptilolith als Barrierematerial zum Rückhalt von Schwermetallen aus Dachabflüssen zu evaluieren. Dabei wurde ein dreiteiliges Forschungsprogramm durchgeführt: Versuche (a) im Labormaßstab, (b) im Pilot-Maßstab und (c) im technischen Maßstab.

Die Laborexperimente zeigten, dass die effektive Ionenaustausch-Kapazität durch eine gezielte Vorbehandlung des Klinoptiloliths mit 1 M NaCl-Lösung verdoppelt werden kann. Es konnten Werte von 0,12 mmol/g für Zn^{2+}, 0,09 mmol/g für Cu^{2+} und 0,2 mmol/g für Pb^{2+} erzielt werden. Untersuchungen zum Einfluss des pH-Wertes auf den Ionenaustausch-Prozess zeigten, dass der pH-Wert stark die physikalischen Eigenschaften, wie beispielsweise die Oberflächenladung von Klinoptilolith verändern, ebenso die Löslichkeit der Ionen im Niederschlagswasser. Eine pH-Wert-Absenkung des pH-Wertes von pH 5,0 auf pH 3,0 resultiert in einer Verschlechterung der Aufnahmekapazität von Metallen um bis zu 40 %. Im Labormaßstab wurden auch Untersuchungen zum dynamischen Verhalten der Festbett-Klinoptilolith-Säule durchgeführt. Resultat war, dass die beste Ionenaustausch-Kapazität erzielt werden kann, wenn die Säule von unten nach oben durchströmt wird, wenn die Schwermetallkonzentrationen in der wässrigen Lösung niedrig liegen und wenn die Flussrate gering ist. Versuche zur Regenerierung der Klinoptilolith-Säule mit 1 M NaCl-Lösung zeigen eine vollständige Regenerierbarkeit.

Hauptaugenmerk der Versuche im Pilotmaßstab las auf dem Einfluss des Dachmaterials, der Phasenverteilung der Schwermetalle in den Dachabflüssen, des Regenprofils sowie der Abhängigkeit von Trockenwetterperioden auf die Einsetzbarkeit von Klinoptilolith als Barrierematerial. In den beprobten Dachabflüssen eines elf Jahre alten Zink-Daches lag Zink hauptsächlich in gelöster Form vor, während Blei bis zu 97 % partikulär gebunden war. Die Pilotanlage mit Klinoptilolith war in der Lage, Zink aus den Dachabflüssen bis zu 97 % zu eliminieren.

Mit der Anwendung im technischen Maßstab wurde der Einfluss der Qualität der Kupferdachabflüsse, der Ausrichtung des Daches sowie des Profils der Niederschläge auf die

Effektivität von Klinoptilolith als Barriere-Material untersucht. Es konnte festgestellt werden, dass sowohl die Niederschlagsmenge als auch die Niederschlagsrate für die Höhe des Kupfers in den Dachabflüssen verantwortlich sind. Dabei lag Kupfer hauptsächlich gelöst vor. Kein Zusammenhang konnte zwischen dem Kupfer-Gehalt im ersten Spülstoß und vorangehenden Trockenwetterperioden ermittelt werden. Die Anlage im technischen Maßstab mit Klinoptilolith als Barrierematerial konnte eine Eliminationsleistung bezüglich Kupfer von bis zu 98 % erreichen.

Zusammenfassend kann festgestellt werden, dass sich Klinoptilolith als Barriere-Material zum Rückhalt von Schwermetallen aus Dachabläufen sehr gut eignet und, in entwickelten Filtereinheiten eingesetzt, die Möglichkeit einer schadstofffreien Versickerung auch dort eröffnet, wo kein Platz für eine oberirdische Versickerung über einen Oberboden besteht. Dies ist vor allem in urbanen Gebieten der Fall.

Abstract

On-site infiltration may be considered as the promising way of managing roof rainwater situations in urban areas, provided the hydrological and geological conditions allow infiltration, and provided the pollutants contained in the collected water are effectively removed before the rainwater enters the soil and the groundwater body. Otherwise, the pollutants may accumulate in the soil leading eventually to highly contaminated sites, and they may contribute to deterioration of the groundwater quality.

The aim of this study was to evaluate the feasibility of the application of clinoptilolite as a barrier material to eliminate heavy metals, such as copper, zinc and lead, from roof runoff. The research program was divided into three scales: research (a) at lab scale; (b) in a pilot plant; and (c) in a full scale application.

In the lab scale experiments, it was found that the chemical conditioning of clinoptilolite with 1 M NaCl solution almost doubled the effective ion exchange capacity of the natural material, regarding the studied heavy metals, and gave values of the order of 0.12 mmol/g for Zn^{2+}, 0.09 mmol/g for Cu^{2+} and 0.20 mmol/g for Pb^{2+}. The physical characteristics of clinoptilolite, such as surface charge, as well as the metal ion speciation were strongly affected by the value of the pH of the metal solution. As a consequence, the metal uptake rate of clinoptilolite was reduced up to 40 % by decreasing the pH from 5.0 to 3.0. The influence of dynamic conditions on the performance of a fixed clinoptilolite bed with respect to heavy metal elimination was also examined. The operating ion exchange capacity of the clinoptilolite bed was favoured in up flow modus, at low metal concentrations and by low volumetric flow rates. Regeneration of the clinoptilolite bed with 1 M NaCl solution was successful.

The pilot plant experiments demonstrated the influence of roof material, heavy metal phase distribution, rain profile and duration of the dry weather period on the performance of the clinoptilolite bed, regarding heavy metal elimination. The phase distribution of zinc concentration in the roof runoff of an eleven years old zinc roof was dominated by the dissolved phase. By contrast, the lead concentration in the same roof runoff was dominated by the particulate phase up to 97 %. The clinoptilolite barrier material managed to reduce the zinc concentration from the roof runoff by a factor up to 97 %.

The full scale application demonstrated how the quality of the copper roof runoff, the roof orientation and the profile of the precipitation event could affect the performance of the clinoptilolite barrier material. It was found that the amount and the rate of a precipitation

event were responsible on the magnitude of the copper runoff rate. The phase distribution of the copper concentration in the roof runoff was dominated by the dissolved phase. No correlation was found between the first flush phenomenon and the antecedent dry weather period. The retention facility equipped with clinoptilolite as a barrier material managed to reduce copper from the roof runoff by a factor up to 98 %.

Summing up, it can be stated that on site infiltration using clinoptilolite as an artificial barrier material is an effective way of managing roof runoff situations in urban areas provided the hydrological and geological conditions allow infiltration.

Table of contents

1. Introduction

Roof surfaces account for about half of the total runoff volume from impermeable surfaces in urban areas of the industrialised countries (Förster et al., 1996). Rolled zinc and copper sheets are commonly used for roofing and drain water systems in countries all over the world. The use of copper as a roofing material has a long tradition in Europe way back to the 16th century when copper sheet began to be used in the Scandinavian countries, originally to prevent buildings from catching fire. Zinc sheet has been used as a roofing material for over 200 years. Both roofing materials are considered to be maintenance free, have a long life time and are easily adapted to various design styles from traditional to modern.

Any metal exposed to atmospheric conditions is subjected to corrosion processes in which corrosion products are formed and accumulate on the surface. During a precipitation event, one part of the corrosion products formed will retain on the surface (patina) and one part will be released and washed off the surface and driven in the roof runoff.

Traditionally, the roof runoff is sent to sewers through which the rainwater is either directly transported to the receiving water or, in case of combined sewer systems, sent to wastewater treatment facilities. From an economical point of view, this solution is far from being optimal because of the high costs for providing sewer capacity which is rarely exploited. Ecologically, the traditional urban drainage concept is to be critically assessed as well, since it leads to two negative effects, pollution of the receiving water by direct discharge of polluted storm water or by sewer overflow, and lowering of the groundwater table underneath the urban area.

On-site infiltration may be considered as the promising way of managing roof rain water situations in urban areas, provided the hydrological and geological conditions allow infiltration, and provided the pollutants contained in the collected water are effectively removed before the rain-water enters the soil and the groundwater. Otherwise, the pollutants may accumulate in the soil leading eventually to highly contaminated sites, and they may contribute to deterioration of the groundwater quality. Major pollutants of concern are heavy metals (Zn, Cu and Pb) stemming from the roof material and from piping.

To avoid such a negative effect it is proposed to pass the roof rain-water runoff through an artificial barrier before it will enter soil and groundwater. The problem is that only very little contact time between the rainwater and the barrier material is available. Thus, the pollution removal mechanism has to be very fast. Secondly, one must consider that the barrier material has to achieve high pollution removal rates during rain events which are following long dry

periods. Thirdly, it has to be realized that some categories of pollutants may appear in enhanced concentration only at the beginning of a rain event, whereas pollutants from roof rainwater runoff, particularly heavy metals, may remain in enhanced concentrations for a prolonged period of time.

The aim of this study was to evaluate the feasibility of using clinoptilolite as a barrier material to eliminate heavy metals from roof runoff. Lab scale experiments were carried out, first. The results obtained, led to the design and operation of a pilot plant. Finally the experiences of the first two steps were combined for the construction of a full scale infiltration unit for the treatment of the runoff of a particular copper roof.

2. State of the Art

A course of water is considered contaminated or polluted when its composition is changed directly or indirectly by human activities in such a way that major impacts are posed on natural aquatic systems. The progressive growth of urban areas, extensive farming activities, and the industrial development are the main reasons for the progressive pollution of groundwater bodies, rivers, lakes and seas, adversely influencing or even destroying fauna and flora and breaking the equilibrium of the ecosystem, as well as the harmony between human beings and their environment.

2.1 Quality of urban storm water runoff

Urban storm water, which includes roof and road runoff, originates from the flowing of meteoric water, such as rain, snow or hail, over impermeable areas. In preceding studies, *Dauber et al.*, (1979) and other scientists (Harrison et al., 1985; Herrmann et al., 1994) clearly showed that runoff from highways contains high level of heavy metals, mainly in particulate form, suspended matter and hydrocarbons. However, in the worldwide field of urban drainage management, little attention has been paid to the quality of roof runoff until recently (Förster et al., 1996). With respect to its pollutants, roof runoff is considered by some authors as non-polluted or at least not significantly polluted (Shinoda et al., 1990; Krejci et al.; 1990; DWA – A 138), compared to waste waters and highway runoff, since it consists of rainwater flowing over various, in general non-abrasive materials, such as tiles, bitumen, metals and concrete. On the other hand there are reports which state that this runoff is severely polluted (Pratt et al., 1984; Leschber et al., 1991). Of major importance is the contribution of runoff from metal roofs, like zinc and copper, to the pollution of wet weather flows (Gromaire et al., 1999 and 2001; Athanasiadis et al., 2005).

Major pollutants of concern are heavy metals like zinc, lead, copper, cadmium, chromium and nickel. Other heavy metals could not be measured in relevant concentrations. Their concentrations in roof runoff highly depend on the situation of the test site and the material of roof and piping (Förster et al., 1999).

2.2 Heavy metals in storm water runoff

Heavy metals are of particular interest in storm water runoff due to their toxicity, ubiquity and persistence. Taking also into consideration that they are not biodegradable and they tend to accumulate in living organisms, it is obvious that they represent a serious threat to aquatic life, to animal and to human health, and to the ecological system as a whole.

2.2.1 Sources of heavy metals

Heavy metals enter water and wastewater from either natural or anthropogenic sources. Some of these natural sources are chemical and physical weathering of igneous and metamorphic rocks and soils that often release heavy metals into the sediment and into the air. Also, the decomposition of plant and animal detritus, precipitation or atmospheric deposition of airborne particles from volcanic activity, wind erosion, forest fire smoke, plant exudates and oceanic spray also contribute to the release of such metals.

Anthropogenic sources are related to the extent of economic activities such as traffic, industrial production, domestic waste incineration, energy generation, agriculture; etc, that are carried out by humans. It is important to state that anthropogenic inputs of metals exceed natural inputs.

Many of these natural and anthropogenic sources contribute to air pollution, generating atmospheric emissions of mostly sub-micron particles. These particles may be transported by the wind over large distances, a phenomenon which is called remote pollution, and affect areas situated far away from the emission source (Thevenot et al., 1999). Nevertheless, local sources affect the pollution of an area most strongly, in comparison.

The sources of metals in urban storm water are diverse, but the major contributors of metals in non-industrial areas are automobiles and structures that use metallic components.

   a) **Zinc**

Zinc belongs to the materials that are traditionally used in the construction of roofs. It is used on roofs for gutters, downspouts, casing sheets for chimneys and roof hatches, as well as for the covering of whole roofs or parts of them. For out door use, two different types of zinc panels are generally used. Galvanised materials only have a very thin layer of zinc covering a construction made out of steel. The most commonly used composition on roofs is zinc with purity of 99.7 – 99.995 %. In order to make the zinc processible, traces of titanium and copper

are mixed to it in varying fractions (Cu-Ti-Zn). Buildings of brick, concrete and painted wood structure are also sources of this heavy metal.

From automobile brakes, according to *Davis et al.*, (2001) the estimated contribution of Zn is of 89 µg/km-vehicle (Fig. 1); in addition Zinc is added to automobile tires as filler, which is released by tire wear.
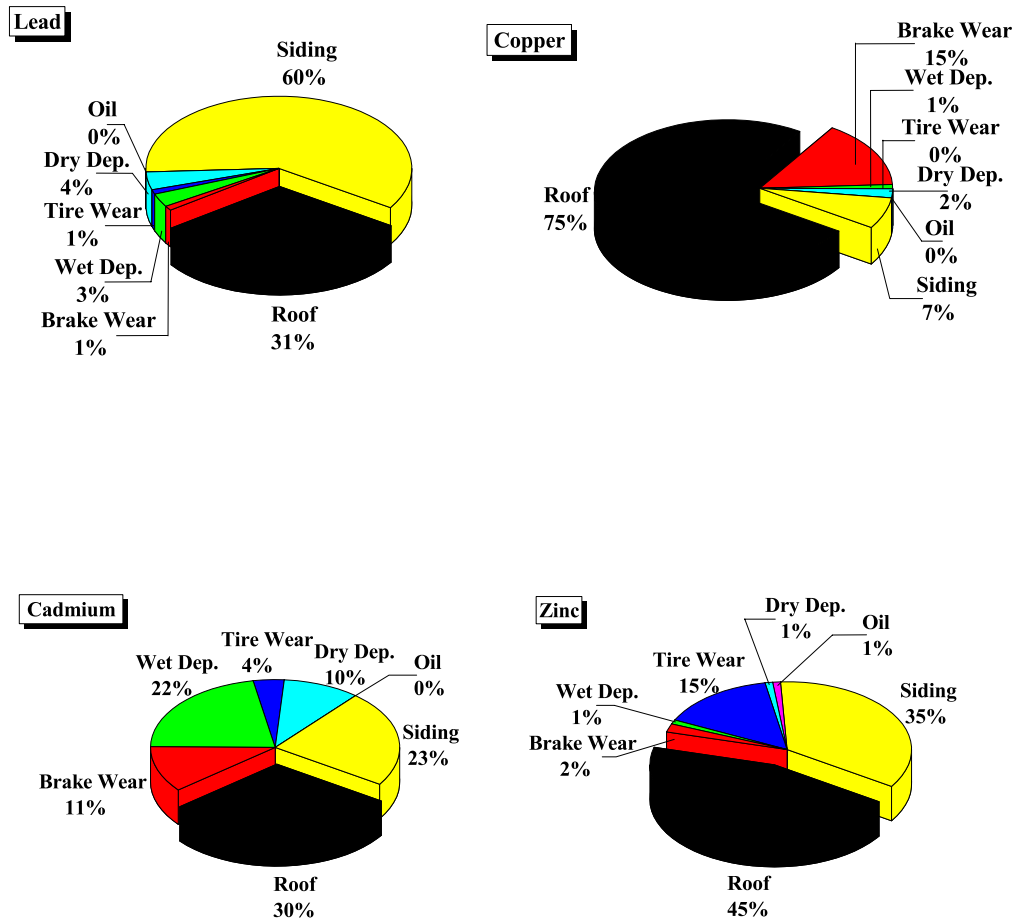
Fig. 1: Estimated contributions of various sources of metals in urban storm water runoff (Davis et al., 2001).

b) Lead

Buildings of brick and painted wood structure are responsible for the presence of this heavy metal in the urban storm water runoff (Davis et al., 1999). Another source of lead in the roof runoff is the use of antimony-free solder (L-PbSn$_{40}$) as a sealing material on roofs, e.g. to seal up chimneys on the roof.

Some years ago, the main source of lead came from the exhaust pipe of the automobiles. However, since the use of leaded fuel has been prohibited, the concentration of this element in storm water runoff has decreased. Brake pad material contains a small percentage of lead. An estimated contribution of Pb is of 3 µg/km-vehicle (Fig. 1).

c)   Copper

Copper is, on the one hand, a natural component in most ecosystems and, on the other, a metal that always has found many applications in old and modern societies, e.g. in jewellery and statues, in plumbing, as a building material, in electronics and in many other industrial artifacts. Nowadays, copper is extensively used for partial roof coverings, full roofs, facades and guttering. Elevated concentrations of copper are obtained in roof runoff from these surfaces, as well as from drains and wood impregnated with copper compounds (Persson et al., 2001).

Brake pad material contains copper, zinc, and brass (which contains a percentage of lead). During brake wear these metals are released into the environment. According *Davis et al.,* (2001) an estimate for copper release from automobile brake abrasion is 75 µg/km-vehicle.

In agriculture, applications of copper-containing fungicides are also a source that contributes to the load of soil and groundwater, even though the fluxes of copper from agriculture are spread over big areas at low deposition rates.

Several studies on copper washed off from different types of roofs state that the contribution from atmospheric deposition of copper becomes nearly negligible when copper sheets are used on roofs (Boller et al., 2002; Davis at al., 2001).

2.2.2 Bioavailability and ecotoxicity of heavy metals

Bioavailability is defined as the degree to which contaminants like heavy metals in environmental media can be assimilated by an organism. The bioavailability of a chemical to the receptor will depend upon its chemical and physical characteristics, and the characteristics of the media it is in. That means that the toxicity of a contaminant depends on its bioavailability. The more bioavailable a chemical is the higher the toxic potential.

a)   Zinc

According *Heijerick et al.,* (2002) zinc is present in the roof runoff (zinc based materials for roofing applications) almost completely (94.3 – 99.9 %) in its most bioavailable form, as an

ion (Zn^{2+}). In general the released zinc amount after a rain event may be of such a magnitude that toxic effects are observed for algae, due to the physico-chemical characteristics of rainwater which shifts the speciation towards the most bioavailable form (Zn^{2+}).

b) Copper

Copper is an essential element required by plants and animals, but only to a certain degree. When this element exceeds certain concentrations, it becomes toxic. Studies by *Karlen et al.*, (2002) revealed that the majority (60-100%) of released copper, from copper based materials used for roofing applications, was present as the free hydrated cupric ion, $Cu(H_2O)_6^{2+}$, the most bioavailable copper species. Also other bioavailable forms of copper such as, e.g. $Cu(OH)^+$ and $Cu_2(OH)_2^{2+}$, were found in the runoff water. The copper containing runoff water caused significant reduction in growth rate of the green algae (Karlen et al., 2002).

It can be mentioned that both results reported from *Heijerick et al.*, (2002) and *Karlen et al.*, (2002) described the runoff situations immediately after release from the zinc and copper roof respectively and not the real environmental ecotoxicity. Risk assessments should take into consideration dilution effects of both heavy metals, changes in their chemical speciation and bioavailability during environmental entry, and type and sensitivity of the receiving ecosystem.

2.3 Pollution of roof runoff

The pollution of roof runoff and its variability is influenced by:

a) local sources

- Industrial activities (e.g. PAHs from incineration for heating purposes)

- Agricultural activities

b) roof itself

- material (e.g. copper or zinc sheets)

- inclination

- age of the roof

c) air pollution (e.g. dry deposition, SO_2, NO_x)

d) profile of the rain event (e.g. wet deposition)

- rain intensity

- rain volume

- antecedent dry period

e) meteorological conditions

- season

- wind speed

- wind direction and finally

f) the pollutant's physico-chemical properties.

These factors generate a high degree of variability within single storms, between different rain events, between different roof materials as well as between different roof locations, and the pattern differs also for different group of pollutants (Förster et al., 1996; Wallinder et al., 2000; Förster et al., 1999). Also patterns of a high degree of pollution of roof runoff at the beginning of a rain event are observed. This is the so called first flush phenomenon, where a high concentration of pollution is followed by an exponential decrease as the rain event proceeds (Boller et al., 1997; Wallinder et al., 2001). According to *Wallinder et al.*, (2001) the first flush phenomenon is furthermore related to prevailing environmental conditions prior to a precipitation event, e.g., to dry and wet deposition of corrosive pollutants and to the duration of dry and wet periods during which corrosion products are dissolved and re-precipitated. Surfaces of varying inclination positioned in different orientations will experience different degrees of dry deposition and length of dry and wet periods and, hence, differences in metal concentration in the first flush.

2.3.1. Pollution process

2.3.1.1 Primary pollution

Pollutants from the atmosphere reach the surface of the roof as dry or wet deposition.

a) Dry deposition

Dry deposition is defined as the accumulation of dust, aerosols and gases as they come into contact with soil, water or vegetation on the earth's surface (EEA-**E**uropean **E**nvironment **A**gency). During dry periods, numerous pollutants are emitted into the environment. They originate almost exclusively from anthropogenic sources like incineration, traffic, chemical

industry, etc. The density and the size of the particles are of particular interest. Heavy particles precipitate from the atmosphere after a short residence time due to gravitation, and settle on the ground, depending on the climatic conditions (accumulation). Fine dust particles of low densities with a diameter of 0.1 – 1 mm and aerosols can be transported by wind over long distances and drift high up into the upper layers of the atmosphere. Due to effects of ``rain out`` and ``wash out``, the particles, gases and aerosols get discharged from the atmosphere and reach the ground as part of wet deposition.

b) Wet deposition

Wet deposition signifies the process by which chemicals are removed from the atmosphere and deposited on the earth's surface via rain, sleet, snow, cloud water and fog (EEA-**E**uropean **E**nvironment **A**gency). The water reaches the atmosphere through evaporation. As those water masses pass through the troposphere, water condenses on nuclei (dirt particles) during the formation of clouds. This process is called ``rain out``. Heavy metals and other kinds of pollutants are absorbed from aerosols and the fine dust which is diffused in the atmosphere. During the precipitation event, rain absorbs those compositions of particles. Absorbed gaseous elements migrate into the liquid phase. The process of washing out from the atmosphere and distributing the wet deposition across the earth surface is called ``wash out``. Its constitution depends on the size and the quantity of aerosols, the amount of precipitation and the diameter of drops (Dierkes et al., 1999).

2.3.1.2 Secondary pollution

Secondary pollution signifies the contamination of roof runoff sourced from the roof itself. Major factors which influence the quality and degree of secondary pollution in roof runoff are the roof itself, meteorological conditions, the profile of the rain event and air pollution.

a) Roof

- **Roof material**

The pollution effect detected in runoff is much greater when the source of the pollutants is the roof material itself. This situation occurs when the roof or parts of it consist of metallic compounds like copper or zinc (see Table 1).

- **Corrosion of the roof**

Atmospheric corrosion of metal materials such as copper, zinc and lead used in roof construction results in the loss of these metals from the exposed materials to the environment. This process involves two steps:

o Initially the metallic compound is converted into its oxidized state M^{2+}, adhering to the surface of the material in the form of very slightly soluble or insoluble corrosion products as the so-called patina layer. This conversion of the metallic compound into its ionic state is the actual corrosion step

o Subsequently the corrosion products or soluble salts derived from them are washed away from the roof surface by precipitation. This is the actual runoff step which determines the flux of metals to the environmental compartments.

Therefore the corrosion process can be quantified by two different parameters: The rate of conversion of metallic compound into its ionic form and the loss of soluble ionic metal from the patina layer. The first parameter is denoted as the corrosion rate, while the second parameter is called runoff rate.

The metal corrosion rate differs from the runoff rate. The runoff rate is considerable lower than the corrosion rate. According *Wallinder et al.*, (2001) a new copper roof which was exposed for one year in an urban atmosphere showed a corrosion rate of 6.7 g/m^2 y and an almost constant run off rate of 1.3 g/m^2 y. The runoff rate represents only a fraction ($\approx$ 20 %) of the total amount of corroded metal. A new zinc roof exposed under the same conditions showed a corrosion rate of 5 g/m^2 y and a relative stable runoff rate of 3.1 g/m^2 y. This value represents almost 60 % of the total amount of corroded zinc.

This difference between the corrosion and the runoff rate is exhibited because during a rain event a part of the corroded products which were formed on the surface of the roof (patina) will be retained there, whereas a part will be washed off.

Table 1. Quality of roof runoff regarding heavy metal concentration

Constituent		Mean concentration in runoff				
		Roof Tile	Polyester	Gravel	Zinc sheet	Copper sheet
	Unit					
Zn_{total}	µg/l	48.0	115	9.0	7000	-
Pb_{total}	µg/l	41.0	24.0	2.7	17.3	-
Cu_{total}	µg/l	304	842	18.0	8.2	1800
Reference		Zobrist et al., (2000)	Zobrist et al., (2000)	Zobrist et al., (2000)	Athanasiadis et al., (2005)	Persson et al., (2001)

- **Age of the roof**

The effect of roof age has been investigated, in field and laboratory studies, by many researchers (Wallinder et al., 2001; Crammer et al., 1990; Wallinder et al., 1997). The results obtained showed that naturally aged copper exhibits somewhat higher average runoff rates (2 g/m^2 y) than new copper, probably due to weather conditions (see Table 2). No significant difference in runoff rate could be found between new and naturally aged zinc.

Table 2. Runoff rates for one year exposures of new and aged roofs (g/m^2 y)

Zinc sheet [*]		Copper sheet [**]	
Roof Age	Runoff rate	Roof Age	Runoff rate
pure	3.02	pure	1.30
15 years	2.94	40 years	2.10
39 years	3.05	100 years	1.90

[*] Korenromp et al., 1999

[**] Odnevall Wallinder et al., 2001

- **Orientation and inclination of the roof**

At a given precipitation quantity impinging on a given roof surface area, the corresponding collected precipitation volume per square meter depends on the inclination angle (see Fig. 2). There is a difference between the precipitation volume (l/m^2) and the precipitation quantity. The precipitation quantity (mm/y) is a meteorological value.

For a given precipitation quantity, with constant pH and intensity, the amount of metal run off from the roof surface depends from its inclination. This is illustrated in Fig. 3 for zinc, which shows that the amount of the metal in roof runoff increases during a specific rain event as the inclination angle decreases. The same results have been reported for a copper roof (Wallinder et al., 2000).
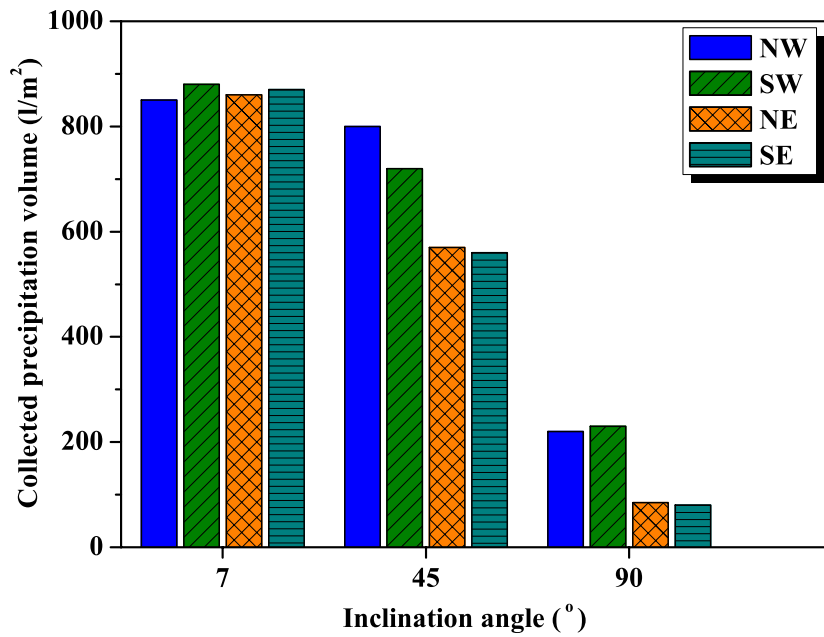
Fig. 2: Total precipitation volume collected from the zinc surfaces on a model roof after one year of exposure (Wallinder et al., 2000).
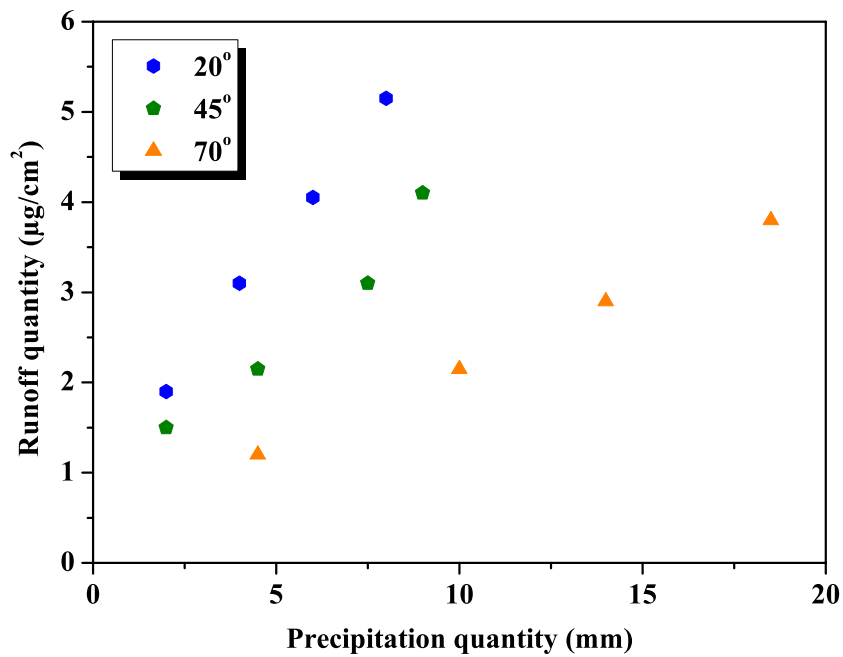
Fig. 3: Accumulated amount of zinc runoff as a function of the precipitation quantity for different surface inclinations (Wallinder et al., 2000).

b) Meteorological factors

Both primary and secondary pollution are highly dependent on meteorological conditions. Factors such as wind direction, wind speed and season influence the metal quantity in roof runoff.

- **Seasonal variations in runoff rate**

According *Wallinder et al.*, (2001) the seasonal differences in corrosion rates that could be discerned in rural areas were mainly attributable to differences in relative humidity. In urban areas no seasonal effect could be observed indicating that other parameters influenced the corrosion kinetic. While corrosion rates exhibit a continuous decrease with exposure time, the yearly metal runoff rates are independent of time.

- **Wind direction and speed**

The orientation of a roof at a given inclination has an effect on the runoff rate. The difference in runoff rates between different roof orientations is mainly connected to the prevailing wind direction and speed during the exposure period. The wind carries the rain differently onto the faces of the roof which results in differences in rain volume hitting the surfaces (Fig. 4).
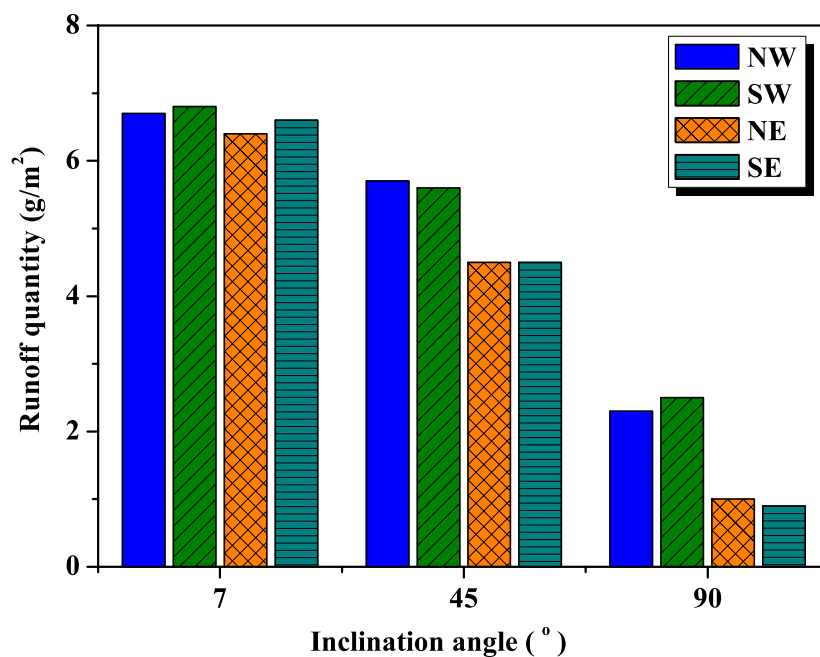
Fig. 4: Total accumulated zinc runoff after one year of exposure (Walinder et al., 2000).

c) Air pollution

Sulphur compounds and chloride ions are the most common and important atmospheric corrosive agents, as has been reported by different authors all over the world (Arroyave et al., 1995; Feliu et al., 1993). Particulate species can also accelerate corrosion of metals in several ways, for example by increasing the conductivity of the surface layer after dissolution of soluble ions from the particulate (Lobnig et al., 2003). The effect of particles of $(NH_4)SO_4$ on the corrosion of zinc and copper has been reported by *Lobnig et al.,* (2003) and *Lindström et al.,* (2002). During the last decades atmospheric SO_2 concentrations have significantly decreased and metal corrosion and runoff rates have decreased accordingly (Table 3).

Table 3. Corrosion and runoff data on zinc

Test site	Corrosion rate $(g/m^2\,y)$	Runoff rate $(g/m^2\,y)$	Ratio (%)	SO_2 conc. $(\mu g/m^3)$	Rainfall (mm/y)	Reference
Stockholm	4.6	3.0	65	3.5	450	Wallinder et al., 1998
Olen[*]	-	7.5	-	39	1026	Wallinder et al., 1998
Hoboken[*]	-	14.3	-	73	1083	Wallinder et al., 1998
Chaufontaine	4.4	2.3	52	9	821	Verbiest et al., 1997
Chaufontaine	5.1	2.4	47	9	898	Verbiest et al., 1997
Hannover	7.8	4.5	58	22	635	Lehmann et al., 1995
Olen	13.3	6.9	52	39	706	Wallinder et al., 1998
Hoboken	21.4	12.6	59	73	748	Wallinder et al., 1998

- not measured
* extrapolated data

d) Profile of the rain event

- **Precipitation volume**

The effect of precipitation volume on runoff behavior is shown in Fig. 5. The accumulated metal runoff quantity increases with increasing precipitation volume. However, the runoff rate, expressed as runoff quantity per mm rain is significantly higher during the initial part of the rain episode after which the rate becomes lower and more or less constant.
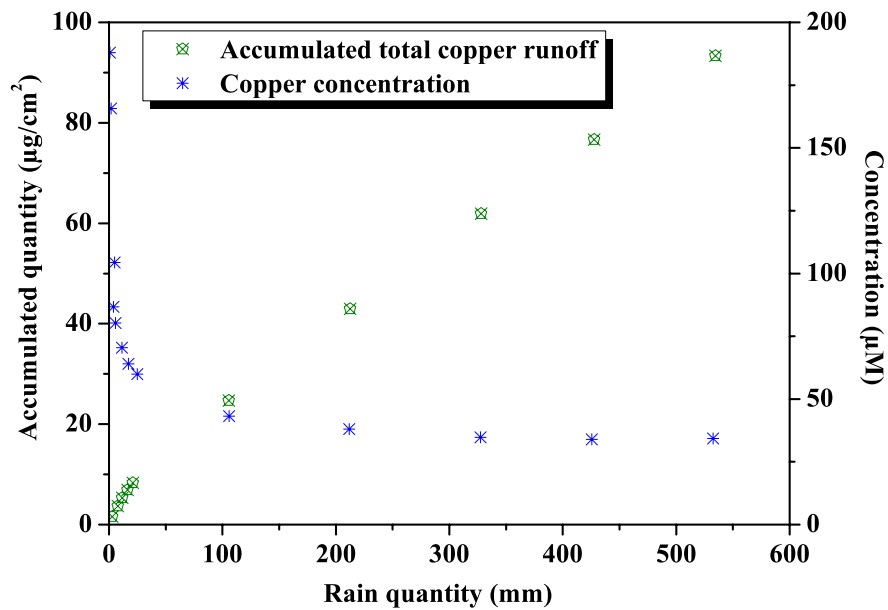
Fig. 5: Accumulated total copper runoff and concentration as a function of rain volume (He et al., 2001).

- **Rain intensity**

A sufficient rain volume is required to be able to transport soluble corrosion products from the roof surface. The contact period between rainwater and the roof surface is governed by precipitation intensity and determines the rate at which the easily soluble corrosion products can be removed, thus determining the magnitude of the first flush phenomenon. According *He et al.*, (2001) extreme low intensity rain events (drizzle, < 1 mm/h), with the longest surface contact time, resulted in an increased amount of released copper (Fig. 6). The same author also reported that there was no significant difference between precipitation events of light rain (≈ 8 mm/h) and moderate rain (≈ 20 mm/h).

- **Antecedent dry period**

The time between two rain events is called the antecedent dry period. The magnitude of the first flush is also dependent on this period. A long period of dry conditions will introduce cracks and defects within the corrosion layer of the roof and hence facilitate the trapping of corrosive species and humidity within the layer (He et al., 2001). A long period with wet conditions, without a wash off event, will increase the residence time of water which is trapped in the corrosion layer and will prolong the time during which the corrosion products
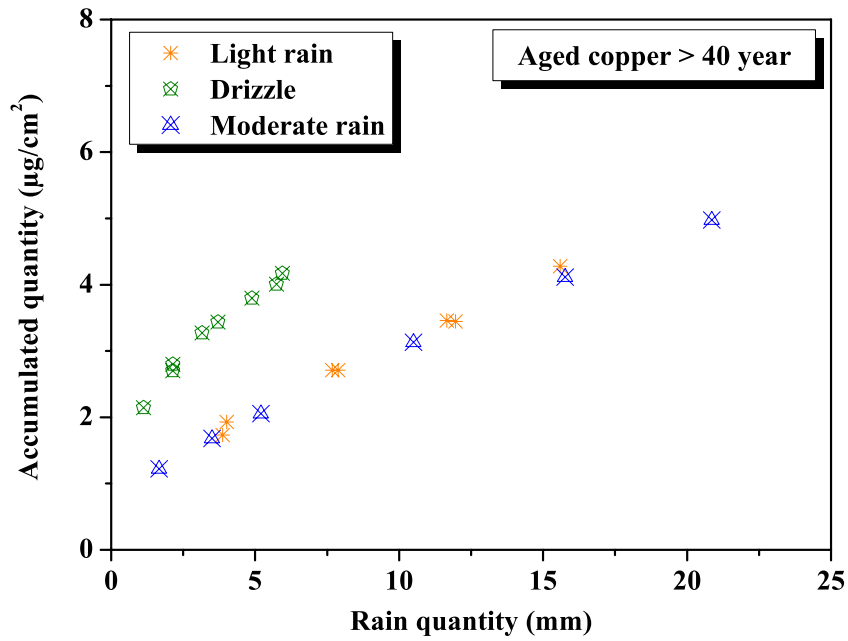
Fig. 6: Effect of rain intensity on the runoff behavior of copper roof as a function of rain quantity (He et al., 2001).
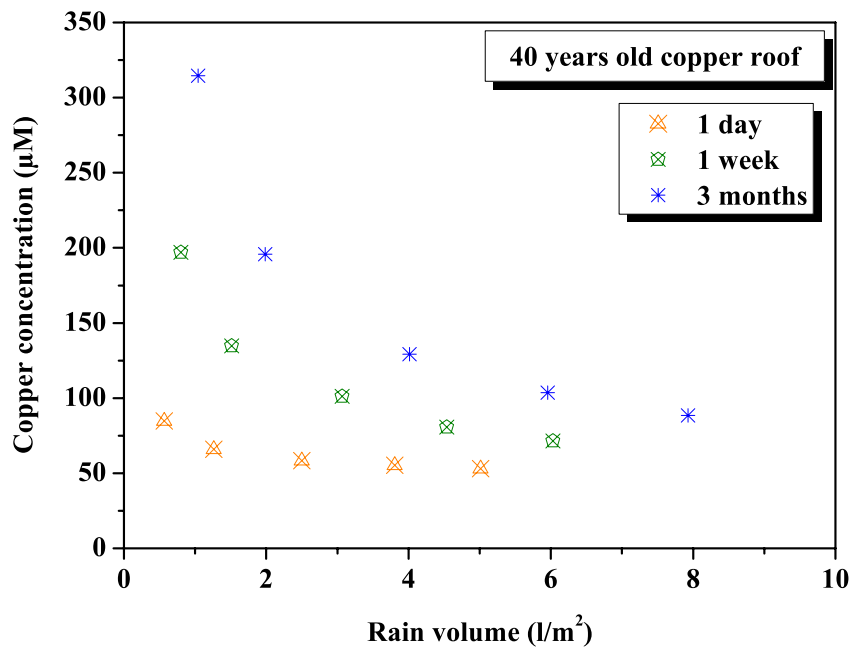
Fig. 7: Effect of duration of dry periods between two rain events on the copper concentration in runoff from copper roofs (He et al., 2001).

can be dissolved (He et al., 2001). The effect of duration of dry period is illustrated in Fig. 7.

According to *He et al.*, (2001) the duration of dry periods results in an increased amount of dry deposited species in the corrosion layer so that more easily soluble corrosion products as well as poorly adherent corrosion products can be removed during the first flush phenomenon.

2.4 Roof runoff management

The primary objective of urban drainage systems is to protect and maintain the health and safety of communities. In practice this means, to prevent flooding and to remove human waste in order to maintain a sanitary environment. The second objective of urban drainage systems is to protect the natural environment including flora and fauna. This is currently achieved by maintaining environmental standards involving limits on the pollution of natural watercourses, land and the atmosphere. Nowadays another objective is introduced and is under discussion: systems should be "sustainable".

A sustainable storm drainage management in urban areas intents not only to achieve effective and conveyance of floodwater and pollution control but also to provide self-supporting ecological and aesthetic benefits.

2.4.1 Traditional urban drainage system

Urban drainage systems are generally networks of sewers which carry urban wastewater and rain water runoffs to one or more terminal points, where it is treated and / or discharged to the environment.

a) Combined sewer system

A combined sewer system (CSS) conveys domestic and industrial wastewater together with storm water in one piping system. The drainage system is designed to transport all type of excess waters as completely and as fast as possible out of urban areas, to wastewater treatment facilities or directly to water bodies. The aim of such a system is to maintain hygienic conditions in the metropolitan area as well as to avoid flooding of residential or industrial areas (Fig. 8).
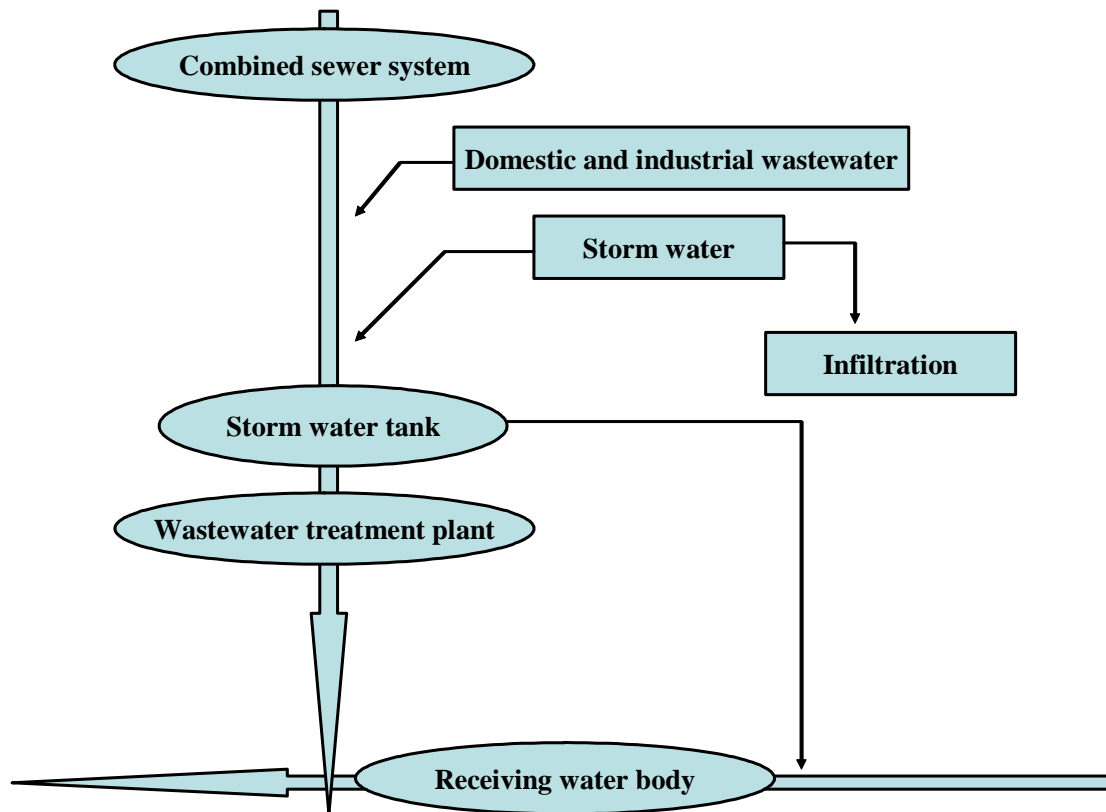
Fig. 8: Schematic representation of a combined sewer system.

From an economical as well as an ecological point of view the combined sewer system presents disadvantages,

o Necessity to provide excess but only rarely used capacity for sewer systems, as well as for wastewater treatment plants (Dormoy et al., 1999)

o Contribution to high flow rates in receiving water bodies under extreme weather conditions

o Pollution of the receiving water when combined sewer overflow occurs

o Decrease in the groundwater level underneath the urban area because natural groundwater discharge is interrupted

o Loading of sewer sludge's with pollutants stemming from roofs and roads.

For cadmium, lead and zinc, *Gromaire et al.*, (2001) have demonstrated that roof runoff was the main source of wet weather pollutants on the ``Marais`` catchment in Paris, due to the erosion of roof covering materials (Table 4).

Table 4. Percentage of the total runoff pollutants loads from the ``Marais`` catchment attributable to each type of runoff (Gromaire et al., 2001)

	Roof runoff			Courtyard runoff			Street runoff		
	10%	median	90%	10%	median	90%	10%	median	90%
Cd	84	88	92	3	5	8	4	7	10
Cu	48	64	85	3	5	8	11	32	43
Pb	80	88	93	2	3	7	4	9	17
Zn	88	93	96	1	2	5	2	5	7

b) Separated sewer system

Separated sewer systems are comprised of two independent piping systems, one for sewage and another one for storm water (Fig. 9). This way domestic and industrial water is transported to wastewater treatment plants (WWTP) and storm water is conveyed directly to receiving water bodies such as, e.g. lakes, rivers and the sea. The system maintains hygienic conditions and prevents metropolitan areas from flooding, like the combined sewer system.
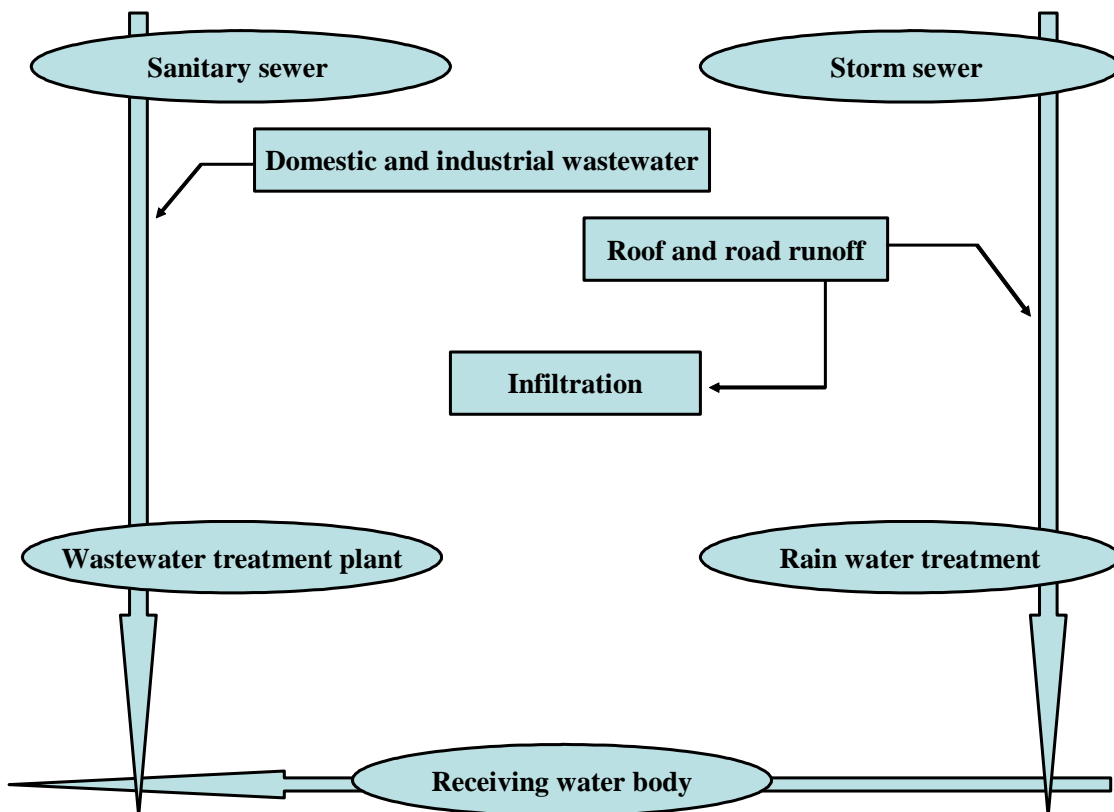
Figure 9: Schematic representation of a separated sewer system.

The disadvantages presented by this system are:

- Contribution to high flow rates in receiving water bodies under extreme rain weather conditions

- Pollution of the receiving water, especially when the water body is small

- Accumulation of contaminants in the sediments of the receiving waters (Marsalek et al., 1997)

- Decrease in the groundwater level underneath urban areas

2.4.2 On-site infiltration

The advantage of on-site storm water infiltration facilities is that they do not append demands on existing wastewater treatment plants and drainage systems and consequently during extreme rain events do not increase discharge from the combined sewer storm overflow. Also, they recharge the groundwater. Their application, however, includes certain risks which have to be taken into consideration by policy makers and by system designers and managers. These risks relate to soil and groundwater pollution by urban runoff water, rapid deterioration of installations by clogging, and possible superstructure damage due to the presence of water in soil.

2.4.2.1 Legal framework, regulations and guide lines

The worksheets A 138 and M 153 of the German Association for Water, Wastewater and Waste (DWA) are the most extensive guidelines regarding the design of infiltration facilities, yet don't deal with the qualitative requirements. According A 138, the infiltration of roof runoff water from metal roofs is only tolerable in exceptional cases. Corresponding to §9 section 1 in the German BauGB (`Baugesetzbuch`), the infiltration of rain water is not listed explicitly, whereas according to §3 section 1 No. 5 in the German Federal Water Act (WHG), the infiltration of runoff water from metal roofs such as copper, zinc or lead with a metal surface area bigger than 50 m^2 requires permission. Other guidelines contain the requirement of pre-treatment of the runoff water before infiltration, in case the water is not passing the overgrown, biological active top soil layer (Dachflächenwässer-tech. Richtlinie – 1996; BBodSchV 1999).

2.4.2.2 Filter strips and swales

Filter strips and swales are vegetated surface features that drain water evenly off impermeable areas (Fig. 10). Swales are long shallow channels, while filter strips are gently sloping areas of ground. They allow run-off to flow in sheets through vegetation, slowing and filtering the flow. Swales also act as temporary storage facilities prior to infiltration into the ground. Sediments are removed from the water, and vegetation can take up any nutrients in the water. Swales and filter strips can be integrated into the surrounding land use, for example, road verges. Local grasses and flower species can be introduced for visual effect and to provide a wildlife habitat. Maintenance consists of regular mowing, clearing litter and periodic removal of excess silt.

Figure 10: Vegetated filter strip and vegetated swales in an urban landscape.

2.4.2.3 Filter drains and permeable surfaces

Filter drains consist of permeable materials located below ground to store run-off. Run-off flows to the storage area via a permeable surface (Fig. 11). The permeable surface can be in the form of grassed or gravelled areas, paving blocks with gaps between individual units or paving blocks with vertical voids built in. Water is therefore collected from a large surface area, stored in the filter drains and allowed to infiltrate through the soil. The permeable fill traps sediments and thereby cleans the run-off. Filter drains and permeable surfaces are

currently used for road verges and car parks. The surfaces should be kept clear of silt and cleaned regularly to keep the voids clear. Weed control may be necessary.

2.4.2.4 Infiltration devices

Infiltration devices drain water directly into the ground. They include soak ways and infiltration trenches, which are located below ground, and into which storm water run-off is directed. They function by storing water and allowing the water to infiltrate into the ground.

Figure 11: Drains and permeable surfaces.

They work well when the soil is permeable and the groundwater table is distance away from the surface. Maintenance consists of regular inspection to ensure the infiltration capacity is maintained. Areas draining to an infiltration device should be kept clear of silt, as this will get washed into the device and reduce its permeability as well as filling up space that should be used for storage.

2.4.2.5 Basins and ponds

Basins are areas for storage of run-off that are dry during dry weather, whereas ponds are permanently filled with water (Fig. 12). Both store water and therefore attenuate the flow of water during a storm. Flow variation downstream of the basins or ponds can thus be

controlled. Basins and ponds also may act as infiltration devices (Section 2.4.2.3). Basins and ponds are often used at the end of a train of treatment for storm water, and provide additional step if source control does not have an adequate capacity to control run-off. Detention time is of the order of two to three weeks. Both basins and ponds can be vegetated, so that they can have a range of features, including wetlands that have amenity values for passive recreation or wildlife habitat. Run-off water quality is improved upon storage in basins or ponds because of sedimentation of solids, bacterial action and nutrient uptake by vegetation. Water stored in ponds can also be used for irrigation of parks and gardens or for fire-fighting and other purposes. Basins and ponds need to be maintained to control vegetation and removal of accumulated silt.

Figure 12: Pond, basin and constructed wetland for storm water treatment.

2.5 Zeolites

2.5.1 History of zeolites

The history of zeolite application began in 1756 when the Swedish mineralogist *Cronstedt* discovered the first zeolite mineral, stilbite (Cronstedt., 1756). He recognized zeolites as a new class of minerals consisting of hydrated aluminosilicates of the alkali and alkaline earths. Because the crystals exhibited in tumescence when heated in a blow pipe flame, *Cronstedt*

called the mineral a ``zeolite`` derived from two Greek words, ``zeo`` and ``lithos`` meaning ``to boil`` and ``a stone``. In 1840 *Damour* observed that crystals of zeolites could be reversibly dehydrated with no apparent change in their transparency or morphology. *Way* and *Thomson* (1850) clarified the nature of ion exchange in soils. *St. Claire Deville* reported the first hydrothermal synthesis of a zeolite, levynite, in 1862. *Grandjean* in 1909 observed that dehydrated chabazite adsorbs ammonia, air, hydrogen and other molecules and in 1925 *Weigel* and *Steinhoff* reported the first molecular sieve effect. They noted that dehydrated chabazite crystals rapidly adsorbed water, methyl alcohol, ethyl alcohol and formic acid but essentially excluded acetone, ether or benzene. In 1932 *McBain* established the term ``molecular sieve`` to define porous solid materials that act as sieves on a molecular scale.

Thus by the mid-1930 the literature described the ion exchange, adsorption, molecular sieving and structural properties of zeolite minerals as well as numbers of reported syntheses of zeolites. The latter early synthetic work remains unsubstantiated because of incomplete characterization and the difficulty of experimental reproducibility.

2.5.2 Zeolite structures

Zeolites are crystalline aluminosilicates of group IA and group IIA elements such as sodium, potassium, magnesium and calcium (Breck., 1974). Chemically, they are represented by the empirical formula:

$$M_{2/n}O \bullet Al_2O_3 \bullet ySiO_2 \bullet wH_2O$$

where y is 2 to 10, n is the cation valence and w represents the water contained in the voids of the zeolite. Structurally, zeolites are complex, crystalline inorganic polymers based on an infinitely extending three dimensional, four-connected framework of AlO_4 and SiO_4 tetrahedra linked to each other by the sharing of oxygen ions (Fig. 13). Each AlO_4 tetrahedron in the framework bears a net negative charge which is balanced by an extra framework cation. The framework structure contains channels or interconnected voids that are occupied by the cations and water molecules. The cations are mobile and ordinarily undergo ion exchange. The water may be removed reversibly, generally by the application of heat which leaves intact a crystalline host structure permeated by the micro pores and voids which may amount to 50 % of the crystals by volume.

The structural formula of zeolite is based on the crystallographic unit cell, the smallest unit of structure represented by

$$M_{x/n}[(AlO_2)_x(SiO_2)_y] \bullet wH_2O$$
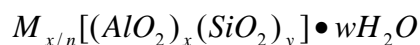
where n is the valence of the cation M, w is the number of water molecules per unit cell, x and
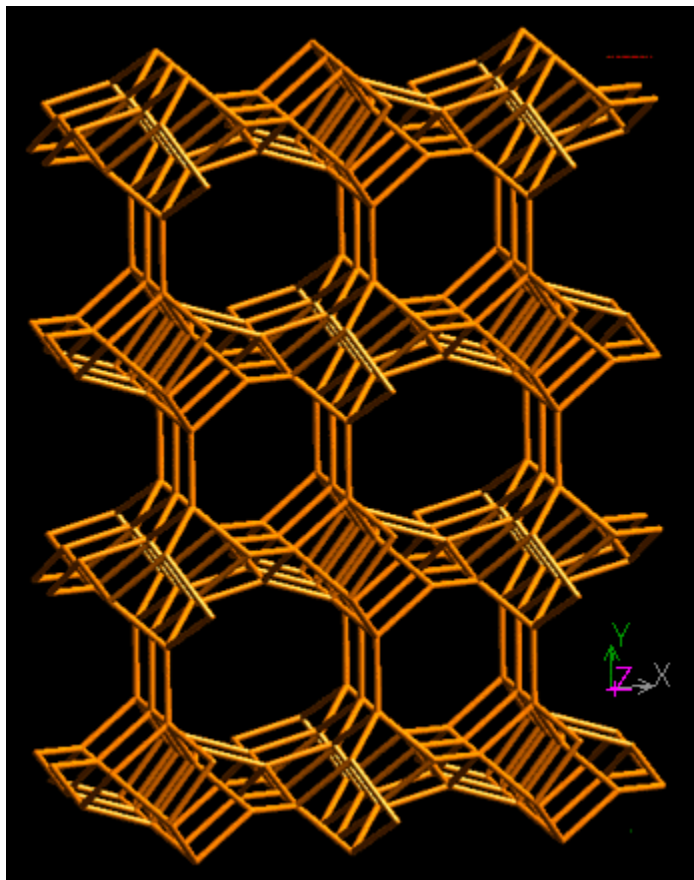
Figure 13: Framework of HEU structure (International Zeolite Association – www. iza-structure.org).

y is the total number of tetrahedra per unit cell, and y/x usually has values of 1-5. In the case of the high silica zeolites y/x is 10 to 100. There are two types of structures: one provides an internal pore system comprised of interconnected cage like voids; the second provides a system of uniform channels which, in some instances, are one dimensional channel systems. The preferred type has two or three dimensional channels to provide rapid intracrystalline diffusion in adsorption and catalytic applications. In most zeolite structures the primary structural units, the AlO_4 or SiO_4 tetrahedra, are assembled into secondary building units which may be simple polyhedra such as cubes, hexagonal prisms or cubo-octahedra. The final framework structure consists of assemblages of the secondary units.

More than 70 novel, distinct framework structures of zeolites are known. They exhibit pore sizes from $0.3 - 1.0$ nm, and pore volumes from about 0.10 to 0.35 cm^3/g. They include small

pore zeolites with eight ring pores with free diameters of 0.30 – 0.45nm, e.g., zeolite A; medium pore zeolites formed by ten ring, 0.45 – 0.60 nm in free diameter, e.g., ZSM-5; large pore zeolites with 12 ring pores, 0.6-0.8 nm, e.g., zeolites X and Y; and extra large pore zeolites with fourteen ring pores, e.g., UTD-1.

2.5.3 Ion exchange in zeolites

Ion exchange is an intrinsic property of most zeolites. As a consequence the phenomenon has either given rise to an admittedly few but nevertheless important number of direct applications, or the phenomenon is used indirectly, as a means of tailoring zeolite structure and hence properties when these materials are used in other ways, such as in catalysis or gas sorption.

Zeolites are normally highly crystalline materials. This means that the ionic framework comprises an extended regular array of silicon, aluminium and oxygen ions which enclose micro-porous channels, these latter being of molecular dimensions. This makes zeolites significantly different from clay minerals or from typical amorphous ion exchange resins. In the following sections the influence of zeolite properties on ion exchange processes will be discussed.

2.5.3.1 Ion sieving and volume exclusion

The size of the pores may be such that some ions are too large to enter some of the cages and channels within the zeolite structure. Thus these ions are sieved out of part of the space which is available for ion exchange within the crystal. This phenomenon may lead to a complete exclusion of one sort of cation from a particular zeolite (Barrer et al., 1978), or partial exchange only occurring (Fletcher and Townsend., 1983), with a clear maximum level of exchange for the entering cation which is less than that one would expect on the basis of the framework Si/Al ratio.

Alternatively, channels within the zeolite structure may be large enough for the ions to diffuse through without severe restriction, but the volume of the individual cation may be such that the sum of the volumes of all the cations of a particular type required to neutralise the anionic framework is greater than the available space within the zeolite (Barrer et al., 1978; Theng., 1971). When this occurs, partial exchange with respect to the entering cation is again observed, not because of a sieving effect but because of a volume exclusion effect.

2.5.3.2 Different exchange sites

The three dimensional extended array which constitutes the zeolite framework may have associated with it quite clearly defined exchange sites. Thus, per unit cell one can commonly define particular sites within the zeolite which differ one from another in terms of the energies of interaction associated with them. A very good example of this is the faujasitic group of zeolites. In these materials a large number of different sites are identified and associated with each type of site is a particular ion population and site energy (Barrer et al., 1978).

It is important to recognize that it can be a difficult and a slow process to remove or exchange cations from certain of these sites even though both the leaving and entering ions are able to move through the channels of the lattice. As a consequence the experimental conditions used in preparing a particular ion exchanged form of zeolite, whether in a mixed or homoionic form can be absolutely critical.

2.5.3.3 Framework flexibility and hysterisis

All zeolite structures exhibit some degree of flexibility as evidenced by for instance the sorption of molecules whose maximum diameters exceed the nominal pore openings of the zeolite (Coker et al., 1998). Distortion of the zeolite framework is necessary to allow passage of the sorbate into the channels. This flexibility allows different cation-exchanged forms of a given zeolite to adopt different symmetries and unit cell sizes, depending upon the rigidity of the framework, the sizes of the cations, the strength of the interaction of the cations with the framework and the degree of hydration. One particularly flexible structure is the gismondinetype zeolite P which is known to convert between three symmetries, depending on hydration (Taylor and Roy., 1965) and cation content (Barrer and Munday., 1971).

2.5.3.4 Stability of the zeolite

Many commonly used zeolites are hydrolytically unstable in solutions of even mildly acid pH, and removal of aluminium from the framework will occur readily. In high aluminium zeolites this can lead ultimately to breakdown of the crystalline structure. This is a phenomenon which has often been neglected in the past, has led to irreproducibility of data and is of particular significance in detergency (Cook et al., 1982; Allen et al., 1983). In addition it is worth noting the limits outside which precipitation of basic salts may occur. Zeolites exhibit an alkaline reaction to their environment and in the presence of many transition metal cations, basic salts

may be precipitated if adequate precaution is not taken (Barrer and Townsend., 1976; Fletcher and Townsend., 1982). Also, one should be aware that many metal ions are speciated in solution (Fletcher and Townsend., 1985). If speciation occurs to a significant extent then the exchange capacity observed will be higher than expected (Sposito et al., 1981). This behaviour has been observed in clay minerals not only with copper but also with calcium and magnesium (Sposito et al., 1983).

2.5.4 Application of zeolites

2.5.4.1 Removal of ammonium from wastewater

One of the first commercial applications of zeolites to ion exchange was the removal of ammonium ions from the effluent of the second purification step of wastewater. The possible use of NH_4^+-selective zeolite in technical dimensions was already demonstrated in the nineteen thirties by several studies and the running of a pilot plant (Leyva Ramos et al., 2004; Beler-Baykal et al., 2004).

2.5.4.2 Detergents industry

Some 20 years ago a growing awareness of the environmental impacts created by the use of polyphosphates in detergents caused detergent manufacturers to look for less problematic replacements. The function of the polyphosphates is the reduction of the hardness of the water by removing Ca^{2+} and Mg^{2+} ions in order to prevent their precipitation by surfactant molecules. The use of zeolites as builders was suggested in the seventies and since then it has been demonstrated that they can effectively carry out the water softening (Gudovicz., 1985; Cruceanu et al., 1985).

2.5.4.3 Separation of radio isotopes

For the treatment of solutions containing radioactive isotopes, organic ion exchange resins were used first. However inorganic materials turned out to have more advantages, like higher stability in the presence of radioactivity, and they are more resistant to aqueous solutions at elevated temperature (Misaelidis et al., 1995). In 1913-1915 *Ames* reported the high selectivity and capacity of zeolite for the cations Cs^+ and Sr^{2+}, which are the major components of radioactive wastewaters.

2.5.4.4 Soil treatment

In Japan around 6000 tons per year of clinoptilolite and mordenite is used to control soil pH, moisture content and manure malodour. The control of pH is related to the ability of zeolite to function as a slow release agent to improve nitrogen retention in the soil. Horticultural applications generally use 5-10% incorporation by weight of clinoptilolite into growing media (International Zeolite Association).

2.5.4.5 Animal feed supplements

The beneficial effect of a 5-6% supplementation to the diet of pigs has been recognised in Japan for many years. Extension to similar studies of pig rearing in the USA, Cuba, Hungary, Austria, etc., has confirmed that pigs taking in clinoptilolite show beneficial weight gains and are less subject to disease than pigs fed by normal diets. Part of the success seems to be derived from ion exchange control of ammonium ion levels in the gut, but some studies show higher levels of blood proteins, globulins and mineral elements in pigs receiving a Ca-K form of clinoptilolite in their feed (International Zeolite Association).

2.5.5 Clinoptilolite

Many different species of zeolites have been identified. Clinoptilolite is the most abundant natural zeolite because of its wide geographic distribution and large size of deposits (Fig.14). It was formed by the diversification (the conversion of glass to crystalline material) of volcanic ash in lake and marine waters millions of years ago.

Clinoptilolite, which means "oblique feather stone" in Greek, received its name because it was thought to be the monoclinic (or obliquely inclined) phase of the mineral ptilolite, as in "oblique ptilolite". But ptilolite was later found to be the earlier named mineral mordenite, consequently ptilolite is no longer in use.

Clinoptilolite belongs to the Heulandite group of minerals. Because of its high content of silicon it is known as high-silica heulandite. Its chemical formula varies depending on its composition and origin, but a typical representation is: $(Na_6((AlO_2)(SiO_2)30)\cdot24H_2O)$. Its characteristic tabular morphology shows an open reticular structure of easy access, formed by open channels of 8-10 membered rings. Exchangeable ions such as Na^+, K^+, Ca^{2+} and Mg^{2+} commonly occupy these channels.

Figure 14: Photo from clinoptilolite with a grain size between 0.5 and 1.0 mm.

It is used in many applications such as a chemical sieve, gas absorber, feed additive, food additive, as an odour control agent, as a water filter for municipal and residential drinking water and as a filter material in aquariums. Clinoptilolite is well suited for these applications due to its large amount of pore space, high resistance to extreme temperatures and chemically neutral basic structure.

3. Hypothesis

The aim of this study was to investigate the applicability of an ion exchanger as an artificial barrier for the elimination of heavy metals, such as e.g. copper, zinc and lead, from the runoff of metal roofs. According to the theoretical considerations presented in section 2 the following hypotheses are stated, which will be assessed in this work:

o   The heavy metal concentration in the runoff of metal roofs is dominated from the dissolved phase (Heijerick et al., 2002; Karlen et al., 2002): thus, ion exchange appears a viable process to remove heavy metals from runoff water

o   The hydraulic load from a roof surface varies in a wide rage depending on rain intensity. Subsequently, the hydraulic loading of any type of reactor applied for heavy metal removal will vary respectively. Under these extreme conditions only an ion exchanger can operate effectively

o   The sorption capacity as well as the ion exchange uptake of an ion exchanger can be optimized through chemical conditioning, using a sodium chloride solution in order to remove specific ions like calcium, magnesium and potassium, from the structure of the material and locate sodium, as more easily removable ion, prior to any application. The final homoionic or near homoionic state of the material was expected to improve its effective ion exchange capacity and performance in ion exchange applications (Inglezakis et al., 2004; Curkovic et al., 1997; Semmens et al., 1988).

o   On site regeneration of the barrier material is possible

Clinoptilolite as an ion exchanger complies with those requirements and at the same time, as a natural material, is inexpensive.

4. Approach

For the development of a filter packed with clinoptilolite as a barrier material the following efforts were made:

4.1 Lab scale experiments

- *Batch experiments*

  - improvement of the ion exchange capacity and ion exchange rate of clinoptilolite through chemical conditioning

  - determination of the ion exchange capacity of clinoptilolite with regard to copper, zinc and lead

  - allocation of the influence of pH and metal ion concentration on the ion exchange process

  - assignment of the kinetics of the ion exchange process

  - definition of the affinity of the material regarding copper, zinc and lead

- *Column experiments*

  - determination of the influence of the volumetric flow rate on the operating ion exchange capacity of clinoptilolite

  - allocation of the metal ion concentration on the operating ion exchange capacity of clinoptilolite

  - definition of the influence of the pH on the ion exchange process

  - assignment of the flow modus (up flow, down flow) on the ion exchange process

  - determination of the regeneration process

4.2 Pilot plant

The barrier material investigated in the lab scale trials was applied in a field study for the treatment of the runoff from an eleven years old zinc roof. The influence of the heavy metal

concentration, the heavy metal phase distribution (dissolved or particulate), and the duration of the antecedent dry weather period on the heavy metal elimination performance of the barrier material was investigated.

4.3 Full scale application

The `know how` obtained during the lab scale and the pilot plant phase was applied in a full scale application at the Academy of Fine Arts in Munich. The target was to define the pollution of the copper roof runoff, regarding weather conditions, roof orientation and profile of the rain event and how it could affect the performance of the barrier material.

5. Materials and Methods

5.1. Lab scale experiments

5.1.1 Chemical conditioning and characterisation of clinoptilolite

The clinoptilolite used was supplied by Silver & Baryte Ores Mining Co. S. A, from Greece. The particle size of the sieved material was in the range of 0.5 – 1 mm. 100 g of it was treated with 1M NaCl solution at a room temperature over a period of 24 hours. Afterwards the clinoptilolite was washed with ultra pure water (18.2 MΩcm) by ultrasonication (SONOREX SUPER RK 514 BH), several times, until the fine fraction was removed. Then the modified clinoptilolite (Na-form) was dried at $105^{o}C$ for 24 hours.

The chemical composition of the natural and modified clinoptilolite was determined by x-ray fluorescence analysis measurements, using the model SRS 303 of Siemens. The density was determined by an autopycnometer from Quanta Chrome Corporation (Ultrapycnometer 1000 Version 2.2). The pore size distribution of the natural and modified clinoptilolite was established with a Mercury-Porosimeter from Porous Materials Inc, Ithaca, New York. For the determination of the zeta-potential, the electro acoustic method from AcoustoPhor, PENKEM was applied.

5.1.2 Batch experiments

- *Equilibrium experiments*

Equilibrium experiments with natural and modified clinoptilolite were conducted as follows: A constant amount of clinoptilolite (1g) was added into a tube (50 ml), containing measured volumes of a different heavy metal solution each time (40 ml). The following concentrations of Zn^{2+}, Cu^{2+} or Pb^{2+} were used: 1, 2, 3, 4, 5 and 10 mM. The experiments for every heavy metal were carried out for initial pH values of 5.0 and 3.0 at room temperature. The suspension was mixed for a period of 24 hours with a vertical rotary shaker (Fig.15) at a speed of 40 rpm. Afterwards 30 ml of every sample was filtrated (0.45 μm cellulose nitrate filter) and pH and temperature values recorded prior to analysis. In order to check for precipitation of metal hydroxides, control samples were conducted at every experiment and analyses were performed for the evaluation of the heavy metals in solution.

- Kinetic experiments

Kinetic experiments were conducted on natural and modified clinoptilolite samples and the experimental details are as follows: A measured quantity of clinoptilolite (1 g) was added into a tube (50 ml), containing measured volumes of a different heavy metal each time (40 ml). The corresponding metal concentrations were approximately 1 and 5 mM. The experiments were carried out for initial pH values of 3.0 and 5.0 at room temperature. The suspension was shaken for a period of 5, 10, 15, 30, 60 and 180 min with the same vertical rotary shaker at a speed of 40 rpm and the same procedure as with the equilibrium runs was followed.
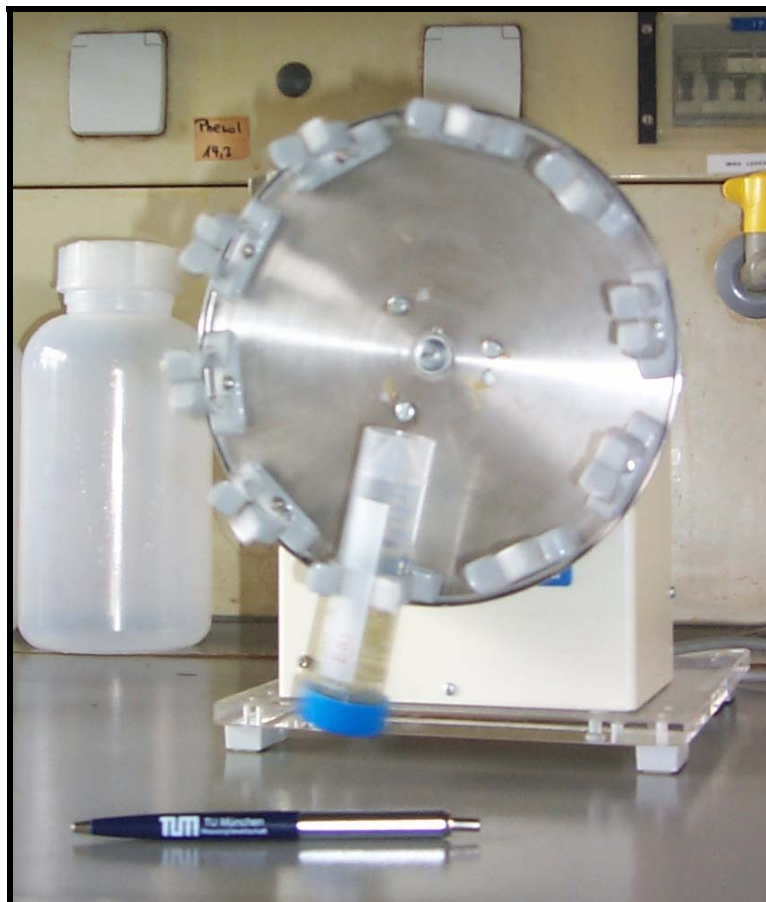

Figure 15: Rotary shaker.

All chemicals used were analytical grade reagents of the highest quality available. Analysis of every heavy metal was performed on the collected samples by means of flame atomic absorption spectrometry (VARIAN SPECTRA A-40). Electric conductivity and pH measurements were performed after collection of each sample. The pH readings were carried

out with a glass electrode (WTW Sentix 60). The EC readings were performed by an EC electrode (WTW TETRACON 325) connected to a WTW LF 340 EC meter.

5.1.3 Column experiments

Column experiments were conducted using vertical glass columns of 25 cm height and 2.5 cm internal diameter (Bed volume of 1.23 l). The packing material was supported on a glass filter of 250 μm pore diameter. The feed was introduced using a high precision 4-channel peristaltic pump, at different volumetric flows, in down and up flow mode (Fig. 16). Samples were withdrawn at the exit of the bed in desired time intervals, depending on the flow rate. All the experiments were carried out at room temperature. As a packing material, the modified clinoptilolite developed through the chemical conditioning process described in paragraph 4.1.1 was used. The particle size of the sieved modified clinoptilolite was in the range of 0.5 – 1mm.
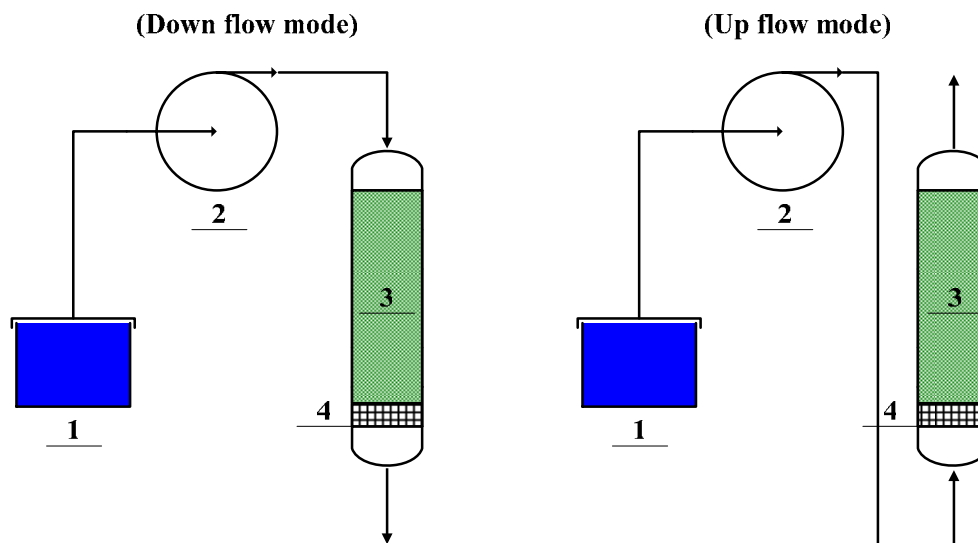
Figure 16: Experimental set-up for column experiments: (1) solution tank; (2) peristaltic pump; (3) clinoptilolite bed; (4) glass filter

Ultra pure water (18.2 MΩcm) with the pH adjusted to 5.0 was pumped through every column (1.7 BV/h) till the pH value remained the same in outlet and inlet. This pre-treatment procedure was followed in every column experiment in order to avoid precipitation problems during breakthrough experiments and to apply as far as possible the same experimental conditions.

Electric conductivity and pH measurements were performed after collection of each sample. The pH readings were carried out with a glass electrode (WTW Sentix 60). The EC readings

were performed by an EC electrode (WTW TETRACON 325) connected to a WTW LF 340 EC meter. Analysis of all heavy metals was performed on the collected samples by flame atomic absorption spectrometry (VARIAN SPECTRA A-40).

- Influence of the pre-treatment column procedure on the ion exchange process

A copper solution of 30 mg/l Cu^{2+} with pH adjusted to 5.0 was pumped (down flow modus) through two different almost water saturated columns under a volumetric flow rate of 8.5 BV/h. On one of them the pre-treatment process described above was applied.

- Influence of pH of the feeding solution

Three pre-treated clinoptilolite columns were fed (down flow modus) with a 30 mg/l copper solution of pH 3.0, 4.0 and 5.0 respectively, under a volumetric flow rate of 8.5 BV/h.

- Influence of flow modus

A copper solution of 30 mg/l Cu^{2+} with initial pH of 5.0 was pumped in an up flow mode through a water saturated column under a volumetric flow rate of 8.5 BV/h. The same solution was fed in a down flow mode through a water saturated column under the same volumetric flow rate.

- Effect of volumetric flow rate

Three packed columns of clinoptilolite were used for this run of experiments. A copper solution of 30 mg/l Cu^{2+} with initial pH of 5.0 was pumped (down flow modus) through three water saturated (almost) columns under a volumetric flow rate of 1.7, 3.4 and 8.5 BV/h, respectively.

- Influence of the metal concentration

Three copper solutions of 5, 15 and 30 mg/l Cu^{2+} with initial pH of 5.0 were pumped (down flow modus) through three water saturated (almost) columns under a volumetric flow rate of 8.5 BV/h.

- Effect of metal speciation

Three metal solutions (Cu^{2+}, Zn^{2+} and Pb^{2+}) of 30 mg/l of pH 5.0 were pumped in down flow modus through three water saturated (almost) columns under a volumetric flow rate of 8.5 BV/h.

- Regeneration studies

A solution of 5 mg/l Cu^{2+} with pH adjusted to 5.0 was pumped in down flow modus through a Na-clinoptilolite column (no pre-treatment procedure was applied) under a volumetric flow rate of 17 BV/h till it became saturated. Then the copper saturated column was regenerated with 1M solution of NaCl. After regeneration the column was fed again with the same copper solution till saturation. The process feeding – regenerating was applied three times.

5.2 Pilot plant

Roof runoff

Rainwater was sampled from a roof of a building on the campus of the Technical University of Munich, in Garching. Two infiltration shafts are located in the courtyard of the building. The location of the shafts is a very good example of situations where limited amount of space is available to install infiltration trenches or ponds. The roof (Fig. 17) is divided into eight surfaces. The total area of the sampling surface was $238m^2$. The roof, the gutters and the down spout are made of Ti-Zn. In order to merge the zinc panels, the standing seam technique was applied. The one big and the four little chimneys all have a round shape and are made of zinc. On their connection to the roof they are soldered with tin–solder which contains fractions of lead. The inclination of all surfaces was 10^0.

Specification of the local conditions

Meteorological conditions, orographic position and emissions from nearby sources influence the constitution of the primary as well as of the secondary deposition on the roof. In this particular case, potential sources of emissions could be a power plant located in a distance of 1.5 km, and an autobahn, 2.2 km apart to the west (Fig.18). For power and heat generation natural gas is used so that only little effects may be expected from this source. The autobahn, however, may be assumed to be a significant source of air pollutants. It is used by more than 130,000 cars per day. 12% of those are trucks. The local weather is dominated by westerly

and sometimes easterly winds, whereas the westerly winds tend to be responsible for the rain events and the easterly winds for the dry periods.

Figure 17: View of the zinc roof with its sampling surface.
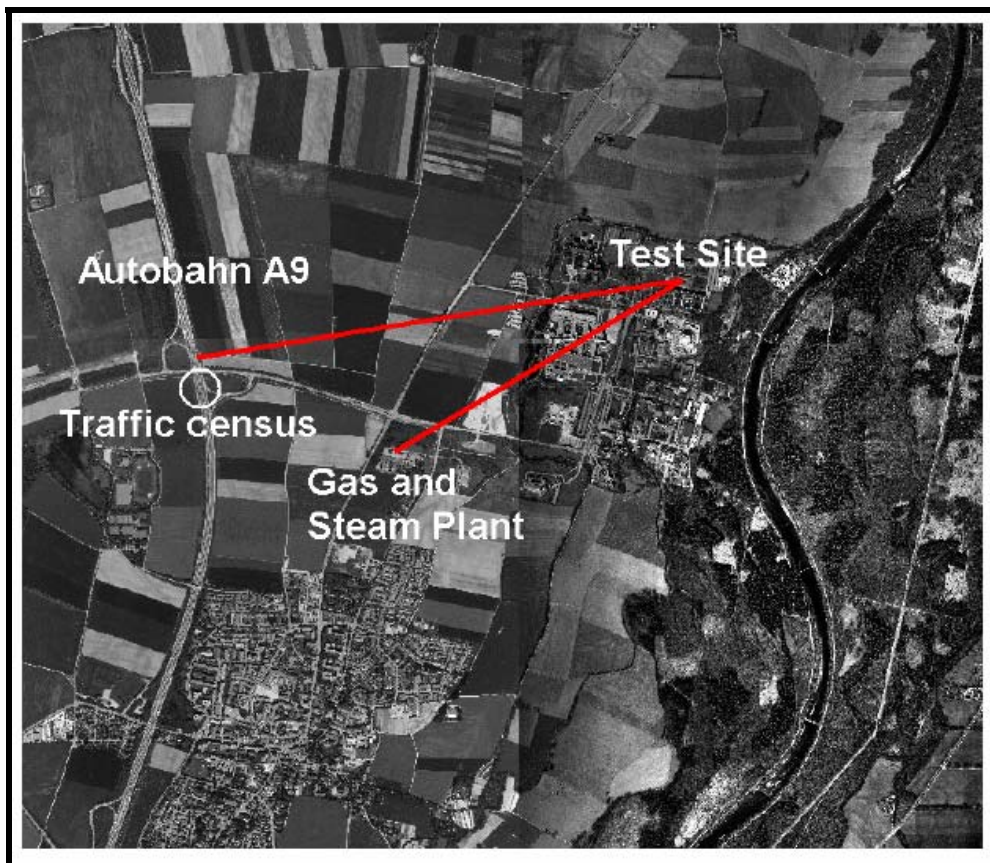
Figure 18: Aerial view of the field site with its surroundings.

Retention facility

A column of stainless steel with an internal diameter of 40 cm and a height of 80 cm was installed into the infiltration shaft and filled with 110 kg of clinoptilolite (Fig. 19).
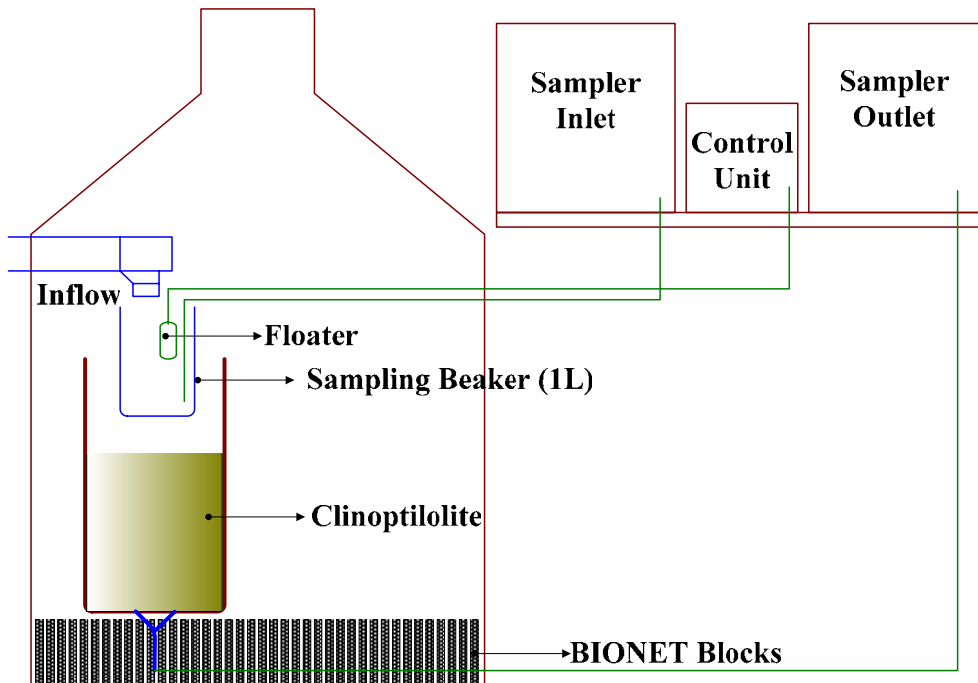
Figure 19: Retention facility with sampling devices.

The clinoptilolite used was the modified one developed through the chemical conditioning process described in paragraph 4.1. The particle size of the sieved modified clinoptilolite was in the range of 0.5 – 1 mm.

Sampling process

Samples were taken from three different points: (1) directly from the rain by means of a sampling device installed at the top of the roof; (2) from the inflow to the infiltration shaft, and (3) from the bottom of the clinoptilolite bed (funnel effluent). 24 hour composite samples were taken by means of two automatic samplers.

A total of 24 bottles could be used for sampling in each of the two automatic samplers. The polyethylene bottles with a volume of 2 l each were washed with a 3 % (V/V) solution of nitric acid prior to every use. The samplers were programmed for a fractionation by runoff time. Samples of maximal 500 ml were taken every 3.5 min and the bottles changed every 7 min.

In the case of a rain event, the runoff entered the infiltration shaft through the inflow pipe, flowed into the beaker and then overflowed into the clinoptilolite filter. When the water level in the beaker rose, the floater gave a signal to both samplers, through the control unit, to start sampling. If a rain event lasted until all 24 bottles from the inflow were filled (168 min), the samplers automatically stopped sampling. In case the rain stopped earlier and the floater gave a signal that the water in the beaker was below the sampling level, the samplers changed the sampling bottle and stopped sampling until the rain started again.

The first two sampling procedures from the outflow (depending mostly on the magnitude of the initial rain and less on the saturation of the clinoptilolite filter) did not carry water or less than 500 ml. The reason was that the beaker first had to be filled with water in order the overflow would be able to reach the funnel which was situated directly underneath the filter.

Analysis of samples

Fifteen rain events were analysed for the following constituents using the methods described as follows:

- Total and dissolved zinc and lead were measured in acidified samples (1% HNO_3 suprapur) by means of atomic absorption spectrometry (VARIAN SPECTRA A-40). The dissolved fraction was obtained by filtration (0.45 μm cellulose nitrate filter) prior to acidification.

- pH values were measured in the lab with a glass electrode (WTW Sentix 60).

5.3 Full scale application

5.3.1 Description of the field site

The Academy of Fine Arts is located in the centre of Munich, Germany (Fig. 20). The building is surrounded by four major streets: Leopold Street, Akademie Street, Türken Street and Georgen Street. The Leopold Street is one of the main roads in Munich with a daily vehicular flow of 40,000 cars. The traffic load of the other streets is less than 2000 vehicles per day.

The four years old copper roof of the Academy of Fine Arts covers a total area of 4,800 m^2. The roof runoff is channelled into ten retention facilities (RF) where each can treat the runoff from almost 500 m^2 roof surface. Four of them were chosen to be monitored (Fig. 21); one at the west site (RF I), two at the south (RF III and RF IV) and one at the east (RF II).

Figure 20: Photo of the south west site of the Academy of Fine Arts in Munich, Germany.
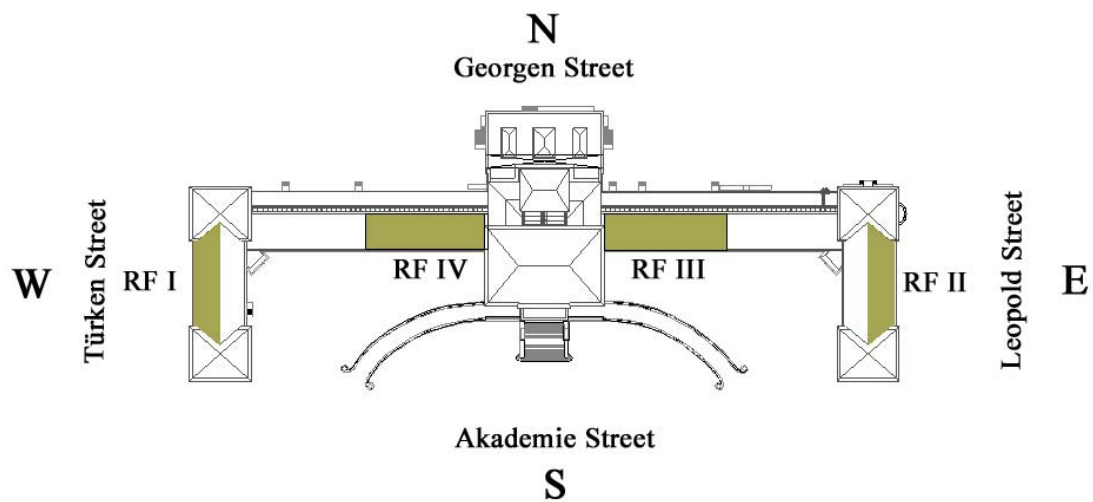
Figure 21: Sampling roof surfaces from the copper roof of the Academy of Fine Arts in Munich.

The retention facility at the west site (RF I) is a technical system which has been developed by the company KME-Mall (Fig. 22). The system is composed of a silt trap and a filtration

tank equipped with a zeolite cartridge (Fig. 23). After saturation of the barrier material, the cartridge can be replaced with a new one. The outflow of the filtration tank is infiltrated into the ground by means of an infiltration ditch.
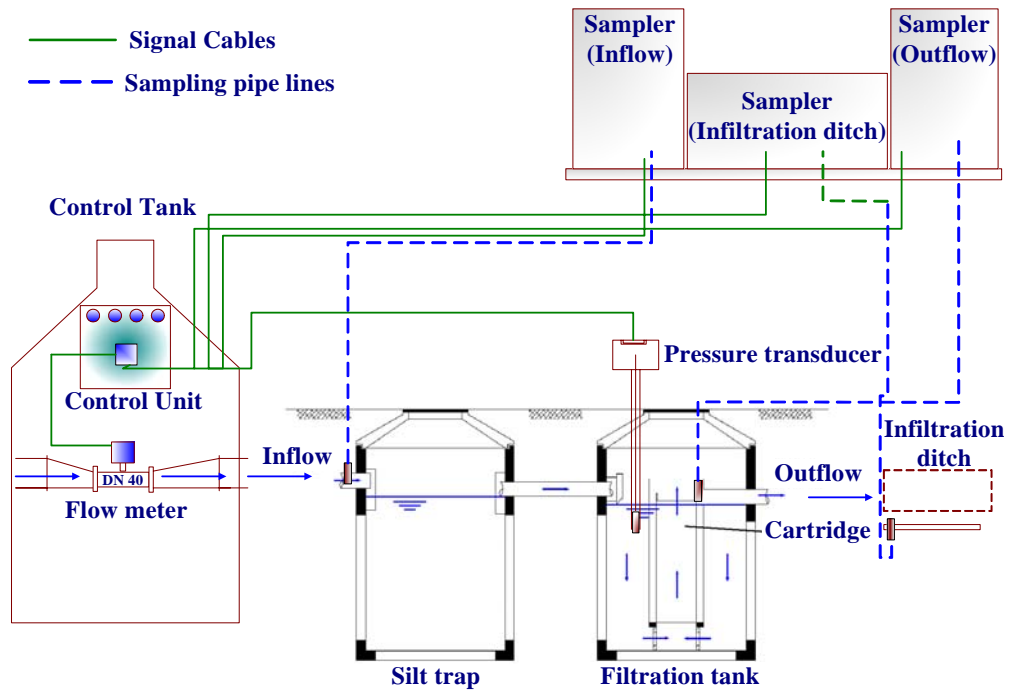
Figure 22: Technical system from KME-Mall with monitoring devices.

Figure 23: Filtration tank with the zeolite cartridge.

The other three retention facilities use the technical system which has been developed by the company HydroCon (Fig. 24). The system is composed of a filtration tank followed by an infiltration ditch. The roof runoff is channelled into the cyclone separator tangentially. Over the hydrodynamic separator is installed the filter unit with the barrier material. Since the barrier material could fail (hydraulic) under extreme rain weather conditions, an emergency overflow is arranged, so that the runoff can reach the infiltration ditch without passing through the barrier material.
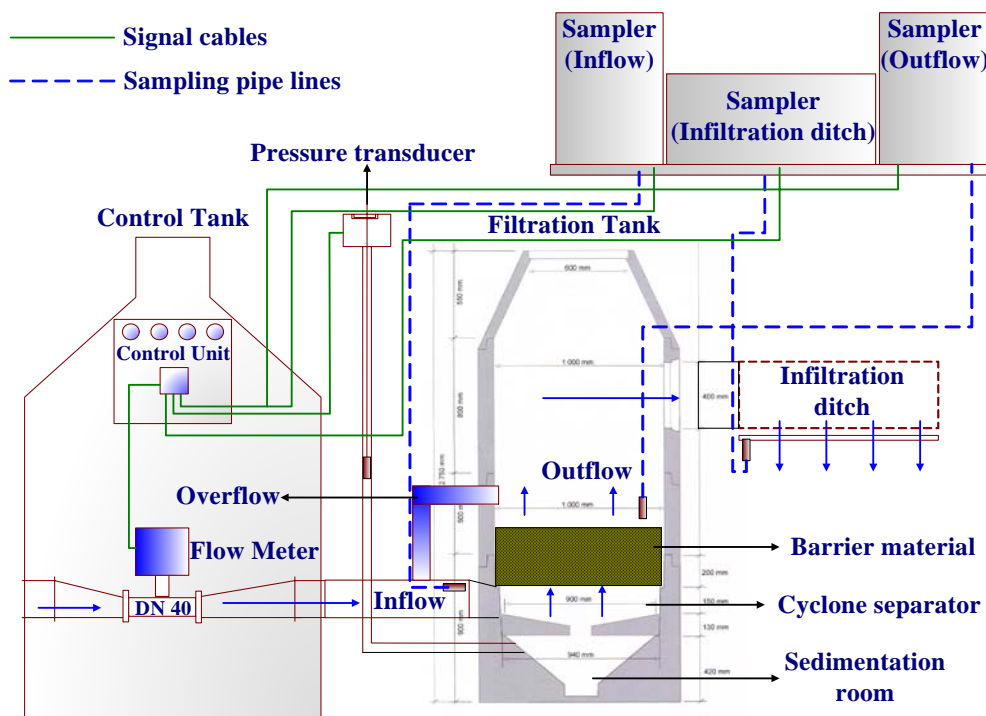
Figure 24: Technical system from Hydrocon with monitoring devices.

The difference between these three retention facilities, using the technical system from HydroCon, is the barrier material. At the east site a barrier material from porous concrete, with a high concentration of $CaCO_3$, coated with iron hydroxide has been used (Fig.25). This barrier material is developed by HydroCon (Dierkes et al., 2002). At the south-east site a mix of chabazite-philipsite (750 kg) is applied (Fig. 26). Finally at the south-west clinoptilolite (750 kg) is used as a barrier material (Fig. 27). Both barrier materials are chemically conditioned as it is described in paragraph 4.1.1. The grain size of both barrier materials ranges between 1 and 2 mm.

Figure 25: The porous concrete barrier material (HydroCon).

Figure 26: Filter unit equipped with a mix of chabazite-philipsite as a barrier material (Technical University of Munich).

Figure 27: Filter unit equipped with clinoptilolite as a barrier material (Technical University of Munich).

As mentioned above the outflow of both technical systems, KME-Mall and HydroCon, is infiltrated into the ground by means of an infiltration ditch. The applied infiltration ditch is a special construction which contributes to an additional reduction of the copper concentration. The ditch consists of a partial seeping pipe of impermeable concrete in the lower part (bottom of the pipe) and of a porous concrete with a high concentration of $CaCO_3$, coated with iron hydroxide, in the remaining part. The infiltration ditch has also been developed by HydroCon.

5.3.2 Instrumentation of the monitoring system

As it is shown in Figures 22 and 24 all the retention facilities are equipped with a control tank. A control unit with a digital writer and a flow meter device were installed in every control tank.

Magnetic induction flow meter device (MID)

Every flow meter device has been industrially calibrated in the range of 0 to 100 l/min and is able to function competently under rain water conditions down to 5 µS/cm.

Sampler (Inflow and Outflow – Bühl)

Every sampler has a capacity of 12 bottles with a volume of 2.5 l each. The sampling process lasts about 2 minutes. During this time the sampler empties away the water which is stagnated in the sampling pipe line from the last process and then sucks a new sample of 250 ml into the collecting bottle. The temperature in the samplers is set to 5 ± 1 ^{0}C.

Sampler (Infiltration ditch)

The sampler comprises a glass bottle of 15 l and a suction pump. The pump delivers the percolation water which is collected from a halved pipe (diameter of 20 cm) installed 25 cm all the way long underneath the infiltration ditch. The halved pipe is packed with washed gravel of 7 mm grain size (Fig. 28).

Figure 28: Installation of the sampling unit underneath the infiltration ditch.

Pressure transducer

A pressure transducer is installed in every filtration tank. The load cell of the transducer is arranged 25 cm underneath the level of the infiltration ditch. The measuring range of the device is between 0 and 0.25 bar.

Control unit

The control unit equipped with a digital writer controls and navigates the sampling process during a rain event. The signals from the flow meter, the pressure transducer and from the samplers are digitally recorded (20 s interval modus).

Weather monitoring station

The rain data of every rain event regarding rain height, rain intensity as well as air temperature, air humidity, wind strength and wind direction are recorded from the weather station of the Ludwig Maximilian University of Munich (LMU) which is located at Theresien Street, 200 m away from the Academy of Fine Arts.

5.3.3 Monitoring process

In the case of a rain event the roof runoff runs through the flow meter. If the flow velocity is faster than 1 l/min the control unit activates the samplers of the inflow and of the outflow. The sampler of the infiltration ditch is activated after 10 minutes but only when the flow velocity remains faster than 1 l/min. If the flow velocity is slower than 0.6 l/min, the control unit stops the sampling process. A flow velocity faster than 1 l/min activates the system again and the new sampling process uses a new bottle of the sampler. For the sampler's inflow and outflow there is a potential to arrange a 4X250 ml sampling process in the same bottle. A sampling process lasts about 2 min. This means that the system can monitor a non-stop rain event for almost 96 minutes.

5.3.4 Sampling

Samples are taken from four different points. (1) Directly from the rain by means of a sampling device installed at the top of the roof; (2) from the inflow of every retention facility; (3) from the outflow of every retention facility and (4) underneath the infiltration ditch.

Analysis of samples

All samples were analysed for the following constituents using the methods described as follows:

- Total and dissolved copper was measured in acidified samples (1% suprapur HNO_3) by means of atomic absorption spectrometry. The dissolved fraction was obtained by filtration (0.45 μm cellulose nitrate filter) prior to acidification

- pH values were measured in the lab with a glass electrode (WTW Sentix 60)

- The electric conductivity (EC) readings were performed by an EC electrode (WTW TETRACON 325) connected to a WTW LF 340 EC meter

6. Results and Discussion

6.1 Batch experiments

6.1.1 Chemical conditioning and characterisation of clinoptilolite

The chemical composition of the modified and natural clinoptilolite is presented in Table 5. According to the chemical analysis the theoretical cation exchange capacity (CEC) is 2.23 ± 0.15 meq/g. This capacity is the result of the presence of cations such as Na, Ca, Mg and K which are considered to be exchangeable and cannot change during any pre-treatment method of the material (Tsitsishvilli et al., 1992; Maliou et al., 1992; Helfferich F. 1995; Pabalan et al., 1994). The Si/Al ratio is 4.34 − 5.52 (mol/mol). According to publicised literature this ratio generally ranges between 4 and 5.5 and is typical for clinoptilolite (Inglezakis et al., 2002; Langella et al., 2000; Tsitsishvili et al., 1992; Malliou et al., 1992; Loizidou et al., 1992).

Table 5. Chemical composition of clinoptilolite (% w/w)

Oxide	Natural	Modified	±
SiO_2	67.1	67.9	0.2
Al_2O_3	12.2	12.1	1.50
Fe_2O_3	1.0	0.86	0.20
Na_2O	0.55	1.65	0.15
CaO	3.3	2.34	0.15
MgO	1.08	0.99	0.15
K_2O	1.76	1.62	0.15
MnO	0.0298	0.0272	0.00
TiO_2	0.16	0.15	0.05
P_2O_5	0.018	0.011	0.005
S	<0.001	<0.001	0.00
F	<0.5	<0.5	0.5
Loss on ignition	13.28	12.46	0.2

The purpose of chemical conditioning of clinoptilolite is to remove specific ions like Ca, Mg and K, from the structure of the material and locate Na, as more easily removable, prior to any application. In practice, the result of the chemical conditioning is the transformation of the natural material to a homoionic form (Na-clinoptilolite). The final homoionic or near homoionic state of clinoptilolite was found to improve its effective ion exchange capacity and

performance in ion exchange applications (Inglezakis et al., 2004; Curkovic et al., 1997; Semmens et al., 1988).

The effect of the chemical conditioning of clinoptilolite on its physical properties such as structure, surface area, bulk density, pore size distribution and surface charge (zeta potential) was investigated. Bulk density of the natural clinoptilolite was 2.33 ± 0.04 g/cm^3 and of the modified 2.32 ± 0.04 g/cm^3 respectively. Through the chemical conditioning of the material it was found that the fine fraction, dust produced during the grinding process, makes up about 8 % (w/w) of the clinoptilolite. BET analysis has shown that the natural clinoptilolite has a specific surface area of 25.7 m^2/g and the modified of 25.1 m^2/g respectively. In Figures 29 and 30 are presented typical XRD diagrams of the natural and modified clinoptilolite.
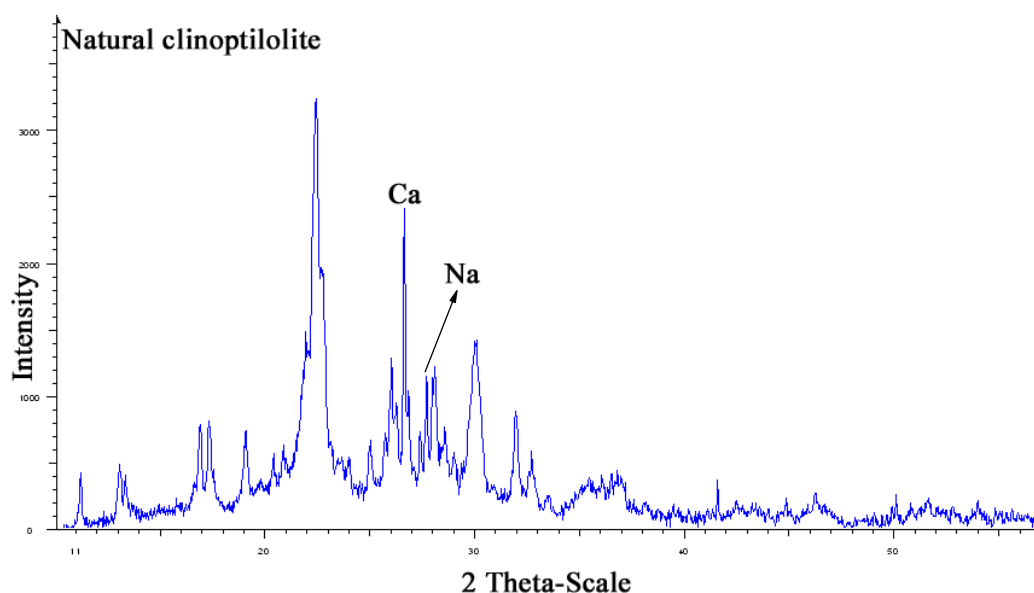
Figure 29: The XRD pattern of natural clinoptilolite.

It is evident that the three most intense d-spacings (peak width) are essentially the same, thus the crystal structure has not been altered during the chemical conditioning. On the contrary, there is a significant change on the relative intensity (signifies the type of atoms and their position) of calcium and sodium peaks between the modified sample and the natural, due to chemical conditioning.
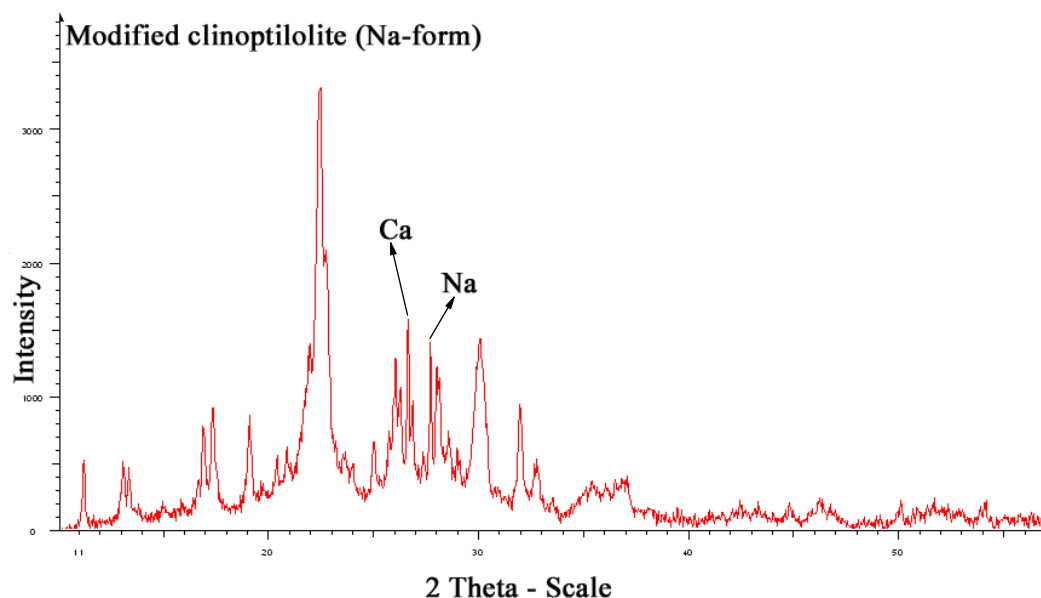
Figure 30: The XRD pattern of modified clinoptilolite.

In Figures 31, 32 and 33 are presented the results of the mercury porosimetry analysis of the modified and natural clinoptilolite. The natural material had a pore volume of 0.071 cm^3/g and a pore surface of 14.5 m^2/g. The median pore diameter, based on volume was 181 Å and 98 Å based on the surface area. The average pore diameter of the natural clinoptilolite was 195 Å. On the contrary, the modified clinoptilolite had a pore volume of 0.055 cm^3/g and a pore surface area of 9.1 m^2/g. The median pore diameter based on volume was 100.6 μm and 99 Å based on surface area. The average pore diameter of the modified clinoptilolite was 239 Å.

The natural clinoptilolite is characterized 60 % as mesoporous and 40 % as macro porous since the 60 % of its pore volume is accumulated in a pore radius of 70 – 200 Å and 40 % in a pore radius of 60 – 235 μm. By contrast, the modified material is characterized 45 % as mesoporous and 55 % as macro porous. It is evident that the clinoptilolite surface and pore openings are partially covered by the dust produced during the grinding process resulting in pore clogging which leads, as it will be shown below, to smaller ion exchange capacity and slower ion exchange rates.
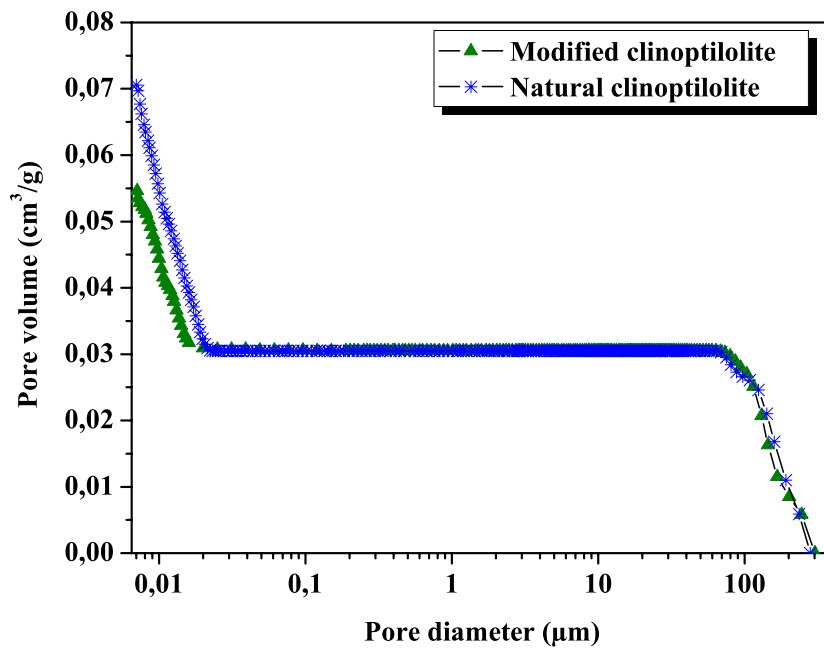
Figure 31: Cumulative pore size distribution by volume.
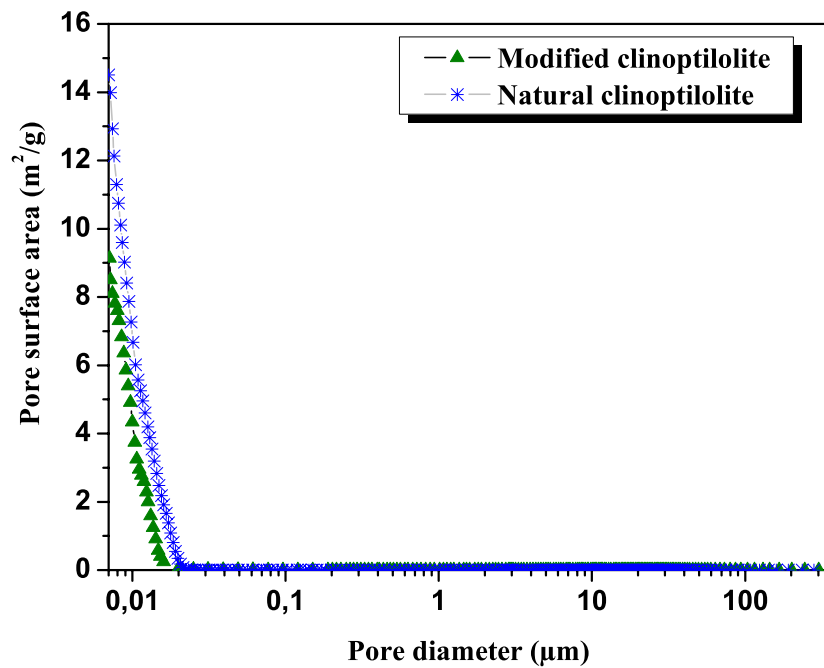
Figure 32: Cumulative pore size distribution by surface area.
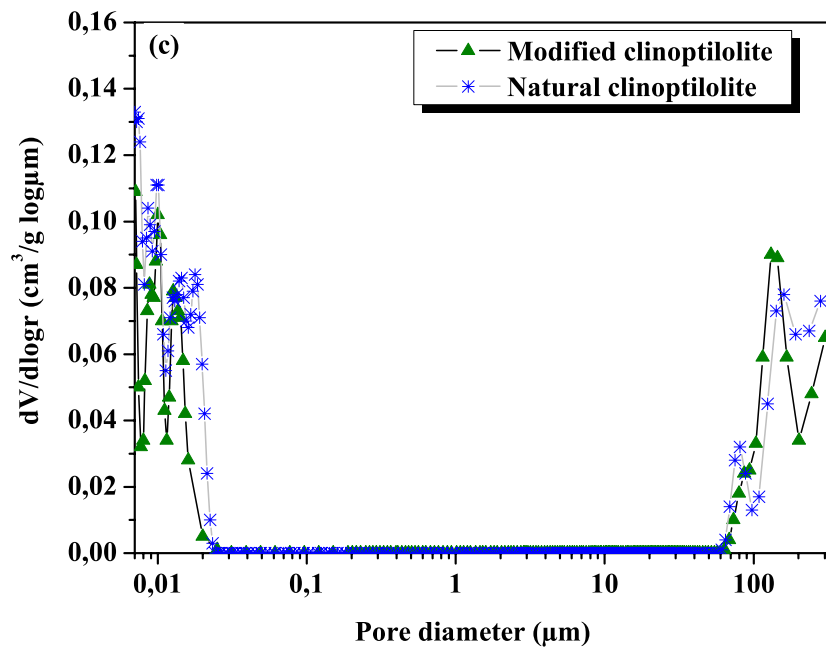
Figure 33: Relative pore size distribution by volume.
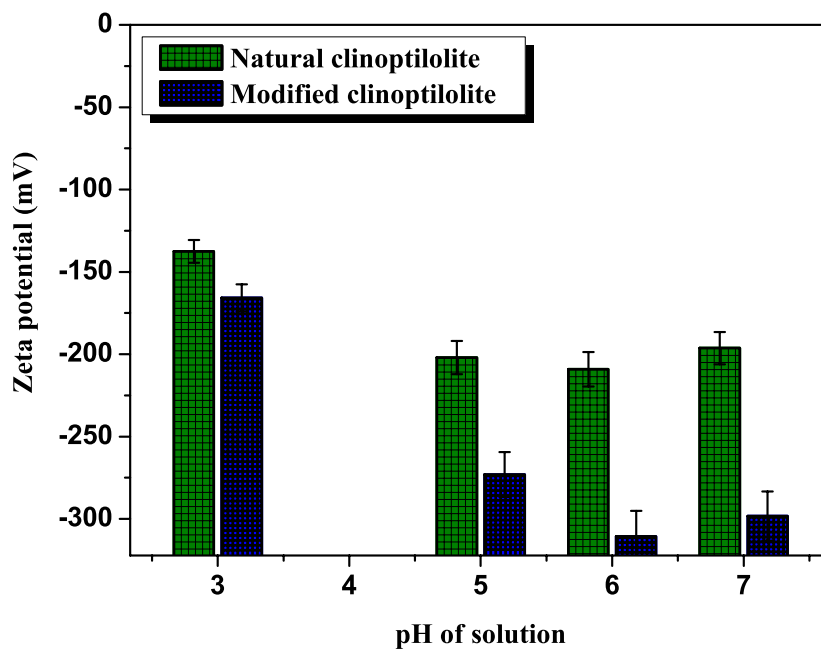
Figure 34: Zeta potential of natural and modified clinoptilolite.

The zeta potential measurements revealed that the clinoptilolite surface has a negative charge in water at the investigated pH values (Fig. 34). The negative charge results from the Al^{3+} substitutions for Si^{4+} within the clinoptilolite lattice (isomorphic substitution), the broken bonds at the Si-O-Si generated at the particle surface during the grinding process and the lattice imperfections (Kraepiel et al., 1998; Van Hooff et al., 1991; Breck et al., 1974; Grim et al., 1968).

6.1.2 Equilibrium and kinetic experiments

6.1.2.1 Influence of the chemical conditioning on the ion exchange

The plots in Figure 35 show the uptake degree of natural and modified clinoptilolite of zinc ion as a function of the initial concentration. The degree of uptake (η) is defined as:

$$\eta = \frac{C_i - C_e}{C_e} x100 \qquad (1)$$

C_i is the initial concentration and C_e is the equilibrium concentration of the zinc ion. Equilibrium was obtained after 24 hours.
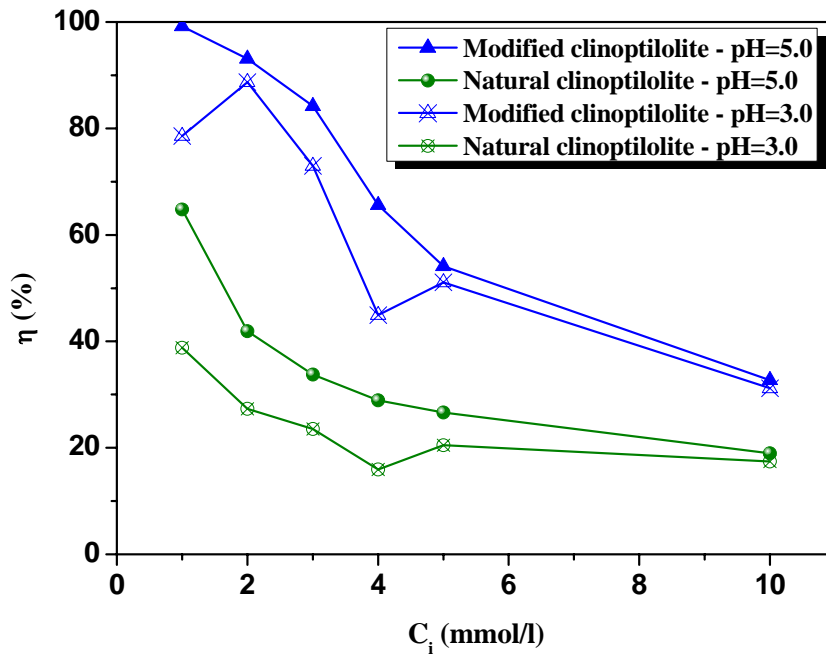
Figure 35: Removal efficiency of Zn^{2+} ions by natural and modified clinoptilolite as a function of initial concentration.

1 g of modified clinoptilolite sorbed 0.1223 mmol Zn^{2+} at pH 5.0 and 0.104 mmol at pH 3.0. By contrast the natural one managed to take up 0.0673 mmol Zn^{2+} and 0.0489 mmol respectively. This means that the modified clinoptilolite has reached up to 100% higher effective sorption capacity than the natural one. This capacity represents only 11% of the theoretical ion exchange capacity regarding the modified material and 6% regarding the natural at pH 5.0.

The sorption of ions in aquatic systems by inorganic porous materials depends on the origin of the material and its surface heterogeneity in addition to the treatment conditions. All natural zeolites such as clinoptilolite have heterogeneous surfaces. Isomorphic substitutions, broken bonds generated during the grinding process and lattice imperfections all affect the sorption properties of the adsorbent in addition to the effects on porous structure and surface irregularities. The adsorption phenomena for such systems are complex, thus the Langmuir and Freundlich models are not able to explain the equilibrium relations (Balci et al., 2004; Peric et al., 2004; Altin et al., 1997; Kinniburgh et al., 1986). On the contrary, isotherm models which take into consideration surface irregularities (heterogeneity factor β) seem to have an advantage over Langmuir and Freundlich models in explaining the equilibrium relations (Peric et al., 2004; Altin et al., 1998).

The equilibrium experimental results of Zn^{2+} ions uptake by natural and modified clinoptilolite at pH 5.0 have been fitted by non-linear equations of the adsorption models presented in Table 6. The adjustable parameters, K and β of each isotherm were estimated by non linear least squares regression analysis (NLLS) using the experimental results of the amount of zinc ion sorbed per gram of clinoptilolite (mmol/g) versus its equilibrium concentration in the solution (mmol/l). The maximum ion exchange capacity, parameter M, was based on the experimental results and it was found to be 0.1223 mmol/g for the modified clinoptilolite and 0.0673 mmol/g for the natural clinoptilolite, at pH 5.0.

Table 6. Adsorption isotherm equations

Isotherm	Equation	Adjustable model parameters	Reference
L	$n=KC_eM/(1+KC_e)$	K,M	Kinniburgh et al., (1983)
L-F	$n=(KC_e)^\beta M/(1+(KC_e)^\beta)$	K,M,β	Nederlof et al., (1990)
T	$n=KC_eM/(1+(KC_e)^\beta)^{1/\beta}$	K,M,β	Stumm et al., (1970)
R-P	$n=KC_eM/(1+(KC_e)^\beta)$	K,M,β	Yong et al., (1992)
D-R	$\log n=-\beta(\log^2(KC_e))+\log M$	K,M,β	Iwata et al., (1995)

Note: L=Langmuir; L-F= Langmuir-Freundlich; T=Toth; R-P=Redlich-Petersen; D-R= Dubinin-Radushkevich;
n=ions sorbed per gram of clinoptilolite (mmol/g); C_e=equilibrium ion solution concentration (mmo/l);
M=maximum amounts of ions sorbed per gram of clinoptilolite (mmol/g); β=degree of heterogeneity ($0<\beta<1$);
K=surface adsorption equilibrium constant (l/mmol).

The adjustable parameters found from the NLLS regression analysis, with the correlation coefficient used as an indicator of fitting of the experimental data to the models proposed, are listed in Table 7. In Tables 8 and 9 are presented the results of the analysis of variance (ANOVA) obtained from the application of the NLLS regression analysis.

Table 7. Adjustable parameters and correlation coefficients

	Modified clinoptilolite				Natural clinoptilolite			
				Zn^{2+}				
Isotherm	K	β	M	r	K	β	M	r
L	9.671	-	0.1223	0.904	0.801	-	0.0673	0.927
L-F	18.416	0.555	0.1223	0.982	0.765	1.098	0.0673	0.929
T	141.524	0.482	0.1223	0.976	0.450	1.532	0.0673	0.936
R-P	10.732	1.012	0.1223	0.910	0.679	0.879	0.0673	0.963
D-R	0.053	0.049	0.1223	0.992	0.053	0.230	0.0673	0.954

Note: L= Langmuir; L-F=Langmuir-Freundlich; T=Toth; R-P=Redlich-Petersen; D-R=Dubinin-Radushkevich.

Table 8. Analysis of variance for all models applied for the sorption of Zn^{2+} ions on modified clinoptilolite at pH 5.0 (ANOVA)

Isotherm Models	Source	Degrees of freedom	Sum of squares	Mean square	F statistic
			Modified clinoptilolite		
L	Regression	1	0.0523751	0.0523751	
	Residual error	5	0.000922859	0.000184572	
	Uncorrected total	6	0.053298		283.7651
	Corrected total	5	0.00505729		
L-F	Regression	2	0.0531212	0.0265606	
	Residual error	4	0.000176748	0.0000441869	
	Uncorrected total	6	0.053298		601.0967
	Corrected total	5	0.00505729		
T	Regression	2	0.053067	0.0265335	
	Residual error	4	0.000230961	0.0000577402	
	Uncorrected total	6	0.053298		459.5325
	Corrected total	5	0.00505729		
R-P	Regression	2	0.0524311	0.0262155	
	Residual error	4	0.000866886	0.000216722	
	Uncorrected total	6	0.053298		120.9637
	Corrected total	5	0.00505729		
D-R	Regression	2	0.0532209	0.0266105	
	Residual error	4	0.0000770504	0.0000192626	
	Uncorrected total	6	0.053298		1,381.4594
	Corrected total	5	0.00505729		

Note: L=Langmuir; L-F=Langmuir-Freundlich; T=Toth; R-P=Redlich-Petersen; D-R=Dubinin-Radushkevich.

Table 9. Analysis of variance for all models applied for the sorption of Zn^{2+} ions on natural clinoptilolite at pH 5.0 (ANOVA)

Isotherm Models	Source	Degrees of freedom	Sum of squares	Mean square	F statistic
			Natural clinoptilolite		
L	Regression	1	0.0118655	0.0118655	
	Residual error	5	0.00021722	0.0000434441	
	Uncorrected total	6	0.0120827		273.1211
	Corrected total	5	0.00154069		
L-F	Regression	2	0.0118709	0.00593546	
	Residual error	4	0.000211815	0.0000529539	
	Uncorrected total	6	0.0120827		112.0873
	Corrected total	5	0.00154069		
T	Regression	2	0.0118934	0.00594671	
	Residual error	4	0.000189308	0.0000473269	
	Uncorrected total	6	0.0120827		125.6518
	Corrected total	5	0.00154069		
R-P	Regression	2	0.011971	0.00598552	
	Residual error	4	0.000111694	0.0000279235	
	Uncorrected total	6	0.0120827		214.3542
	Corrected total	5	0.00154069		
D-R	Regression	2	0.0119447	0.00597235	
	Residual error	4	0.000138034	0.0000345084	
	Uncorrected total	6	0.0120827		173.0695
	Corrected total	5	0.00154069		

Note: L=Langmuir; L-F=Langmuir-Freundlich; T=Toth; R-P=Redlich-Petersen; D-R=Dubinin-Radushkevich.

The plots in Figures 36 and 37 graphically show the fitting of the experimental results to the curves of the adsorption models applied. With respect to the coefficient of correlation, the Redlich-Petersen and the Dubinin-Radushkevich isotherms described the sorption of Zn^{2+} ions on natural clinoptilolite better than the other models. The most commonly used isotherm Langmuir showed an inadequate fit to the experimental data giving a value of the coefficient of determination of 0.86. The Langmuir-Freundlich and the Toth isotherms failed to explain the experimental data by giving a surface heterogeneity factor β almost equal to 1.0 and 1.5 respectively. Dubinin-Radushkevich and Redlich-Petersen fitted the data giving surface heterogeneity factors lower than one, since the adsorption mechanism could be explained with the presence of less available active sites in comparison with the ideal isotherm (Langmuir model).

Regarding the fitting of the isotherm models to the experimental data for the modified clinoptilolite it was evident that the isotherms in which the surface heterogeneity (factor β) was taken into account explained the data better than the Langmuir isotherm. The R-P
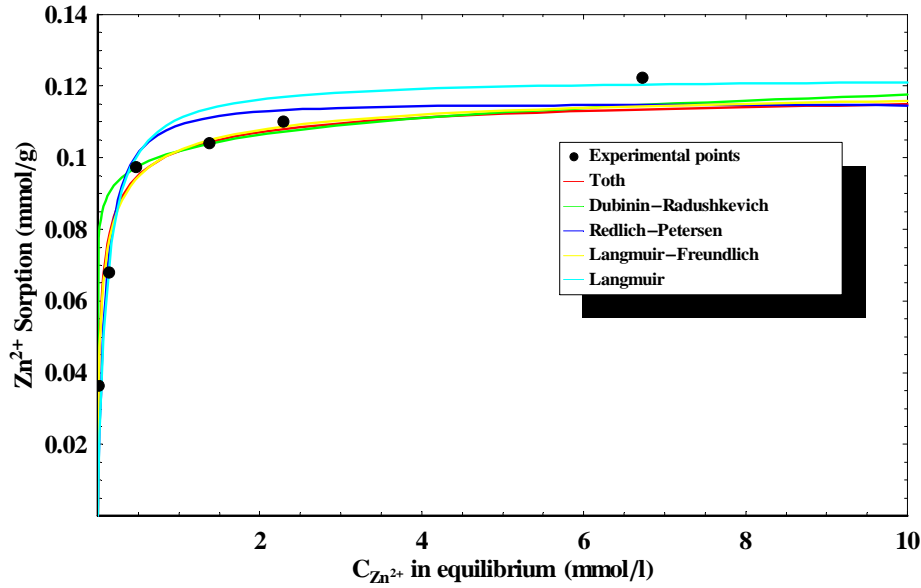
Figure 36: Comparison of adsorption isotherms for the sorption of Zn^{2+} ions on modified clinoptilolite at pH 5.0.
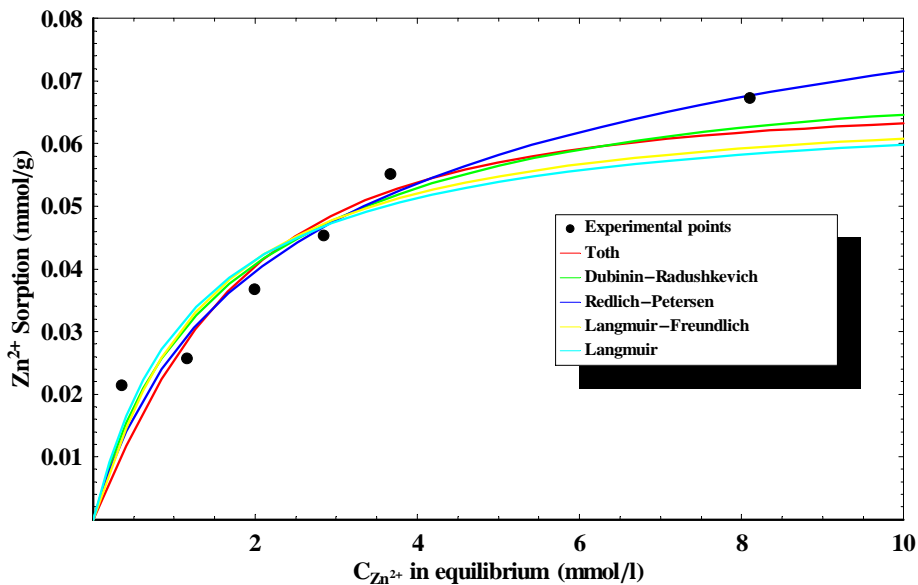
Figure 37: Comparison of adsorption isotherms for the sorption of Zn^{2+} ions on natural clinoptilolite at pH 5.0.

model failed to explain the experimental data by giving a heterogeneity factor β equal to 1.0. As expected, with respect to the correlation coefficient, the Dubinin-Radushkevich model described the sorption of Zn^{2+} ions on modified clinoptilolite better than the other models (see Table 7). D-R isotherm fitted the data giving a surface heterogeneity factor lower than the

other models. The equilibrium constant value was also lower than the ones estimated from the other models.

In Figures 38 and 39 are presented the ion exchange kinetic curves of zinc uptake by natural and modified clinoptilolite at pH 5.0 and 3.0 for 1 and 5 mM Zn^{2+} solution. At a pH value of
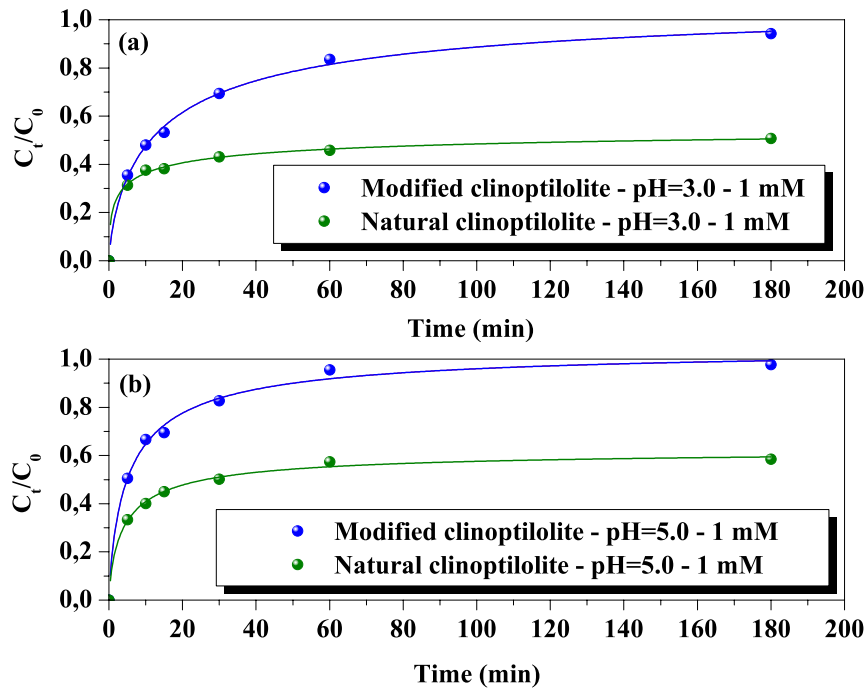
Figure 38: Ion exchange kinetic of zinc uptake by natural and modified clinoptilolite at pH 5.0 and 3.0 for 1 mM zinc solution.

5.0 the modified clinoptilolite was able to sorb zinc in concentrations of 1mM up to 50 % and in that of 5 mM up to 16 % in the very first 5 minutes. At pH 3.0 the material was able to remove within the first 5 minutes up to 35 % and 17 % respectively. On the contrary the natural clinoptilolite at a pH value of 5.0 sorbed zinc in concentrations of 1mM up to 33 % and in that of 5 mM up to 12 % in the first five minutes. At pH 3.0 it was able to remove up to 32 % and 11 % respectively. Through the chemical conditioning of the clinoptilolite it was found that the fine fraction, dust produced during the grinding process, made up about 8 % (w/w) of the clinoptilolite. The clinoptilolite surface and the pore openings were partially covered by this dust resulting in pore clogging which led to smaller ion exchange capacity and slower ion exchange rates. Pore clogging by fine particles has also been reported as the

possible cause of smaller ion exchange capacity and slower ion exchange rates of clinoptilolite (Athanasiadis et al., 2005; Inglezakis et al., 1999; Carland et al., 1995).
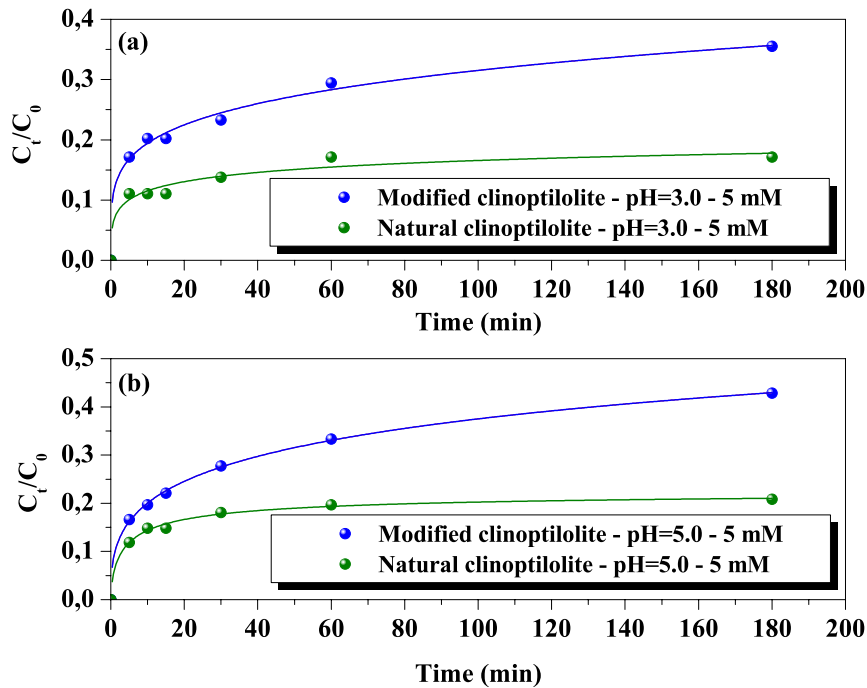
Figure 39: Ion exchange kinetic of zinc uptake by natural and modified clinoptilolite at pH (a) 3.0 and (b) 5.0, for 5 mM zinc solution.

According *Inglezakis et al.,* (1999) the pore clogging can affect the ion exchange capacity by up to 15 %, regarding Pb^{2+}. Pore clogging alone is not able to explain the effective performance of the modified clinoptilolite compared to the natural. Other factors such as zeta potential, pH of the metal solution, metal ion concentration, particle size of the ion exchanger, heat of the solution and cation type are able to modify the ion exchange behaviour of clinoptilolite (Harland et al., 1994; Breck et al., 1974).

The sorption rate of the modified clinoptilolite at pH 5.0 and 1mM Zn^{2+} solution was up to 15 % faster in the first five minutes of the ion exchange process compared to the rate of the natural clinoptilolite under the same conditions. Although it would be expected that the rate of zinc uptake of the modified clinoptilolite would be decreased or remained stable (Zn^{2+} ions concentration in the solution was half of the initial; easily approached ion exchangeable sites were already occupied) after the first five minutes compared to the rate of the natural one, it was observed that it increased up to 25 %. The pH of both clinoptilolite solutions after the

first five minutes had almost reached the value of 6.0 (Fig. 40(b)). It is obvious that at this pH the difference in the surface charge between the modified and natural clinoptilolite (Fig. 34) was the reason for the increased sorption rate of the modified clinoptilolite. Also by making the same comparison at pH 3.0 and 1 mM zinc solution it was demonstrated that the surface charge was responsible for the ion exchange rates achieved in both forms of clinoptilolite.
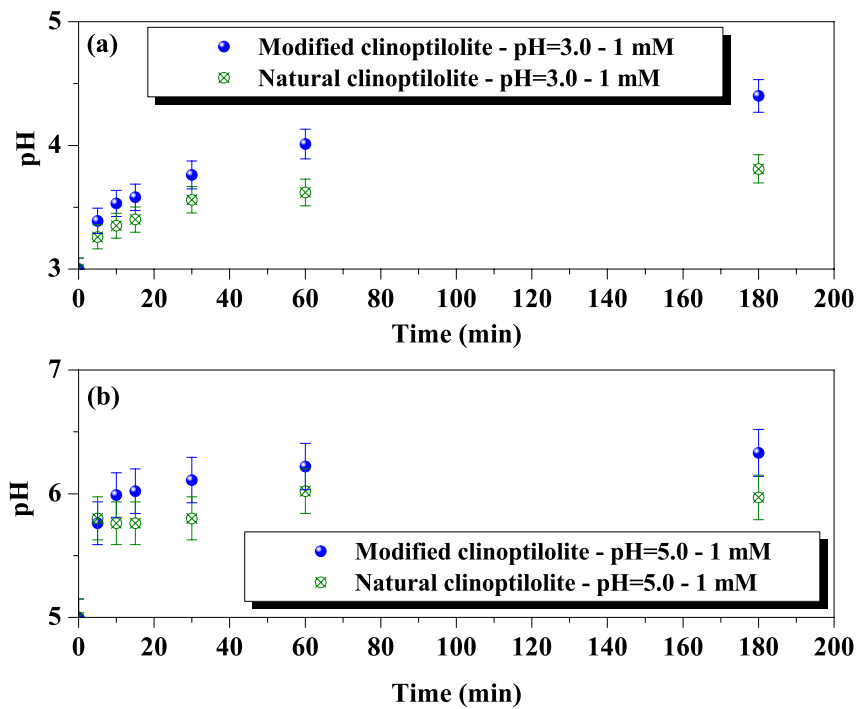
Figure 40: pH profiles during the ion exchange kinetic experiments of zinc uptake by natural and modified clinoptilolite at (a) pH 3.0 and (b) pH 5.0, for 1 mM zinc solution.

6.1.2.2 Selectivity determination of the modified clinoptilolite

In Table 10 are presented the recorded pH values of the equilibrium experiments conducted between the modified clinoptilolite and different concentrations of metal solutions. The maximum recorded pH values were 6.8 for Zn^{2+}, 5.8 for Cu^{2+} and 6.9 for Pb^{2+}. These maximum values are lower than the starting pH for precipitation of hydroxides, corresponding to the initial metal concentrations used.

Table 10. Recorded pH values during the equilibrium experiments of Zn^{2+}, Cu^{2+} and Pb^{2+} on the modified clinoptilolite

Initial metal concentration (mM)	Zn^{2+}			Cu^{2+}			Pb^{2+}		
	Initial pH	T (^{0}C)	Final pH	Initial pH	T (^{0}C)	Final pH	Initial pH	T (^{0}C)	Final pH
1	5.0	24.3	6.8	5.0	22.1	5.8	5.0	22.6	6.9
2	5.0	24.0	6.5	5.0	22.3	5.4	5.0	22.9	6.6
3	5.0	24.1	6.5	5.0	22.8	5.4	5.0	23.2	6.1
4	4.9	23.9	5.9	5.0	22.5	5.3	5.0	23.0	5.6
5	5.0	24.5	6.1	5.0	22.6	5.3	5.0	23.0	5.4
10	5.0	24.4	6.4	5.0	23.1	5.1	5.0	23.2	5.00

The equilibrium isotherms for the metals studied are presented in Figure 41, where X is the reduced concentration of metal in the solution, in respect to initial metal concentration, and Y the relative equilibrium metal concentration in the solid phase with respect to the theoretical cation exchange capacity (CEC_{Na}). Since the homoionic Na-clinoptilolite was prepared through the chemical conditioning process described in the section on material and methods, it seems reasonable to assume that potassium, calcium and magnesium present in modified clinoptilolite were in inaccessible ion exchange sites and did not participate in the ion exchange process. No significant amount of these cations was observed in the metal solution after equilibrium, demonstrating that the systems investigated maybe considered bicationic. In this case, the theoretical cation exchange capacity was calculated from the chemical composition of the modified clinoptilolite presented in table 5, considering that the only exchangeable cation is the Na^+. The calculated CEC_{Na} of the modified clinoptilolite was 0.53 meq/g.

It can be seen that equilibrium is strongly favourable to Pb^{2+} and less favourable to Zn^{2+} and Cu^{2+}. According to the equilibrium isotherms, the selectivity series was $Pb^{2+}>Zn^{2+}>Cu^{2+}$. The maximal exchange levels attained were as follows: $Pb^{2+} \rightarrow 77$ %; $Zn^{2+} \rightarrow 46$ %; $Cu^{2+} \rightarrow 34$ %. The lead exchange isotherm lies above the diagonal over the whole composition range, thereby indicating the high affinity of modified clinoptilolite towards lead. By contrast, the zinc and copper isotherms are above the diagonal only for low concentrations. This means that the affinity of modified clinoptilolite for zinc and copper depends strongly on the metal concentration (Helfferich, 1995; Barrer et al., 1974;). *Langella et al.*, (2000) determined the selectivity of the Na-modified Sardinian clinoptilolite, regarding maximal exchange levels, as $NH_4^+> Pb^{2+} > Cu^{2+} > Zn^{2+} > Cd^{2+}$. *Top et al.*, (2004) obtained the following selectivity sequence $Ag^+ > Na^+ > Zn^{2+} > Cu^{2+}$ for the Na-modified clinoptilolite of Gördes. *Loizidou et*

al., (1989) proposed the following selectivity series for Na-clinoptilolite: $Pb^{2+} > Cu^{2+} > Fe^{3+} > Cr^{3+}$.
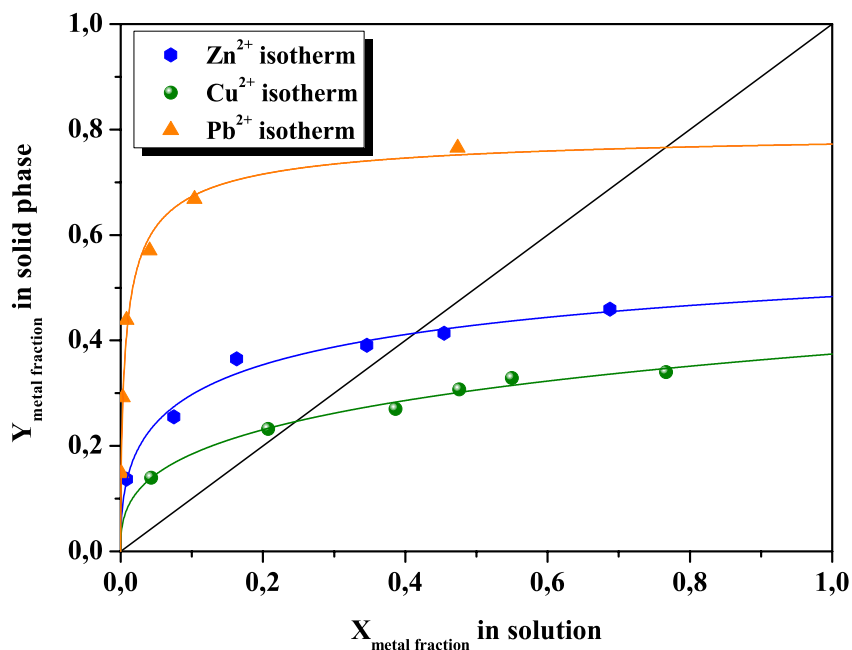
Figure 41: Equilibrium isotherms for Pb^{2+}, Cu^{2+} and Zn^{2+} on modified clinoptilolite at pH 5.0.

In Figure 42 are presented the ion exchange kinetic measurements of zinc, copper and lead uptake on the modified clinoptilolite at pH 5.0 for 1 mM and 5 mM zinc, copper and lead solutions, respectively.

It is evident that the kinetic experiments deduced the same selectivity series with the equilibrium experiments regarding zinc, copper and lead. Differences between selectivity series deduced by kinetic and equilibrium experiments on clinoptilolite have been reported between Zn^{2+} and Cd^{2+} and between $C_2H_5NH_3^+$ and $(CH_3)_2NH_2^+$ (Blanchard et al., 1984; Barrer et al., 1967).

In Figure 43 is presented the copper, zinc and lead mixture uptake on the modified clinoptilolite vs. time, at pH 5.0 with metal concentrations of 1 mM. It can be seen that the selectivity series regarding copper, zinc and lead, follows not the same order obtained through the equilibrium and the single ion exchange kinetic experiments: $Pb^{2+} > Cu^{2+} > Zn^{2+}$.
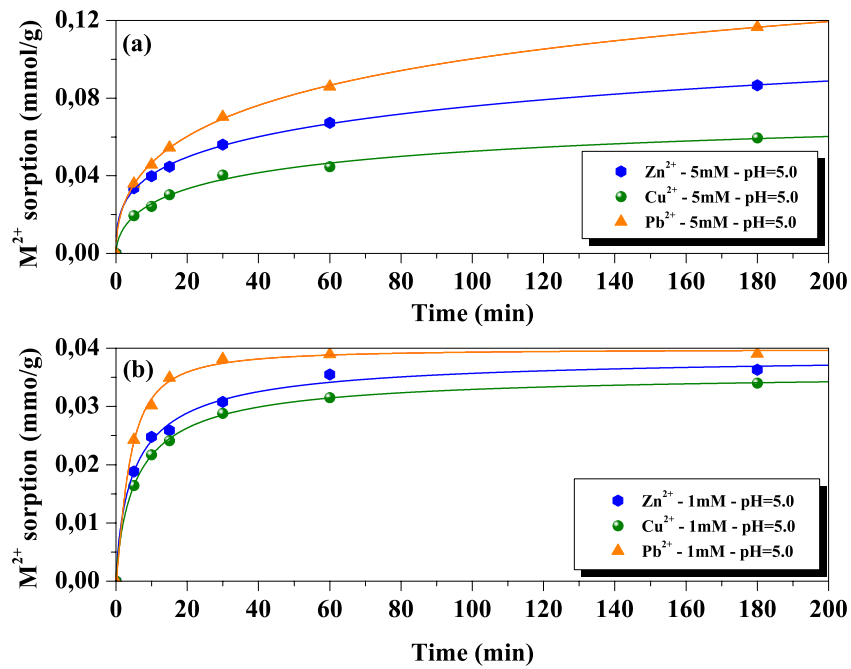
Figure 42: Ion exchange kinetics of Zn^{2+}, Cu^{2+} and Pb^{2+} uptake on modified clinoptilolite at (a) pH 5.0 for 5 mM, and (b) pH 5.0 for 1 mM ion metal solution, respectively.
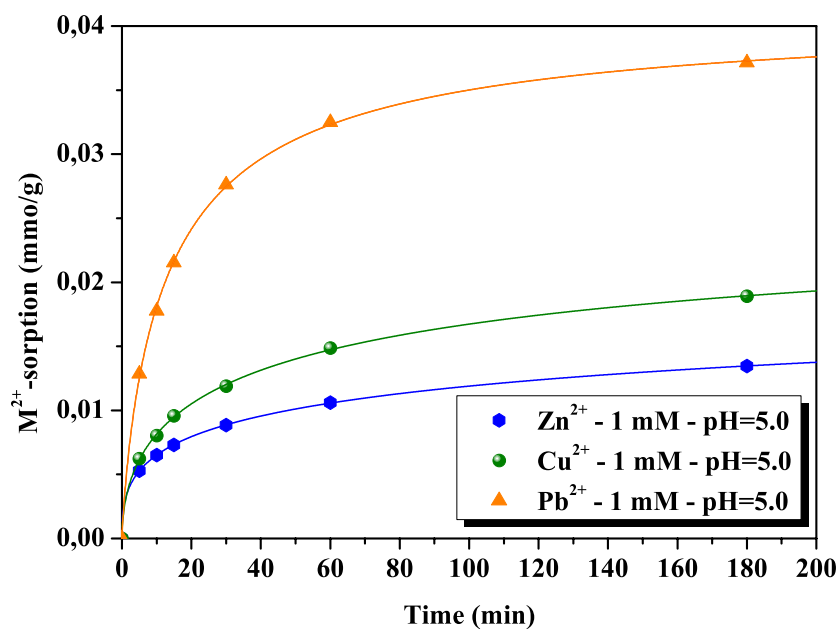
Figure 43: Evolution of total metal uptake for zinc, copper and lead component solution on modified clinoptilolite at pH 5.0 and 1 mM metal concentrations.

The selectivity order and the dependence of the total metal uptake of the modified clinoptilolite on the components of the solution are the result of physicochemical and stereo chemical factors such as stokes radii, the hydration enthalpy of cations and the dimensions of the pores of clinoptilolite (Ouki et al., 1997; Helfferich, 1995). In Table 11 are presented stokes radii (hydration radii) and hydration energies of the interesting metals in pure water at 298^0 K. The concept of the hydration radii, could explain the high selectivity for lead (2.59 Å) and silver (1.49 Å) compared to the lower selectivity for copper (3.44 Å), zinc (3.49 Å) and chromium (4.12 Å). It can be seen that the values obtained are not system specific, thus selectivity ratios can be predicted.

Table 11: Stocks radii and hydration energies of metals in pure water at 298^0 K (Lide 1999)

Metal	Stokes radii (Å)	Hydration energy (kJ/mol)
K^+	1.25	-321
H^+	0.26	-1091
Ag^+	1.49	-475
Na^+	1.84	-405
Cu^{2+}	3.44	-2100
Zn^{2+}	3.49	-2044
Pb^{2+}	2.59	-1480
Cr^{3+}	4.12	-4402
Fe^{3+}	4.06	-4376

6.1.2.3 Analysis of equilibrium data on modified clinoptilolite – a comparison of adsorption isotherms

The plots in Figure 44 show the uptake degrees, obtained after 24 hours equilibrium, on modified clinoptilolite of zinc, copper and lead ions as a function of the initial concentration. 1 g of modified clinoptilolite sorbed 0.1223 mmol Zn^{2+}, 0.090 mmol Cu^{2+} and 0.2038 mmol Pb^{2+} at pH 5.0, respectively. This capacity represents 77 % of the theoretical ion exchange capacity (CEC_{Na}), regarding lead, 46 %, regarding zinc, and 34 % regarding copper.

The equilibrium experimental results of Zn^{2+}, Cu^{2+} and Pb^{2+} ions uptake by modified clinoptilolite at pH 5.0 have been fitted by non-linear equations of the adsorption models presented in Table 6. The adjustable parameters, K and β of each isotherm were estimated by non linear least squares regression analysis (NLLS) using the experimental results of the amount of zinc ion sorbed per gram of clinoptilolite (mmol/g) versus its equilibrium

concentration in the solution (mmol/l). The maximum ion exchange capacity, parameter M, was based on the experimental results, and it was found to be 0.1223 mmol/g for zinc, 0.090 mmol/g for copper and 0.2038 mmol/g for lead at pH 5.0, respectively.
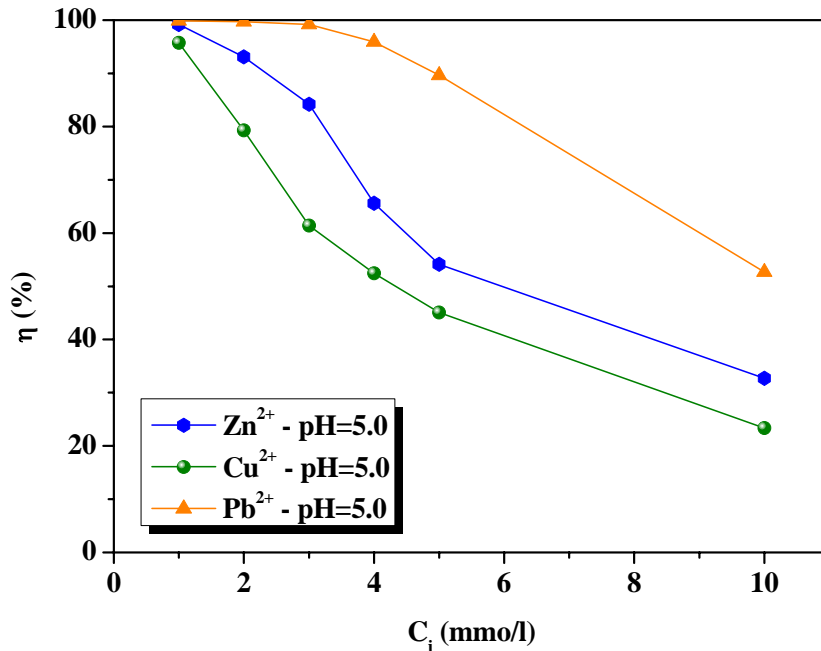
Figure 44: Removal efficiency of Zn^{2+}, Cu^{2+} and Pb^{2+} ions by modified clinoptilolite as a function of initial concentration at pH 5.0.

The adjustable parameters found from the NLLS regression analysis, with the correlation coefficient used as an indicator of the fit of the experimental data to the models proposed, are listed in Table 12. In Table 8, 13 and 14 are presented the results of the analysis of variance (ANOVA) obtained from the application of the NLLS regression analysis.

Table 12. Adjustable parameters and correlation coefficients

	Modified clinoptilolite								
Isotherm	Zn^{2+}			Cu^{2+}			Pb^{2+}		
	K	β	r	K	β	r	K	β	r
L	9.671	-	0.904	8.982	-	0.904	68.951		0.925
L-F	18.416	0.555	0.982	11.821	0.653	0.974	67.614	0.529	0.996
T	141.524	0.482	0.976	36.144	0.605	0.970	667.233	0.454	0.995
R-P	10.732	1.012	0.910	10.768	1.012	0.913	75.705	1.016	0.937
D-R	0.053	0.049	0.992	0.069	0.062	0.990	0.152	0.045	0.998

Note: L= Langmuir; L-F=Langmuir-Freundlich; T=Toth; R-P=Redlich-Petersen; D-R=Dubinin-Radushkevich.

Table 13. Analysis of variance for all models applied for the sorption of Cu^{2+} ions on modified clinoptilolite at pH 5.0 (ANOVA)

Isotherm Models	Source	Degrees of freedom	Sum of squares	Mean square	F statistic
			Modified clinoptilolite		
L	Regression	1	0.0325607	0.0325607	
	Residual error	5	0.000364934	0.0000729868	
	Uncorrected total	6	0.0329256		446.1176
	Corrected total	5	0.001987		
L-F	Regression	2	0.0328217	0.0164109	
	Residual error	4	0.000103906	0.0000259765	
	Uncorrected total	6	0.0329256		631.7595
	Corrected total	5	0.001987		
T	Regression	2	0.0328098	0.0164049	
	Residual error	4	0.000115798	0.0000289495	
	Uncorrected total	6	0.0329256		566.6730
	Corrected total	5	0.001987		
R-P	Regression	2	0.0325949	0.0162975	
	Residual error	4	0.000330675	0.0000826687	
	Uncorrected total	6	0.0329256		197.1423
	Corrected total	5	0.001987		
D-R	Regression	2	0.0328871	0.0164435	
	Residual error	4	0.0000385257	0.00000963143	
	Uncorrected total	6	0.0329256		1,707.275
	Corrected total	5	0.001987		

Note: L= Langmuir; L-F=Langmuir-Freundlich; T=Toth; R-P=Redlich-Petersen; D-R=Dubinin-Radushkevich.

The plots in Figures 36, 45 and 46 graphically show the fitting of the experimental data to the curves of the adsorption models applied. The sorption behaviour of Zn^{2+}, Cu^{2+} and Pb^{2+} on modified clinoptilolite is similar except at the value of their ion exchange capacities. With respect to the coefficient of correlation, the Dubinin-Radushkevich isotherm described the sorption of Zn^{2+}, Cu^{2+} and Pb^{2+} better than the other models. The most commonly used isotherm, Langmuir, showed an inadequate fit to the experimental data giving a value of the coefficient of determination of 0.82 for Zn^{2+}, 0,82 for Cu^{2+} and 0.86 for Pb^{2+}, respectively. The Redlich-Petersen model failed to explain the experimental data by giving a value of the surface heterogeneity factor β almost equal to 1.0 (see Table 12). Thus, simplified models that assume that the site affinity is equally distributed on the clinoptilolite surface do not show a good fit across the whole concentration range. The reason why the Dubinin-Radushkevich model fitted the data better than all the other models is that it assumes that metal ions bind first with the energetically most favourable sites, after which multi-layer adsorption occurs.

Table 14. Analysis of variance for all models applied for the sorption of Pb^{2+} ions on modified clinoptilolite at pH 5.0 (ANOVA)

Isotherm Models	Source	Degrees of freedom	Sum of squares	Mean square	F statistic
		Modified clinoptilolite			
L	Regression	1	0.114683	0.114683	
	Residual error	5	0.00278992	0.000557985	205.531
	Uncorrected total	6	0.117473		
	Corrected total	5	0.0193221		
L-F	Regression	2	0.117329	0.0586646	
	Residual error	4	0.000143345	0.0000358363	1,637.016
	Uncorrected total	6	0.117473		
	Corrected total	5	0.0193221		
T	Regression	2	0.117271	0.0586355	
	Residual error	4	0.000201545	0.0000503862	1,163.721
	Uncorrected total	6	0.117473		
	Corrected total	5	0.0193221		
R-P	Regression	2	0.115126	0.0575628	
	Residual error	4	0.00234704	0.000586761	98.103
	Uncorrected total	6	0.117473		
	Corrected total	5	0.0193221		
D-R	Regression	2	0.117378	0.058689	
	Residual error	4	0.0000944832	0.0000236208	2,484.632
	Uncorrected total	6	0.117473		
	Corrected total	5	0.0193221		

Note: L= Langmuir; L-F=Langmuir-Freundlich; T=Toth; R-P=Redlich-Petersen; D-R=Dubinin-Radushkevich.
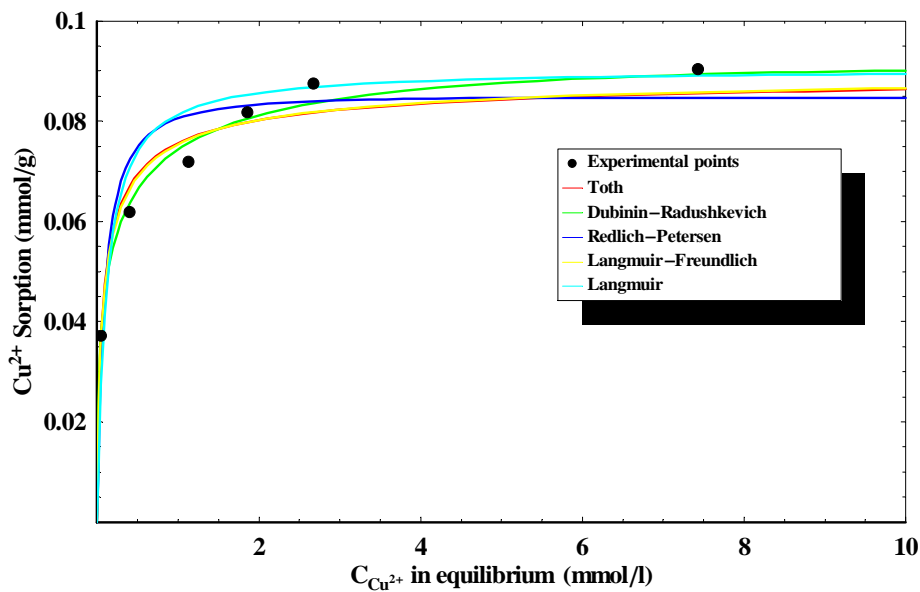
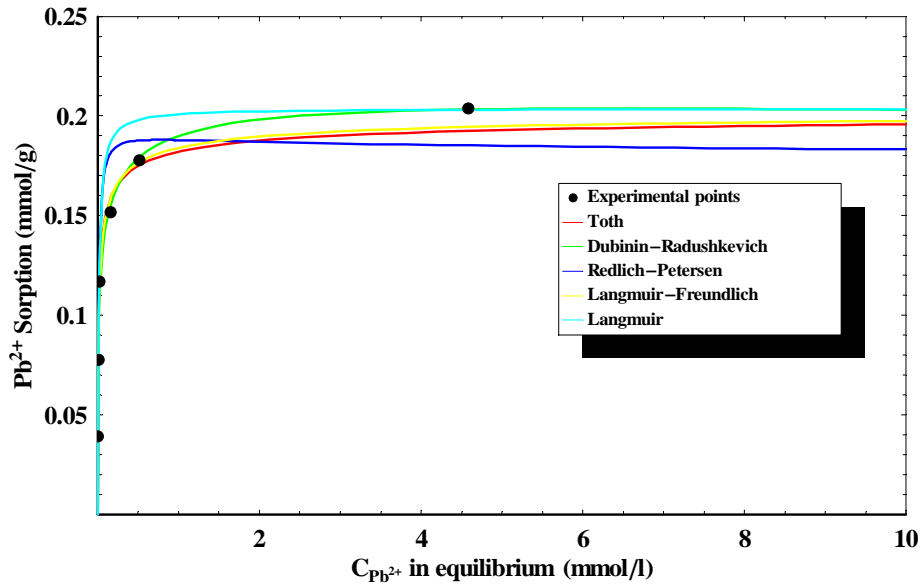**Figure 45:** Comparison of adsorption isotherms for the sorption of Cu^{2+} ions on modified clinoptilolite at pH 5.0.

Figure 46: Comparison of adsorption isotherms for the sorption of Pb^{2+} ions on modified clinoptilolite at pH 5.0.

6.1.2.4 Effect of the pH of the metal solution on the ion exchange kinetic of Zn^{2+}, Cu^{2+} and Pb^{2+} on modified clinoptilolite

In Tables 15 and 16 are presented the recorded pH values of the kinetic experiments conducted between the modified clinoptilolite and 1 mM Zn^{2+}, Cu^{2+} and Pb^{2+} solutions at pH 5.0 and 3.0, respectively.

Table 15. Recorded pH values during the kinetic experiments of Zn^{2+}, Cu^{2+} and Pb^{2+} on the modified clinoptilolite at pH 5.0 and 1 mM metal solution

Time (min)	Zn^{2+}			Cu^{2+}			Pb^{2+}		
	Initial pH	T (^{0}C)	Final pH	Initial pH	T (^{0}C)	Final pH	Initial pH	T (^{0}C)	Final pH
5	5.0	22.4	5.8	5.0	23.3	5.6	5.0	22.5	5.5
10	5.0	22.4	6.0	5.0	23.3	5.7	5.0	22.5	5.6
15	5.0	22.4	6.0	5.0	23.3	5.7	5.0	22.5	5.7
30	5.0	22.4	6.1	5.0	23.3	5.7	5.0	22.5	5.8
60	5.0	22.4	6.2	5.0	23.3	5.8	5.0	22.5	6.0
180	5.0	22.4	6.3	5.0	23.3	5.9	5.0	22.5	6.5

Table 16. Recorded pH values during the kinetic experiments of Zn^{2+}, Cu^{2+} and Pb^{2+} on the modified clinoptilolite at pH 3.0 and 1 mM metal solution

Time (min)	Zn^{2+}			Cu^{2+}			Pb^{2+}		
	Initial pH	T (^{0}C)	Final pH	Initial pH	T (^{0}C)	Final pH	Initial pH	T (^{0}C)	Final pH
5	3.0	23.4	3.4	3.0	23.6	3.2	3.0	22.0	3.3
10	3.0	23.4	3.5	3.0	23.6	3.3	3.0	22.0	3.4
15	3.0	23.4	3.6	3.0	23.6	3.4	3.0	22.0	3.4
30	3.0	23.4	3.8	3.0	23.6	3.5	3.0	22.0	3.5
60	3.0	23.4	4.0	3.0	23.6	3.6	3.0	22.0	3.6
180	3.0	23.4	4.4	3.0	23.6	3.8	3.0	22.0	4.0

The maximum recorded pH values were 6.3 for Zn^{2+}, 5.9 for Cu^{2+} and 6.5 for Pb^{2+}. These maximum values are lower than the starting pH for precipitation of hydroxides, corresponding to the initial metal concentrations used.

In Figure 47 is presented the percentage decrease of metal uptake between pH 5.0 and 3.0 for the modified clinoptilolite at 1 mM initial metal concentration. It can be seen that the acidity
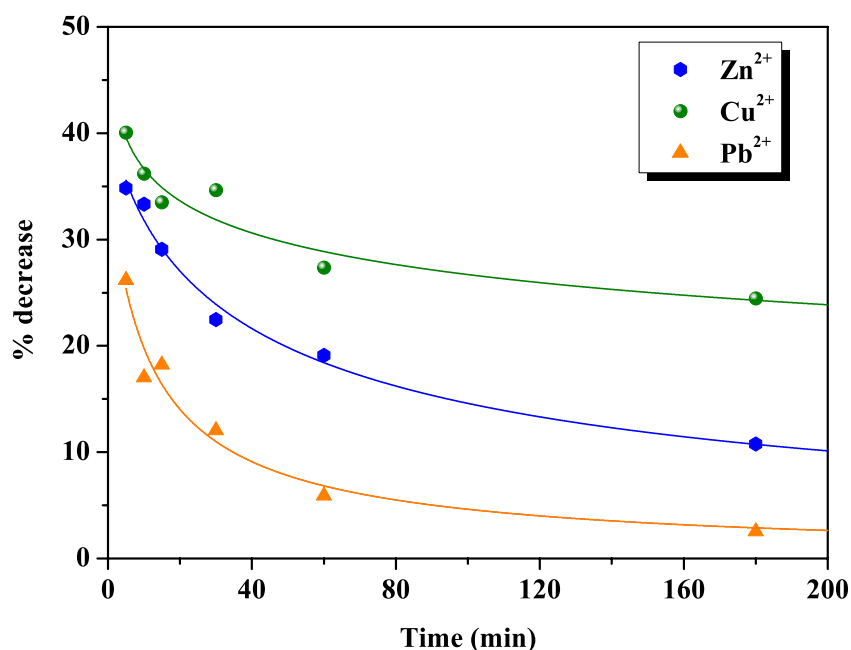
Figure 47: Percentage decrease of metal uptake between pH 5.0 and 3.0 for modified clinoptilolite at1 mM initial metal concentration.

influenced the uptake rates of heavy metals by modified clinoptilolite, especially at the beginning of the ion exchange process. The metal uptake rate of the modified clinoptilolite was reduced by up to 25 %, regarding Pb^{2+}, up to 35 % regarding Zn^{2+} and up to 40 % regarding Cu^{2+} in the first five minutes of the ion exchange process. After one hour of the ion exchange process, the metal uptake rate of modified clinoptilolite decreased by up to almost 5 % for lead, almost 20 % for zinc and up to 30 % for copper. It is obvious that H^+ cations have to be considered as competitive ions in the ion exchange process and therefore the ion exchange of metals on the modified clinoptilolite is favoured by high acidity, which, however has to be lower than the minimum acidity of precipitation for each metal (Ouki et al., 1999; Feng et al., 2000; Panayotova et al., 2001).

pH has a significant impact on the metal uptake by clinoptilolite since it can influence the speciation of the exchanged ions and the character of the clinoptilolite itsself. The extent of the complex cation formation varies with the pH, the cationic concentration and the metal of concern. This means that the exact speciation of the metal (concept of the hydration radius) has a significant impact on the selectivity and on the ion exchange removal efficiency of the clinoptilolite, as was described in chapter 5.1.2.2. The impact of the pH on the surface charge of the clinoptilolite is clearly demonstrated in Figure 34. The surface charge of the modified clinoptilolite was responsible for the higher ion exchange rates achieved, during the ion exchange process (see chapter 5.1.2.1).

6.1.2.5 Adsorption kinetics modelling

The models of sorption kinetics correlate the metal uptake rate, and are therefore important in water treatment process design. The sorption mechanism of Zn^{2+}, Cu^{2+} and Pb^{2+} on the modified clinoptilolite was investigated using the following sorption models:

a. *First-order reversible reaction model*

The sorption of Zn^{2+}, Cu^{2+} and Pb^{2+} on the modified clinoptilolite may be considered as a reversible reaction with equilibrium established between two phases (Arun et al., 1984; Bektas et al., 2004; Hamadi et al., 2001). A simple first-order model was used to correlate the rates of reaction which can be expressed as

$$A \underset{K_2}{\overset{K_1}{\rightleftarrows}} B \tag{1}$$

The reaction rate is expressed as

$$\frac{dC_B}{dt} = -\frac{dC_A}{dt} = K_1 C_A - K_2 C_B = C_{A_i} \frac{dX_A}{dt} = K_1(C_{A_i} - C_{A_i}X_A) - K_2(C_{B_i} - C_{A_i}X_A) \tag{2}$$

where C_B (mmol/g) is the concentration of the metal ion on the modified clinoptilolite and C_A (mmol/l) the concentration of the metal in the solution at any time, C_{B_i} and C_{A_i} the initial metal concentrations on the modified clinoptilolite and in the solution, respectively. X_A is the fractional conversion of the metal and K_1 and K_2 are the first-order rate constants. In equilibrium,

$$\frac{dC_B}{dt} = -\frac{dC_A}{dt} \tag{3}$$

and $X_{A_e} = \dfrac{K_e - (C_{B_i}/C_{A_i})}{K_e + 1} \tag{4}$

where X_{A_e} is the fractional conversion of the metal at equilibrium and K_e is the equilibrium constant defined:

$$K_e = \frac{C_{B_e}}{C_{A_e}} = \frac{C_{B_i} - C_{A_i}X_{A_e}}{C_{A_i} - C_{A_i}X_{A_e}} = \frac{K_1}{K_2} \tag{5}$$

where C_{B_e} and C_{A_e} are the equilibrium metal concentrations on the modified clinoptilolite and in the solution, respectively. The rate equation in terms of equilibrium can be obtained from the equations (2), (4) and (5)

$$\frac{dX_A}{dt} = (K_1 + K_2)(X_{A_e} - X_A) \tag{6}$$

The integration of equation (6) and the substitution for K_2 from equation (5), gives

$$-\ln(1 - \frac{X_A}{X_{A_e}}) = K_1(1 + \frac{1}{K_e})t \tag{7}$$

Equation (7) can be written in the following form:

$$\ln[1 - U(t)] = -K_r t \tag{8}$$

where K_r is the overall rate constant. Furthermore,

$$K_r = K_1(1 + \frac{1}{K_e}) = K_1 + K_2 \tag{9}$$

and

$$U(t) = \frac{C_{A_i} - C_A}{C_{A_i} - C_{A_e}} = \frac{X_A}{X_{A_e}} \tag{10}$$

where U(t) is the fractional attainment of equilibrium.

b. Pseudo-first-order model

According *Ho et al.*, (1998) and *Namasivayam et al.*, (1999) the sorption kinetics of Zn^{2+}, Cu^{2+} and Pb^{2+} on the modified clinoptilolite can also be described by a pseudo-first-order model

$$\frac{dq}{dt} = K_1(q_e - q) \tag{11}$$

where q_e is the amount of the metal adsorbed at equilibrium per unit weight of clinoptilolite (mmol/g), q the amount of metal adsorbed at any time (mmol/g) and K_1 is the adsorption constant. Equation (11) is integrated and then rearranged to obtain the following linear time dependence function:

$$\log(q_e - q) = \log(q_e) - \frac{K_1}{2.303}t \tag{12}$$

c. Pseudo-second-order model

A pseudo-second-order model was also applied to describe the sorption kinetics of Zn^{2+}, Cu^{2+} and Pb^{2+} on the modified clinoptilolite (Ho et al., 1998; Ho et al., 1999). The differential equation is

$$\frac{dq}{dt} = K_2(q_e - q)^2 \tag{13}$$

Equation (13) is integrated and then rearranged to obtain the following linear time dependence function:

$$\frac{t}{q} = \frac{1}{K_2 q_e^2} + \frac{1}{q_e}t \tag{14}$$

$$h = K_2 q_e^2 \tag{15}$$
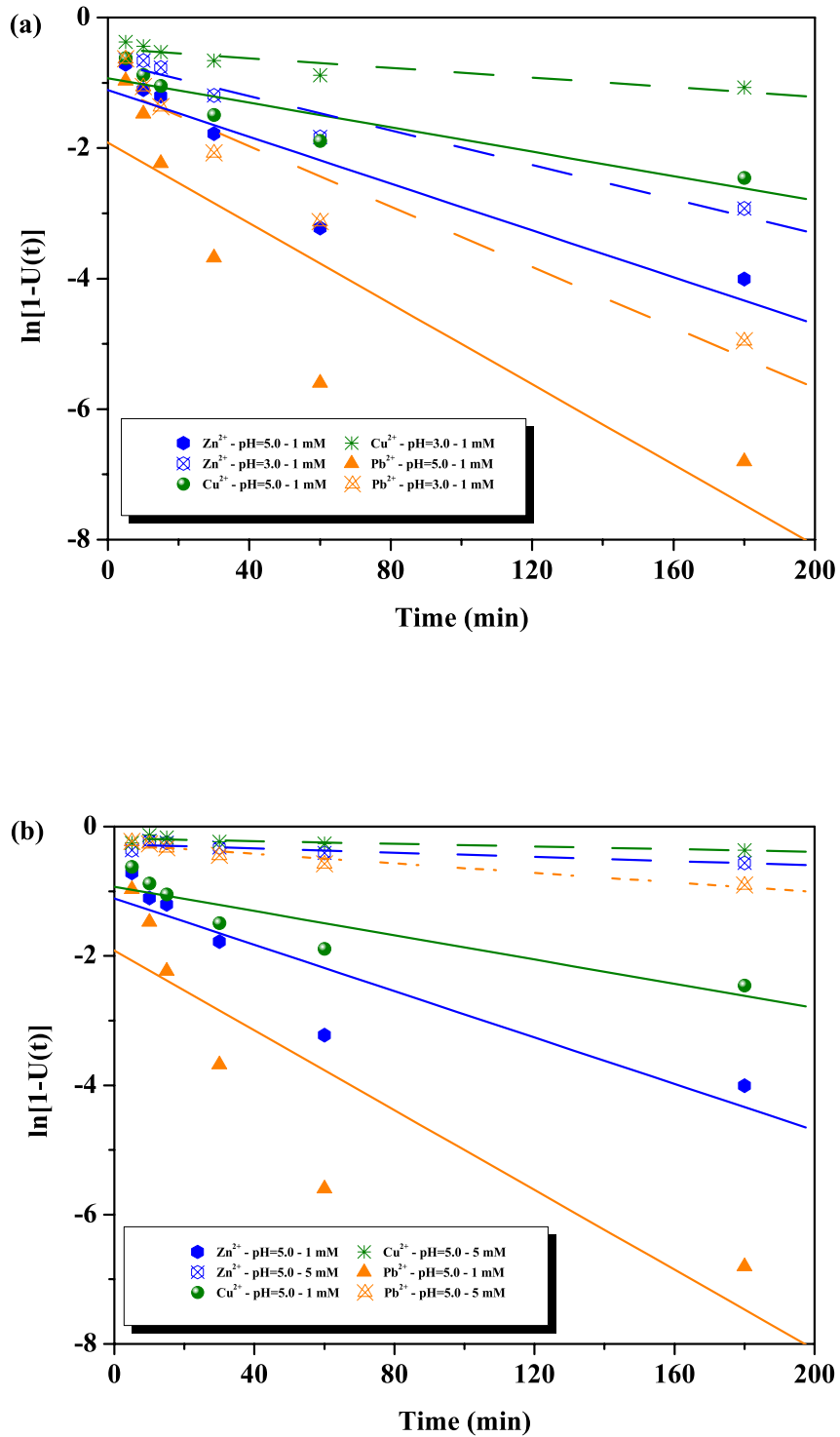
h is the initial metal sorption rate (mmol/g min).

In Figure 48 are presented the plots of the first-order reaction kinetic for the sorption of Zn^{2+}, Cu^{2+} and Pb^{2+} on the modified clinoptilolite at different experimental conditions. Constants K_1, K_2, K_r and K_e were calculated using the equations (5) and (9) and are summarised in Tables 17 and 18. The assumption that the sorption of Zn^{2+}, Cu^{2+} and Pb^{2+} on the modified clinoptilolite could be predicted for all pHs and all initial metal concentrations by the linear first-order reversible reaction model demonstrated satisfactory results. Correlation coefficients were found to be between 0.849 and 0.975 which means that there is a good agreement but not an optimum one.

Table 17. First-order reaction rate constants for the sorption of Zn^{2+}, Cu^{2+} and Pb^{2+} on the modified clinoptilolite at different pHs.

Initial metal concentration (1 mM)	pH	K_1 (min^{-1})	K_2 (min^{-1})	K_r (min^{-1})	K_e	r
Zn^{2+}	5	0.0147	0.0032	0.0179	4.55	0.909
	3	0.0020	0.0112	0.0132	0.1771	0.975
Cu^{2+}	5	0.0044	0.0049	0.0094	0.8959	0.909
	3	0.0005	0.0032	0.0037	0.1718	0.907
Pb^{2+}	5	0.0315	0.0008	0.0308	39.34	0.878
	3	0.0240	0.0006	0.0232	40.00	0.961

Table 18. First-order reaction rate constants for the sorption of Zn^{2+}, Cu^{2+} and Pb^{2+} on the modified clinoptilolite at different initial metal concentrations of pH 5.0.

Metal	Initial metal concentration (mM)	K_1 (min^{-1})	K_2 (min^{-1})	K_r (min^{-1})	K_e	r
Zn^{2+}	1	0.0147	0.0032	0.0179	4.55	0.909
	5	7.7 10^{-5}	0.0016	0.0016	0.0480	0.892
Cu^{2+}	1	0.0044	0.0049	0.0094	0.8959	0.909
	5	3.3 10^{-5}	0.0010	0.0010	0.0326	0.849
Pb^{2+}	1	0.0315	0.0008	0.0308	39.34	0.878
	5	0.0009	0.0027	0.0037	0.3461	0.972

Figure 48: First-order kinetics plots for sorption of Zn^{2+}, Cu^{2+} and Pb^{2+} on the modified clinoptilolite at (a) different pHs and (b) different initial metal concentrations.

In Figure 49 are presented the plots of the pseudo-first-order model for the sorption of Zn^{2+}, Cu^{2+} and Pb^{2+} on the modified clinoptilolite at different experimental conditions. Constant K_1 for all applied conditions has been calculated and is summarised in Tables 19 and 20. The assumption that the sorption of Zn^{2+}, Cu^{2+} and Pb^{2+} on the modified clinoptilolite could be predicted for all pHs and all initial metal concentrations by the pseudo-first-order model demonstrated satisfactory results. Correlation coefficients were found to be between 0.794 and 0.980 which means that as with the first-order reversible reaction model, there is a good agreement but not a perfect one.

Table 19. Pseudo-first-order reaction rate constant for the sorption of Zn^{2+}, Cu^{2+} and Pb^{2+} on the modified clinoptilolite at different pHs.

Initial metal concentration (1 mM)	pH	K_1 (min^{-1})	r
Zn^{2+}	5	0.0316	0.976
	3	0.0082	0.931
Cu^{2+}	5	0.0092	0.903
	3	0.0063	0.913
Pb^{2+}	5	0.0197	0.794
	3	0.0131	0.885

Table 20. Pseudo-first-order reaction rate constant for the sorption of Zn^{2+}, Cu^{2+} and Pb^{2+} on the modified clinoptilolite at different initial metal concentrations of pH 5.0.

Metal	Initial metal concentration (mM)	K_1 (min^{-1})	r
Zn^{2+}	1	0.0316	0.976
	5	0.0064	0.980
Cu^{2+}	1	0.0092	0.903
	5	0.0046	0.955
Pb^{2+}	1	0.0197	0.794
	5	0.0045	0.972

Figure 49: Pseudo-first-order plots for sorption of Zn^{2+}, Cu^{2+} and Pb^{2+} on the modified clinoptilolite at (a) different pHs and (b) different initial metal concentrations.
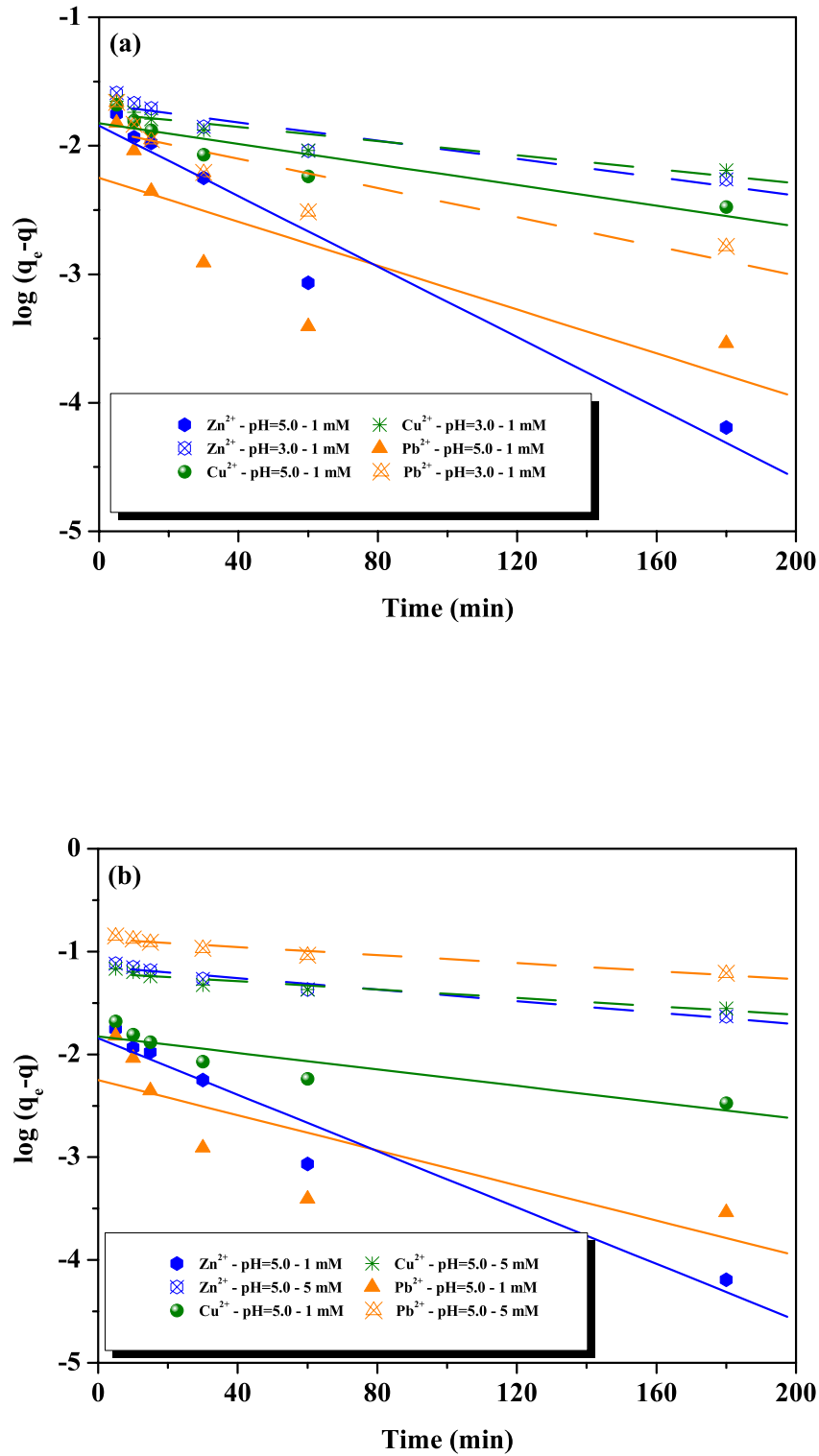
In Figure 50 are presented the plots of the pseudo-second-order model for the sorption of Zn^{2+}, Cu^{2+} and Pb^{2+} on the modified clinoptilolite under different experimental conditions. The constant K_2 for all applied conditions has been calculated from the plots of Figure 50 and is summarised in Tables 21 and 22. Excellent fits were observed for the pHs and initial metal concentrations applied, indicating that the sorption reaction of Zn^{2+}, Cu^{2+} and Pb^{2+} on the modified clinoptilolite can be predicted with the pseudo-second-order kinetics model.

Table 21. Pseudo-second-order reaction rate constant for the sorption of Zn^{2+}, Cu^{2+} and Pb^{2+} on the modified clinoptilolite at different pHs.

Initial metal concentration (1 mM)	pH	K_2 (g/mmol min)	h (mmol/g min)	r
Zn^{2+}	5	4.89	0.0069	0.999
	3	2.52	0.0030	0.999
Cu^{2+}	5	4.47	0.0055	0.999
	3	3.54	0.0026	0.999
Pb^{2+}	5	11.35	0.0178	0.999
	3	4.68	0.0072	0.999

Table 22. Pseudo-second-order reaction rate constant for the sorption of Zn^{2+}, Cu^{2+} and Pb^{2+} on the modified clinoptilolite at different initial metal concentrations of pH 5.0.

Metal	Initial metal concentration (mM)	K_2 (g/mmol min)	h (mmol/g min)	r
Zn^{2+}	1	4.89	0.0069	0.999
	5	0.6935	0.0060	0.997
Cu^{2+}	1	4.47	0.0055	0.999
	5	0.9061	0.0037	0.997
Pb^{2+}	1	11.35	0.0178	0.999
	5	0.3883	0.0063	0.996
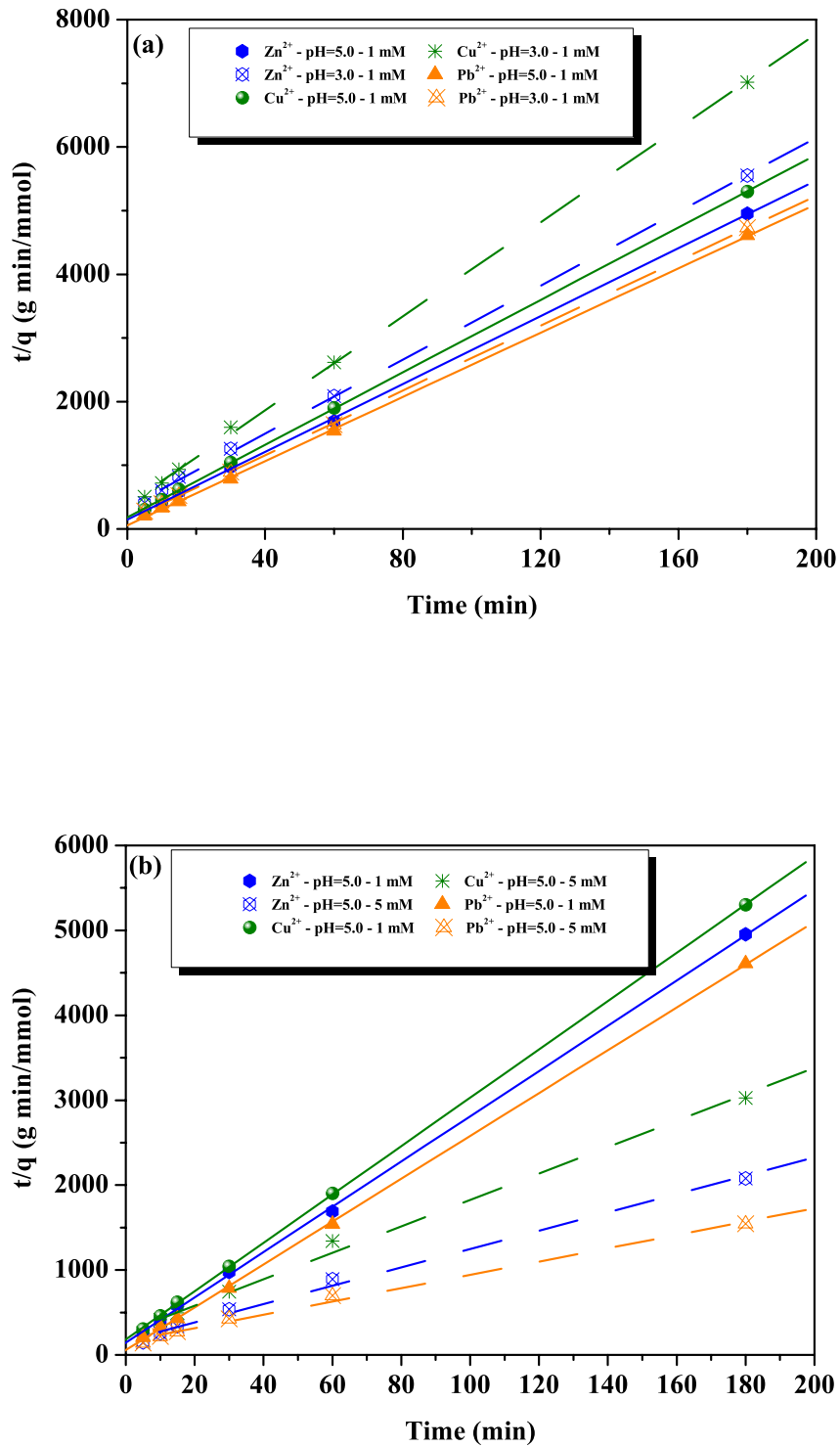
Figure 50: Pseudo-second-order plots for sorption of Zn^{2+}, Cu^{2+} and Pb^{2+} on the modified clinoptilolite at (a) different pHs and (b) different initial metal concentrations.

6.1.3 Conclusions

The following conclusions can be drawn from the results obtained from the batch experiments:

- The chemical conditioning of clinoptilolite with a sodium chloride solution almost doubles the effective ion exchange capacity of the material and give values of the order of 0.12 mmol/g for Zn^{2+}, 0.09 mmol/g for Cu^{2+} and 0.2 mmol/g for Pb^{2+}.

- The clogging of the pores of the natural material resulted in smaller ion exchange capacity and in slower ion exchange rates. Removal of the fine fraction prior to application of clinoptilolite is advisable

- The selectivity series deduced from the equilibrium isotherms and ion exchange kinetic experiments was $Pb^{2+} > Zn^{2+} > Cu^{2+}$.

- At low metal concentrations the factor that controlled the ion exchange behaviour of clinoptilolite and thus the ion exchange rate, was the surface charge.

- The zeta potential of the modified clinoptilolite, and therefore the surface charge, was strongly affected by the pH of the metal solution.

- The removal efficiency of clinoptilolite was strongly affected by the pH of the metal solution.

- The pseudo-second-order chemical reaction model can predict the sorption reaction of Zn^{2+}, Cu^{2+} and Pb^{2+} on the modified clinoptilolite.

Regarding these results the application of clinoptilolite as a barrier material for the elimination of heavy metals from roof runoffs can be considered as a viable solution.

6.2 Column experiments

Most ion exchange operations, whether in the lab or in full scale, are carried out in columns. A solution is passed through a fixed bed of ion exchanged material and its composition is changed either by ion exchange or sorption. The time when the cations of the feeding solution first appear in the effluent is termed as the breakthrough point. In practice, the breakthrough point is defined as the time when the effluent cation concentration (C_t) reaches a percentage (5-10 %) of influent cation concentration (C_0) which is considered unacceptable. Then the operation is stopped and the exchanger is to be regenerated or replaced by a fresh one

(Hellferich 1995; McCabe et al., 1993; Crittenden et al., 1978; Michaels 1952). In the present study, the breakthrough point was set at 10 %.

6.2.1 Influence of the pre-treatment column procedure on the ion exchange process

The effect of the pre-treatment column procedure on the Cu^{2+} exchange process on clinoptilolite was examined for 8.5 BV/h volumetric flow rate and the results are reported in Figure 51. It is obvious that in the column where the pre-treatment procedure was applied, a steeper breakthrough curve was obtained and the breakthrough point was moved towards the left on the C_t/C_0 vs. bed volume diagram. The breakthrough points obtained were almost 41 and 194 BV resulting for operating ion exchange capacities of 0.018 and 0.084 mmol/g, respectively. This means that the operating ion exchange capacity of the modified clinoptilolite was decreased by a factor almost 5.0, regarding copper elimination.

Through the pre-treatment procedure, the Na-form of modified clinoptilolite was transformed to H-form. In Table 23 is presented the chemical composition of both materials. The effect of
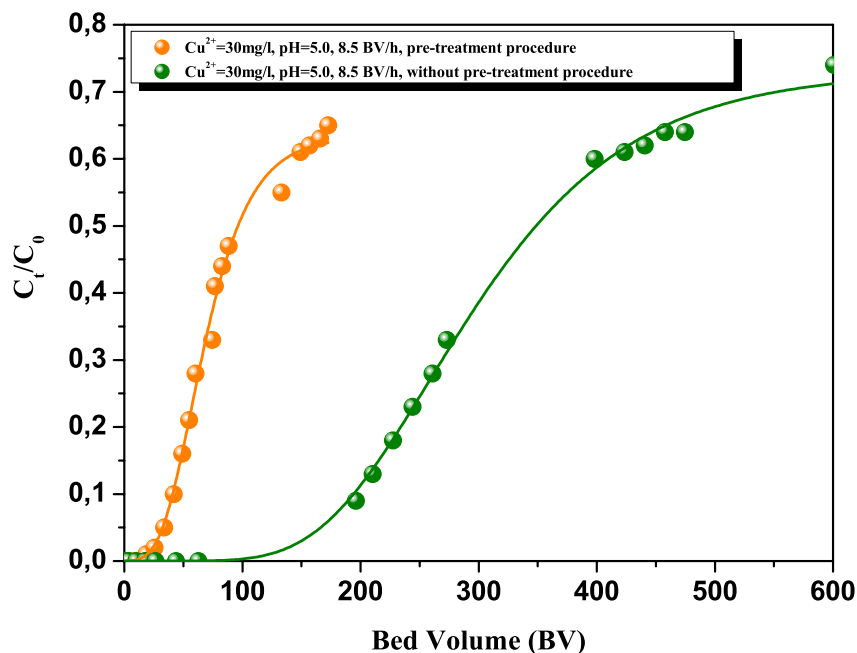
Figure 51: Typical experimental breakthrough curves for the ion exchange of Cu^{2+} on the modified clinoptilolite (Q=8.5 BV/h).

Table 23. Chemical composition of Na- and H-clinoptilolite, % (w/w).

Oxide	Na-clinoptilolite	H-clinoptilolite	±
SiO_2	67.9	67.6	0.2
Al_2O_3	12.1	12.2	1.50
Fe_2O_3	0.86	0.91	0.20
Na_2O	1.65	0.99	0.15
CaO	2.34	2.51	0.15
MgO	0.99	0.96	0.15
K_2O	1.62	1.63	0.15
MnO	0.0272	0.0197	0.00
TiO_2	0.15	0.14	0.05
P_2O_5	0.011	0.014	0.005
S	<0.001	<0.001	0.00
F	<0.5	<0.5	0.5
Loss on ignition	12.46	12.52	0.2

this transformation on its physical properties such as structure, surface area, bulk density, pore size distribution and surface charge (zeta potential) was investigated. Bulk density of the Na-clinoptilolite was 2.32 ± 0.04 g/cm^3 and of the H-clinoptilolite 2.30 ± 0.04 g/cm^3 respectively. BET analysis has shown that the Na-clinoptilolite has a specific surface area of 25.1 m^2/g and the H-form of 26.0 m^2/g, respectively. In Figures 52 and 53 typical XRD diagrams of the Na- and H-clinoptilolite are presented.
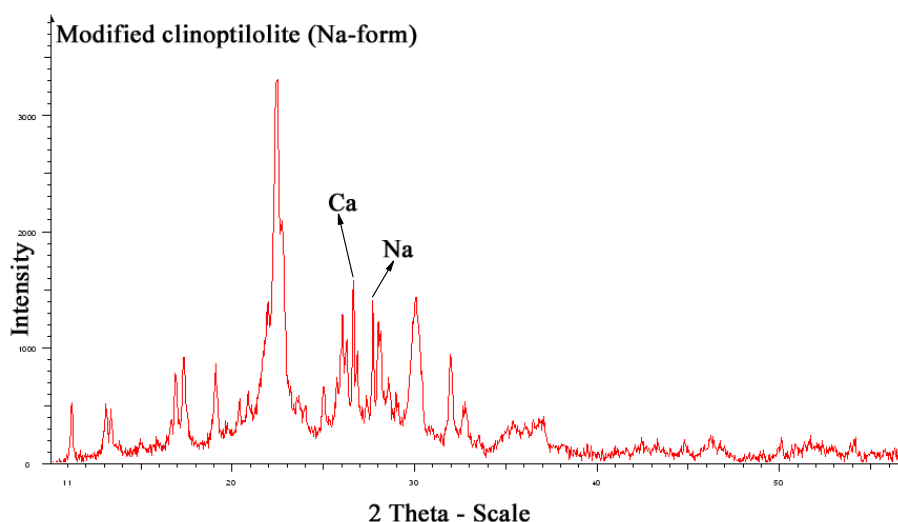
Figure 52: XRD pattern of Na-clinoptilolite.
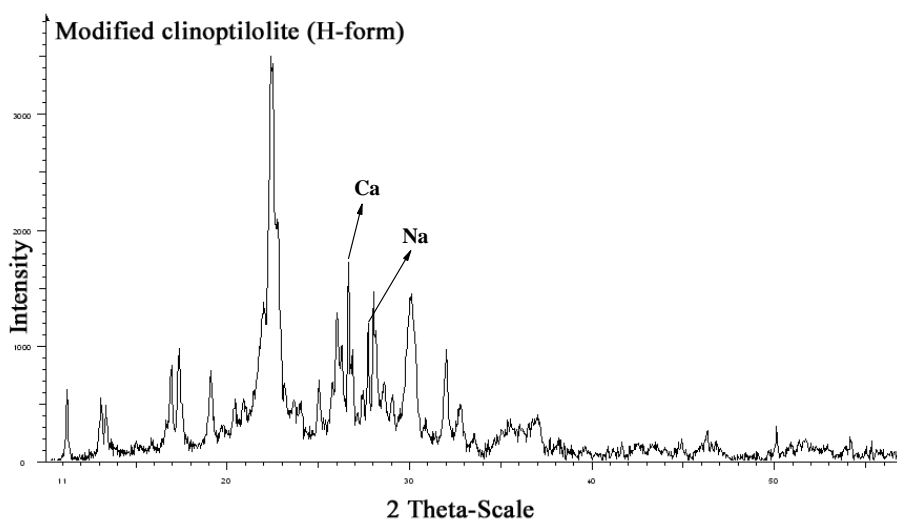
Figure 53: XRD pattern of H-clinoptilolite.

In Table 24 are presented the results of the mercury porosimetry analysis of the Na- and H-clinoptilolite. The Na-clinoptilolite had a pore volume of 0.055 cm^3/g and a pore surface of 9.1 m^2/g. The median pore diameter, based on volume was 100.6 μm and 99 Å based on the surface area. The average pore diameter of the Na-clinoptilolite was 239 Å. By contrast, the H-clinoptilolite had a pore volume of 0.085 cm^3/g and a pore surface area of 12.1 m^2/g. The median pore diameter based on volume was 79.0 μm and 114 Å based on surface area. The average pore diameter of the modified clinoptilolite was 282 Å. The surface area of the

Table 24. Mercury porosimetry analysis of Na- and H-clinoptilolite.

Physical Properties	Modified clinoptilolite	
	Na-clinoptilolite	H-clinoptilolite
Pore volume (cm^3/g)	0.055	0.085
Pore surface (m^2/g)	9.1	12.1
Median pore diameter$_{based on volume}$ (μm)	100.6	79.0
Median pore diameter$_{based on surface}$ (μm)	0.0099	0.0114
Average pore diameter (μm)	0.0239	0.0282

H-clinoptilolite increased by up to almost 30 %. While the surface area increased the pore size changed as well. Change in pore size affects the mobility of the exchanged ions regarding the concept of the stokes radius (see paragraph 5.1.2.2). Similar results were obtained from

Özbelge et al., (1998) on the surface of montmorillonite. According to these results one would expect that the transformation of the Na-clinoptilolite to H-clinoptilolite would result in a higher or at least equal operating ion exchange capacity. This did not occur because of the changes on the surface charge of the H-clinoptilolite (Fig. 54). The surface charge of the H-clinoptilolite was more positive than that of Na-clinoptilolite in the studied pH range, resulting in smaller operating ion exchange capacity.

It is evident that the chemical conditioning of clinoptilolite affects strongly its physical properties, such as pore surface area, pore size and surface charge, and thus affects the operating ion exchange capacity of the material. Consequently it can be concluded that the ion exchange process in this case was predominantly controlled by the surface charge of the clinoptilolite.
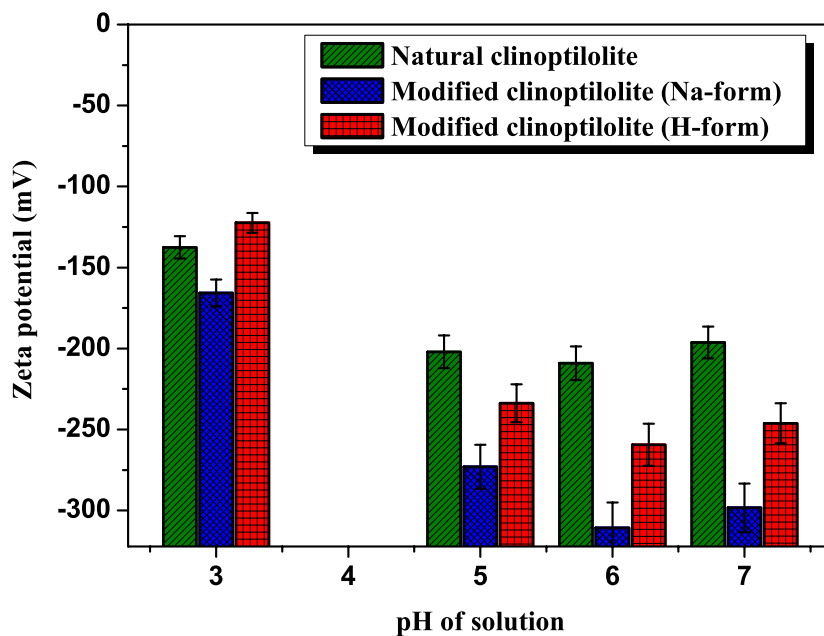
Figure 54: Zeta potential of natural, Na- and H-clinoptilolite.

6.2.2 Influence of the pH of the feeding solution

The effect of the pH of the Cu^{2+} feeding solution (30 mg/l) was examined for 1.7 BV/h volumetric flow rate and the results are reported in Figure 55. It is obvious that at lower pH a steeper breakthrough curve was obtained and the breakthrough point was moved towards the left on the C_t/C_0 Vs bed volume diagram. The breakthrough point was almost 4 BV at pH 3.0,

135 BV at pH 4.0 and 576 BV at pH 5.0. The operating ion exchange capacity of the H-clinoptilolite was 1.6×10^{-3} mmol/g at pH 3.0, 0.058 mmol/g at pH 4.0 and 0.258 mmol/g at pH 5.0, respectively. By lowering the pH of the Cu^{2+} feeding solution from 5.0 to 3.0 the operating ion exchange capacity of the clinoptilolite decreased by a factor near to 160. This decrease resulted from the difference of the clinoptilolite surface charge (see Fig. 54), the copper speciation and the competition between the copper and hydrogen ions for the exchangeable sites of the clinoptilolite. Therefore, the operating ion exchange capacity of clinoptilolite is strongly dependent on pH and is favoured by high pH values.
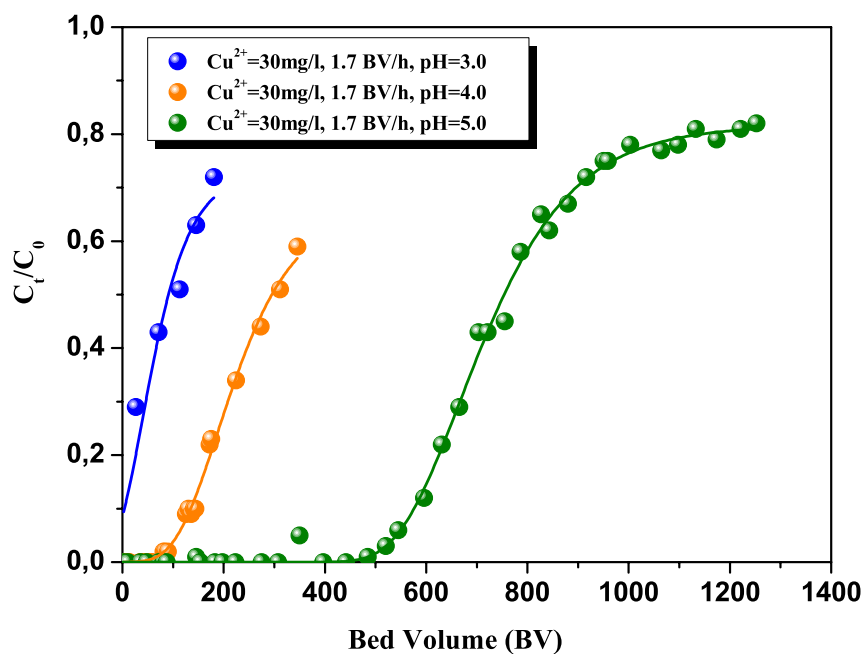
Figure 55: Breakthrough curves for the ion exchange of Cu^{2+} on modified clinoptilolite under different pH conditions and 1.7 BV/h volumetric flow rate.

6.2.3 Influence of the flow modus

The effect of the flow modus on the operating ion exchange capacity of clinoptilolite was examined for 8.5 BV/h volumetric flow rate and the results are reported in Figure 56. The breakthrough point, set at $C_t/C_0 = 10$ %, was almost 41 BV for the down flow modus and 68 BV for the up flow modus. The operating ion exchange capacity obtained was 0.018 mmol/g for the down flow modus and 0.030 for the up flow modus, respectively. Differences between the performance of the down flow and the up flow modus have been reported for ion

exchange clinoptilolite fixed beds (Guangsheng et al., 1988). According to *Inglezakis et al.*, (2001) the hold-ups of the clinoptilolite beds were between 85-100 % for the up flow modus, independent of the value of the superficial velocity. By contrast, in the down flow modus the hold-ups were dependent upon the value of the superficial velocity, ranging between 40 and 95 %. For superficial velocities greater than $0.4 \ 10^{-2}$ m/s down flow hold-ups were equal to those for up flow (Inglezakis et al., 2001). This means that the optimum removal efficiency of an ion exchanged clinoptilolite bed can be only achieved in the up flow modus.
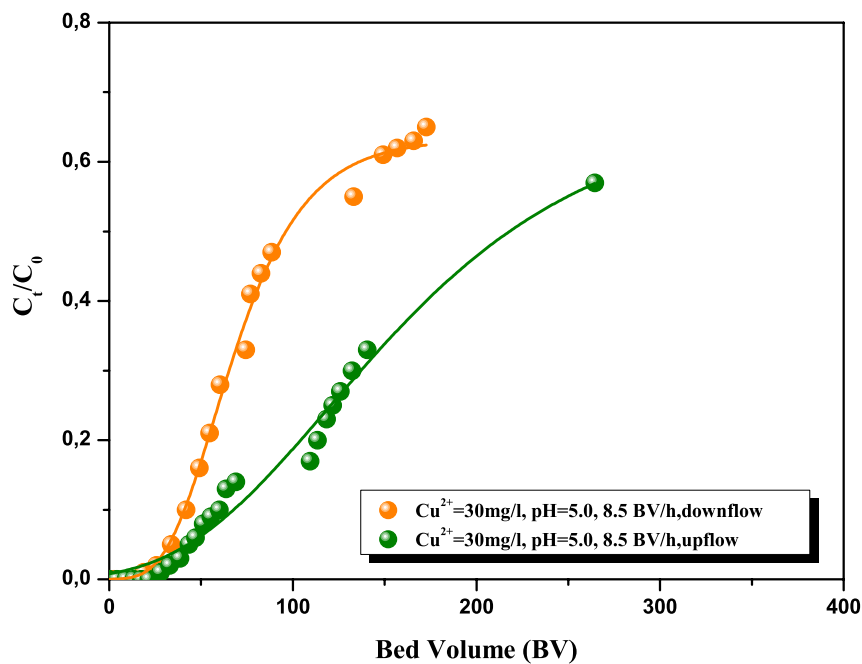
Figure 56: Breakthrough curves for the ion exchange of Cu^{2+} on modified clinoptilolite in down- and up-flow modus for 8.5 BV/h volumetric flow rate.

6.2.4 Effect of volumetric flow rate

The effect of the volumetric flow rate on the operating ion exchange capacity of clinoptilolite was examined for 30 mg/l Cu^{2+} concentration of the feeding solution at pH 5.0. The results obtained are shown in Figure 57. The breakthrough point obtained for a volumetric flow rate of 1.7 BV/h was almost 576 BV, for a flow rate of 3.4 BV/h was 95 BV and for a flow rate of 8.5 BV/h was 41 BV. The corresponding operating ion exchange capacities were 0.258 mmol/g, 0.041 mmol/g and 0.018 mmol/g, respectively. As can be seen, the removal efficiency was favoured by lower volumetric flow rates.
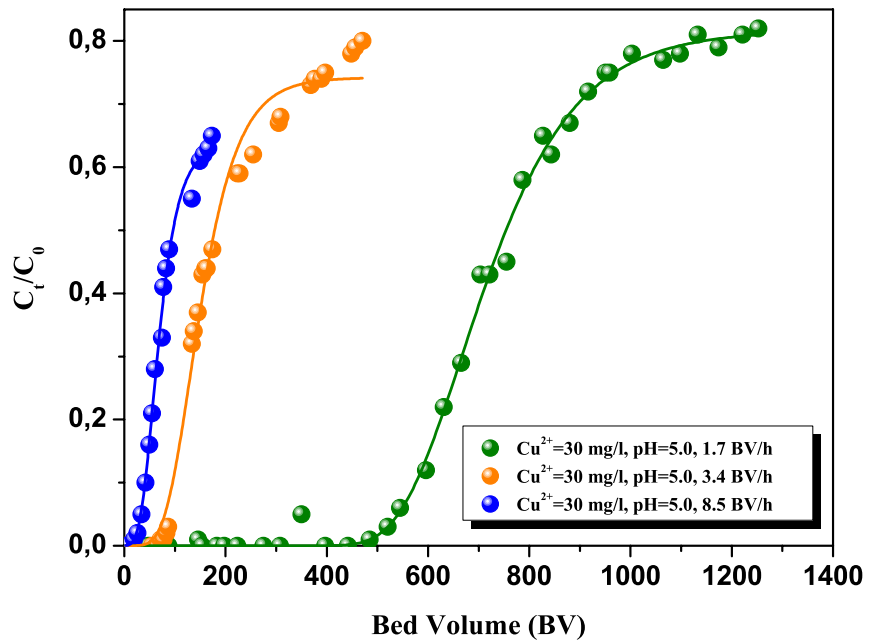
Figure 57: Breakthrough curves for the ion exchange of Cu^{2+} on modified clinoptilolite for different volumetric flow rates.
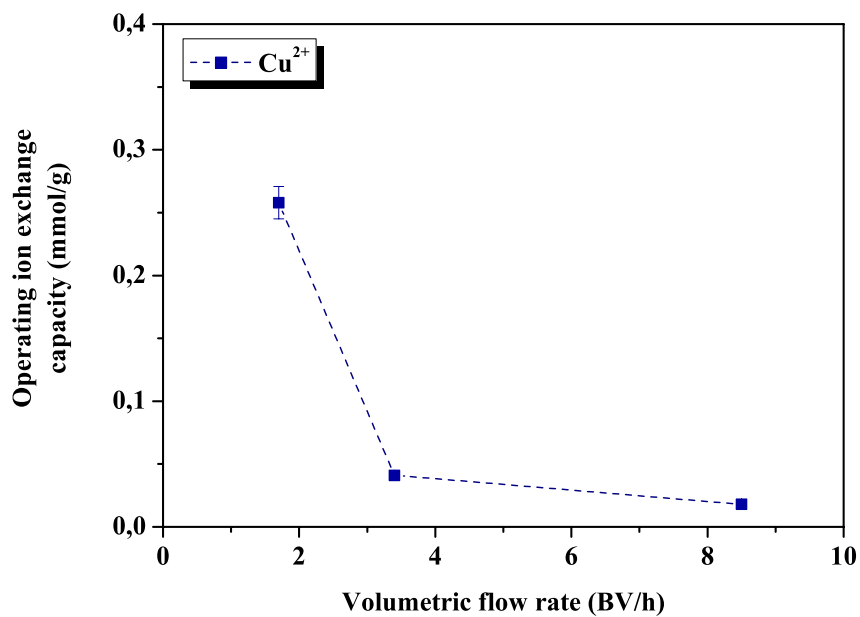
Figure 58: Effect of the volumetric flow rate on the operating ion exchange capacity of the fixed bed of modified clinoptilolite.

The increase in operating ion exchange capacity, however, was not proportional to the flow rate. By lowering the flow rate from 8.5 to 1.7 BV/h the operating ion exchange capacity increased by a factor of 14, for the metal studied (see Fig. 58).

According to *Guangsheng et al*., (1988) the operating ion exchange of Na-clinoptilolite for Cu^{2+} was slightly influenced by the flow rate and increased by a factor of 1.24 by lowering the flow rate from 22.5 to 7.5 BV/h. *Inglezakis et al*., (2004) reported that flow rates lower than 5 BV/h would be beneficial to the removal efficiency of clinoptilolite beds. From the results obtained, it can be concluded that the optimum volumetric flow rates is in the range between 2 and 3 BV/h. Generally by lowering the volumetric flow rate the liquid hold up of the bed is also lowered, especially in the down flow modus, leading to liquid misdistributions which may result in reduced operating ion exchange capacities (Milan et al., 1997).

6.2.5 Influence of the metal concentration

The effect of the solution metal concentration on the operating ion exchange capacity of the modified clinoptilolite was examined for 8.5 BV/h volumetric flow rate and the results are reported in Figure 59. The breakthrough point obtained for a Cu^{2+} concentration of 30 mg/l was almost 41 BV, for a Cu^{2+} concentration of 15 mg/l was 248 BV and for a Cu^{2+} concentration of 5 mg/l was 1458 BV. The corresponding operating ion exchange capacities observed were 0.018 mmol/g, 0.056 mmol/g and 0.107 mmol/g, respectively. It can be seen that the operating ion exchange capacity was favoured by lower Cu^{2+} concentrations and that its increase was proportional to the Cu^{2+} concentration. The regression estimate was obtained by minimising the sum of the squares of the residuals. The coefficient of determination (R^2), the coefficient of correlation (r) and the root mean square error are presented in Figure 60. In Table 25 are presented the results of the analysis of variance (ANOVA).

Table 25. Analysis of variance (ANOVA)

Source	Degrees of freedom	Sum of squares	Mean Square	F statistic	p-value
Regression	1	0.00383	0.00383	24.56406	0.12675
Residual error	1	$1.5602 \ 10^{-4}$	$1.5602 \ 10^{-4}$		
Total	2	0.00399			
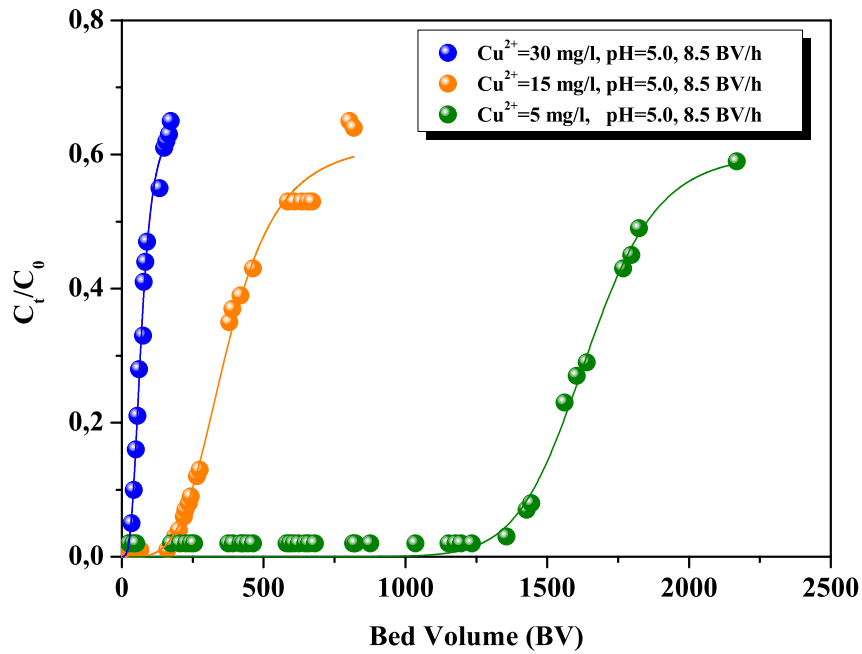
Figure 59: Breakthrough curves for the ion exchange of Cu^{2+} on modified clinoptilolite for different Cu^{2+} concentrations at 8.5 BV/h volumetric flow rate.

Figure 60: Effect of the Cu^{2+} concentration on the operating ion exchange capacity of the fixed bed of modified clinoptilolite.
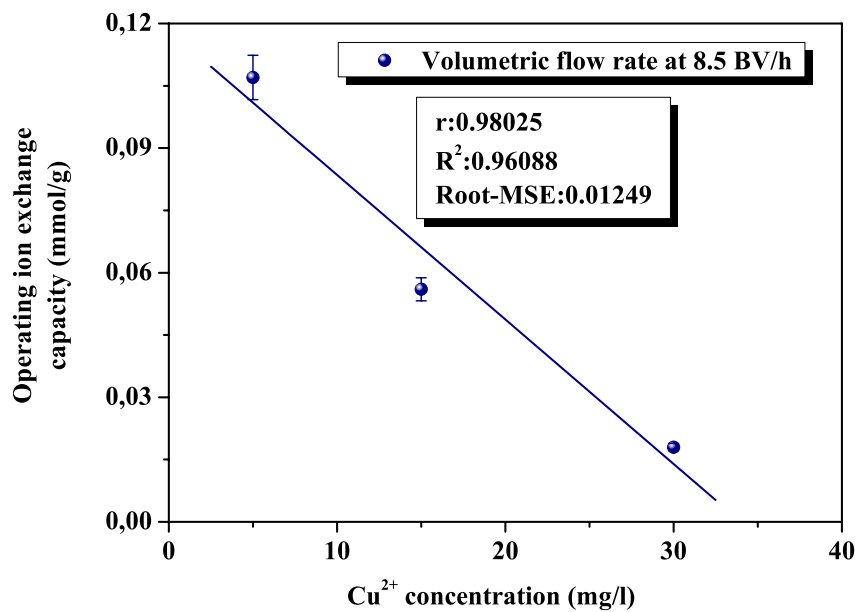
6.2.6 Effect of metal speciation

The effect of the metal speciation on the operating ion exchange capacity of the modified clinoptilolite was examined for 8.5 BV/h volumetric flow rate and the results obtained are reported in Figure 61.
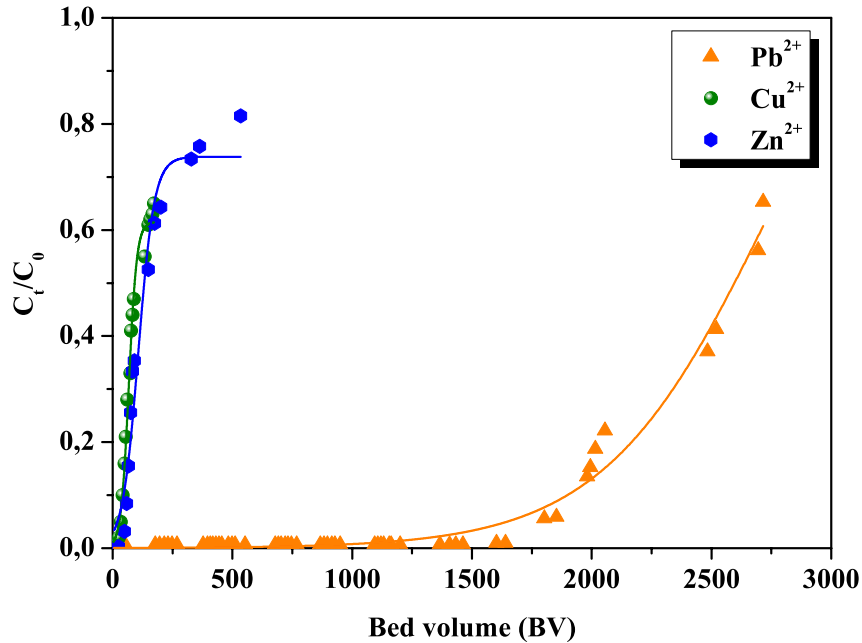
Figure 61: Breakthrough curves for the ion exchange of Cu^{2+}, Zn^{2+} and Pb^{2+} on clinoptilolite for metal concentrations of 30 mg/l at 8.5 BV/h volumetric flow rate.

The breakthrough point obtained for copper was 41 BV, for zinc was 46 BV and for the lead was 1900 BV. The corresponding operating ion exchange capacities were 0.018 mmol/g, 0.020 mmol/g and 0.25 mmo/g, respectively. It can be seen that the operating ion exchange capacity of the fixed clinoptilolite bed was favourable for lead and unfavourable for zinc and copper. The selectivity series obtained was the same as in batch equilibrium experiments and could be explained by the hydration radii concept (see paragraph 5.1.1.2). This means that metals with different physical and chemical properties are influenced in the same manner regarding operating conditions of the fixed clinoptilolite bed (Inglezakis et al., 2004).

6.2.7 Regeneration studies

The Na-clinoptilolite bed saturated (partly) with Cu^{2+} ions was regenerated with 1 M NaCl solution. The first regeneration process was conducted in a continuous flow modus of 2.8 BV/h. The results obtained are illustrated in Table 26.

Table 26. Data of the effluent of the first regeneration process

pH	T (^{0}C)	EC (mS/cm)	T (^{0}C)	BV	$\sum Cu_{desorbed}$ (g)	$\Delta\sum Cu_{desorbed}$ (g)	$\sum Cu_{desorbed}$ (%)
3.3	19.2	71.1	19.2	4.05	0.837	0.837	53.4
3.4	19.4	83.5	19.4	6.07	0.942	0.105	60.1
3.5	19.5	83.7	19.5	8.07	1.020	0.078	65.1
3.5	19.8	83.7	19.8	10.09	1.078	0.059	68.8

It could be observed that with the first 4 BV it was possible to regenerate half of the sorbed Cu^{2+}. Although the regeneration process was continued up to 10 BV, the copper desorption attained was almost 70 %. This means that the regeneration process of a saturated ion exchanged fixed bed of clinoptilolite using a continuous flow modus is probably inappropriate.

The second and the third regeneration processes were conducted in a discontinuous modus. After every 2 BV of regenerant passed through the fixed bed reactor, the regeneration process was stopped for one hour. The results obtained are reported in Tables 27 and 28.

Table 27. Data of the effluent of the second regeneration process

pH	T (^{0}C)	EC (mS/cm)	T (^{0}C)	BV	$\sum Cu_{desorbed}$ (g)	$\Delta\sum Cu_{desorbed}$ (g)	$\sum Cu_{desorbed}$ (%)
2.8	16.1	66.6	16.1	1.94	1.635	1.635	48.9
3.0	17.2	96.9	17.2	3.90	2.478	0.843	74.1
3.2	18.8	99.7	18.8	5.88	2.698	0.220	80.6
3.4	19.2	99.7	19.2	7.88	2.825	0.127	84.5
3.4	19.4	99.7	19.4	9.76	2.897	0.072	86.6

Table 28. Data of the effluent of the third regeneration process

pH	T (^{0}C)	EC (mS/cm)	T (^{0}C)	BV	$\sum Cu_{desorbed}$ (g)	$\Delta\sum Cu_{desorbed}$ (g)	$\sum Cu_{desorbed}$ (%)
3.1	22.4	66.0	22.4	2.03	2.229	2.229	53.7
3.3	22.6	96.9	22.6	3.95	3.506	1.277	84.5
3.6	22.7	99.7	22.7	5.68	3.710	0.204	89.4
3.7	22.6	100.5	22.6	7.51	3.800	0.090	91.6
3.8	22.6	100.5	22.6	9.27	3.848	0.048	92.7

It can be seen that in the second regeneration process a volume of 4 BV of 1M NaCl solution could restore almost 74 % of the sorbed copper and in the third regeneration process the same volume regenerated almost 85 %, respectively. The discontinuous technique achieved sufficiently higher regeneration levels than the continuous under the same regenerant volumes used. This means that the implementation of the regeneration process on clinoptilolite retention facilities can reduce the maintenance cost of those facilities.

The influence of the regeneration process on the operating ion exchange capacity of the fixed clinoptilolite bed is illustrated in Figure 62.
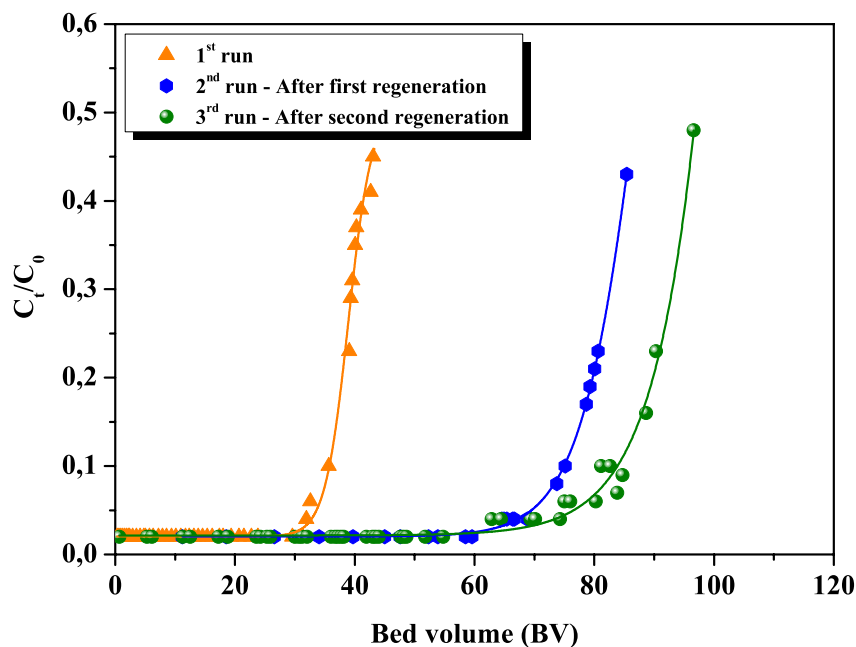
Figure 62: Breakthrough curves for the ion exchange of Cu^{2+} on modified clinoptilolite (Na-form) for Cu^{2+} concentration of 5 mg/l at 17 BV/h volumetric flow rate during regeneration experiments.

The breakthrough point of Cu^{2+}, set at C_t/C_0=10 %, was 36 BV, 75 BV and 84 BV for the first, second and third run. The corresponding operating sorption capacities were 2.5 10^{-3} mmol/g, 5.3 10^{-3} mmol/g and 6.1 10^{-3} mmol/g, respectively. It can be seen that the operating sorption capacity of the regenerated fixed clinoptilolite bed was upgraded by up to 2.1 times after the first regeneration process and by up to 2.5 times after the second regeneration process. These results indicate that the chemical conditioning process in batch modus is less effective than in fixed bed modus. Similar results have been reported in the literature, concluding that the column ion exchange technique is superior to the batch method (Mondale et al., 1995; Carland et al., 1995; Grigoropoulou et al., 2001).

6.2.8 Conclusions

The following conclusions can be drawn from the study of the influence of the operating conditions on the ion exchange capacity of the fixed clinoptilolite bed:

- The chemical conditioning of clinoptilolite strongly affects its physical properties such as pore surface area, pore size and surface charge, and thus can exert a significant influence on the operating ion exchange capacity of the material

- The operating ion exchange capacity of the fixed clinoptilolite bed is strongly dependent from the pH of the metal solution and is favoured by high pH values

- Down flow operation suffers due to channelling of the flow, especially in low volumetric flow rates. Therefore the optimum removal efficiency of an ion exchange clinoptilolite bed can be attained only in up flow modus

- The operating ion exchange capacity is favoured by lower volumetric flow rates and it was increased by a factor of up to 14 by lowering the flow rate from 8.5 to 1.7 BV/h for the metal studied

- The removal efficiency of the fixed clinoptilolite bed is favoured by low metal concentrations and the increase of the operating ion exchange capacity was proportional to the concentration of the metal studied

- The removal efficiency is favourable for lead and unfavourable for copper and zinc

- Regeneration in discontinuous mode is more effective than in continuous mode

6.3 Pilot plant

Fifteen rain events were sampled from the zinc roof in the period between June 2002 and August 2002 (Table 29). Seven samples were analysed from each rain event:

- One from the rainwater before it comes into contact with the roof (RW)

- Three from the roof runoff before it enters the infiltration shaft:

    1. Before the filter: content of the first bottle (1SBF)

    2. Before the filter: content of the second bottle (2SBF)

    3. The remaining rainwater runoff before the barrier material: the water from the remainder bottles was mixed in a beaker and a sample of 500 ml was assayed (RRWBF).

- Three from the treated runoff after the clinoptilolite filter:

    1. From the runoff after passing the barrier material: content of the first bottle (1SAF)

    2. From the runoff after passing the barrier material: content of the second bottle (2SAF)

    3. The remaining runoff after the barrier material: the water from the remainder sampled bottles was mixed in a beaker and a sample of 500 ml was assayed (RRWAF).

6.3.1 Quality of the roof runoff

In the rain water (RW) the pH value varied from 5.1 to 8.2; the mean value was 6.6. The mean pH value of the roof runoff was about 7.0. Considering that the presence of a zinc panel alters the physico-chemistry of the runoff water a comparison of pH measurements reported in the literature is necessary. *Reimann et al.*, (1997) measured pH levels ranging from 4.0 to 5.0 in rainwater collected in Finland, Norway and Russia with measured SO_4^{-2} concentrations varying between 0.8 and 5 mg/l. *Negrel* (1998) reported pH levels ranging from 4.3 to 6.2 in rainwater samples collected in the Massif Central, in France. Measured SO_4^{-2} concentrations were between 0.4 and 4.9 mg/l. The pH is of major interest at the outflow of the artificial barrier due to its impact on the bioavailability of zinc. The lowest pH value measured was 6.4 and the highest 8.2. The increase of the pH value in the roof runoff after its passage through

the clinoptilolite barrier was due to the ion exchange process (Athanasiadis et al., 2005; Doula et al., 2002; Townsend., 1991).

With respect to suspended particles, the mean concentration was 4.5 mg/l in the rain water, almost 24 mg/l in roof runoff at the beginning of the rain event, and was reduced by up to six times during the remaining rain event (see Table 30). Similar results were reported by *Gromaire et al.*, (1999) in roof runoffs in the city of Paris. This means that a preliminary mechanical treatment of the roof runoff is required for the plane operation of clinoptilolite applied as barrier material in retention facilities for the elimination of heavy metals from roof runoffs.

Table 29. Rain event characteristics

Rain event	Date	Rain depth (mm)	Antecedent dry period (d)
1	07.06.2002	4.12	1
2	27.06.2002	1.38	2
3	06.07.2002	1.98	1
4	09.07.2002	10.13	0.1
5	13.07.2002	5.59	2
6	17.07.2002	6.89	1
7	21.07.2002	1.32	2
8	24.07.2002	10.93	2
9	25.07.2002	2.34	0.1
10	31.07.2002	78.53	4
11	01.08.2002	15.40	0.1
12	04.08.2002	24.41	0.2
13	06.08.2002	47.89	1
14	07.08.2002	23.42	0.1
15	21.08.2002	17.51	8

As expected, different amounts of zinc were washed off the roof surface during all sampled rain events. In the rainwater the mean concentration of total zinc was 0.16 mg/l. After contacting the roof material the concentration of zinc in the roof runoff increased significantly. At the beginning of the rain event the concentration of total zinc in the roof runoff varied from 5.6 to 23.5 mg/l and remained as high as 6.6 mg/l (mean value) throughout the rain event (Fig. 63). The phase distribution of zinc concentration in roof runoff was

dominated by the dissolved phase (around 93 % at the beginning of the rain event and almost 98 % during the remaining rain event – Fig. 64).

Table 30. Suspended solids in rain water and in roof runoff

Rain event	SS_{RW} (mg/l)	SS_{1SBF} (mg/l)	SS_{2SBF} (mg/l)	SS_{RRWBF} (mg/l)
1	7.7	64.0	30.3	6.5
2	18.0	53.0	8.0	1.0
3	8.0	9.0	50.0	10.0
4	5.0	35.0	28.0	5.0
5	2.0	27.0	29.0	3.0
6	1.0	14.0	8.0	4.0
7	4.0	6.0	2.0	1.0
8	8.0	1.0	33.0	1.0
9	2.0	6.0	3.0	1.0
10	2.0	75.0	10.0	4.0
11	7.0	27.0	103.0	10.0
12	1.0	3.0	3.0	2.0
13	1.0	13.0	7.0	2.0
14	0.5	2.0	0.5	2.0
15	1.0	24.0	37.0	10.0
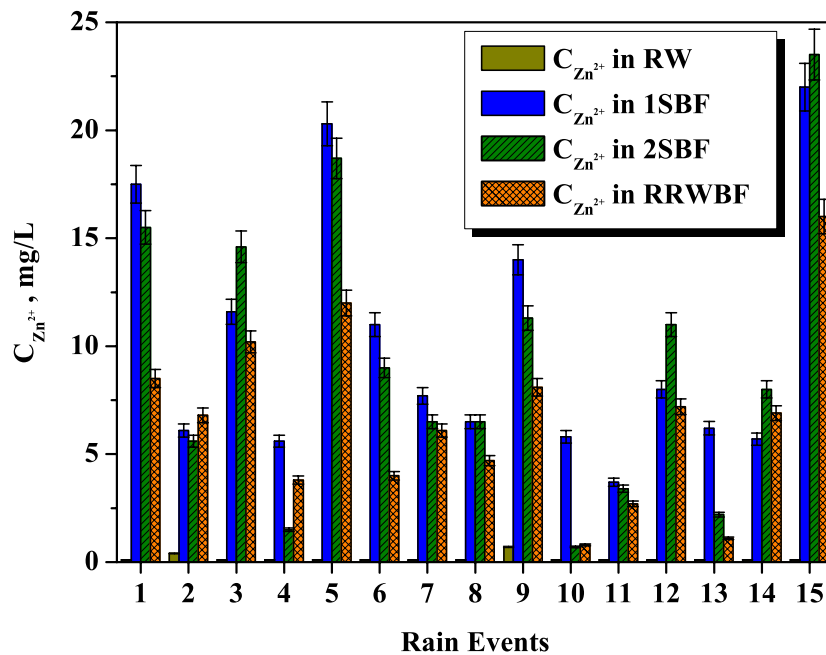
Figure 63: Total zinc concentration in rainwater and in roof runoff.
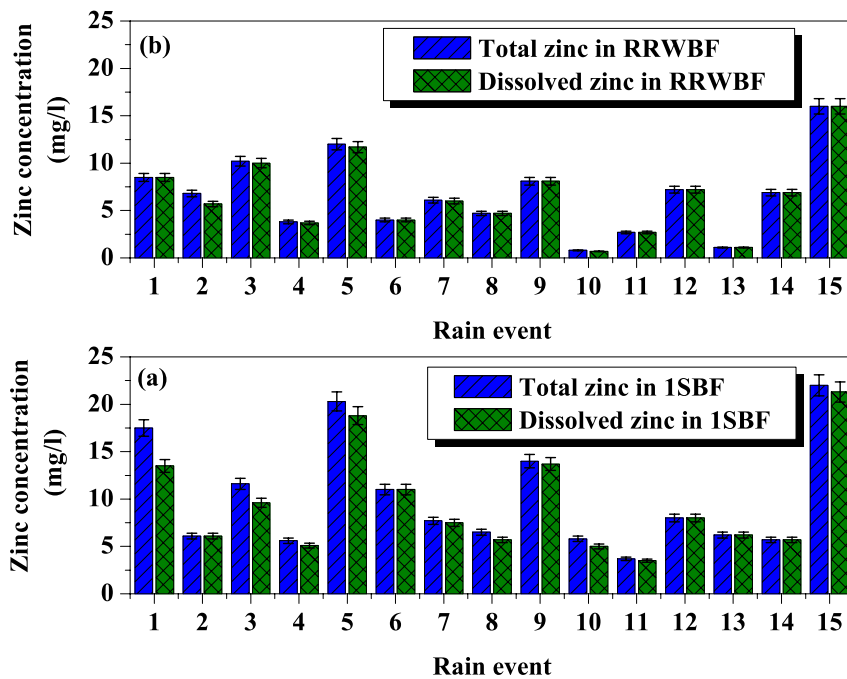
Figure 64: Zinc phase distribution in roof runoff during precipitation.

He et al., (2001) reported zinc concentrations in roof runoff from new non-coated zinc sheets ranging between 2.8 and 4.7 mg/l. Depending on the type of roofing material and the pre-treatment process (e.g. coated zinc, painted zinc, pure zinc, galvanized zinc) runoff concentrations between 0.1 and 10 mg/l were also reported. *Gromaire et al.*, (1999) reported zinc concentrations in roof runoff from the catchment ``le Marais`` in Paris of between 0.8 and 38.1 mg/l. According to his work the main source of zinc pollution (91 %) in the combine sewerage drainage system was the runoff from roofs (Chebbo et al., 2004; - Fig. 65).

This result is of major importance regarding the management of wet weather flow in urban areas. An important reduction of zinc pollution of the combined sewerage drainage system and of the sludge harvested from waste water treatment plants can be reached through the disconnection of the roof runoff from the sewer.

The concentration and the phase distribution of zinc in the roof runoff are of prime importance with regard to its bioavailability immediately after its release from the roof surface, creating a challenge for environmental engineers and decision makers first to develop and then to adopt an adequate removal technique for the construction of a simple and inexpensive on site retention facility.
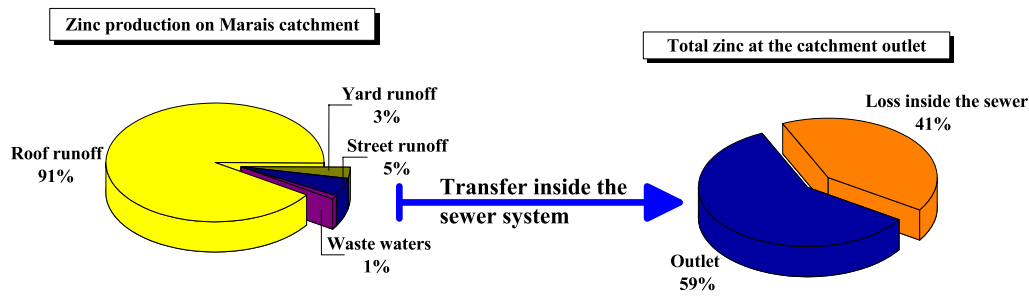
Figure 65: Contribution of the different sources to total zinc loads production and evolution during the transport in the sewer (Chebbo et al., 2004).

Heijerick et al., (2002) reported that zinc was almost completely bioavailable, and thus toxic, for *A. eutrophus* and the green alga R. *subcapitata.* However the toxicity of the zinc roof runoff water should not simply be extrapolated to effects in the environment since dilution processes, organic and inorganic compexations may alter its phase distribution (and hence its toxicity) on its way to the receiving water bodies. According *Mason et al.*, (1999) immediate percolation of roof runoff at the point of discharge to the infiltration pit resulted in a minor retention of the metals Cu, Zn, Pb, Cr and Cd by the top organic rich humus layer. Metals, in particular Cu, Cd and Cr, were transported in soil water downward through the unsaturated zone and could finally reach groundwater.

To identify the factors which mostly influence the concentration of zinc in the roof runoff the mean concentration of zinc in the roof runoff at the beginning of the rain event and the antecedent dry period were correlated in Figure 66. The regression estimate (best linear fit) was obtained by minimizing the sum of the squares of the residuals. The coefficient of determination (R^2), the coefficient of correlation (r) and the sample size are present in Figure 66. The predicted line had an intercept of 7.4 mg/l. This means that after the first flush there is still a significant zinc concentration in the roof runoff. Thus it is important to treat the whole rain event and not only the roof runoff of the beginning of the rain event. In Table 31 are presented the results of the analysis of variance (ANOVA).

Table 31. Analysis of variance (ANOVA)

Source	Degrees of freedom	Sum of squares	Mean square	F statistic	p-value
Regression	1	117.29434	117.29434	3.7828	0.07374
Residual error	13	403.095	31.00731		
Total	14	520.38933			
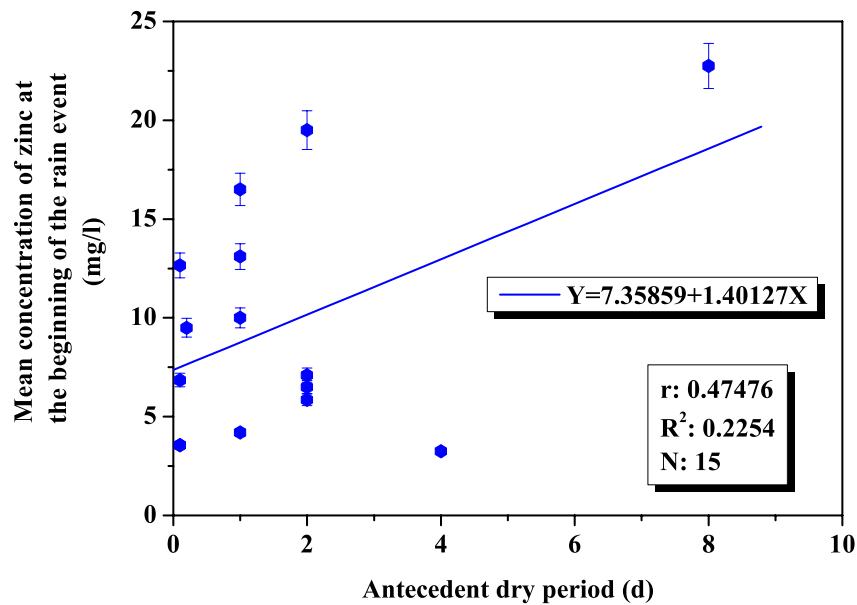
Figure 66: Influence of the antecedent dry period on the zinc concentration in the roof runoff.

The concentrations of lead in the roof runoff as well as in the rain water were originally assumed to be rather low because of the use of lead free gasoline technology and the location of the field site. The rain water of the second sampled rain event contained 16.3 μg/l of lead. In all other rain events the concentration of lead in the rain water was lower than 5 μg/l (detection limit). In the roof runoff the lead concentration varied from less than 5 to 84 μg/l. Taking the limitations of 10 μg/l from the EC Drinking Water Directive into consideration, the magnitude of these concentrations becomes obvious. As can be seen in Table 32 lead was present in the roof runoff from only six of the fifteen sampled rain events. The high values of lead in the roof runoff resulted from the sealing material used to seal the chimneys on the roof (see Fig. 67). The antimony-free solder which was applied on the roof contained 40 % tin and 60 % lead (L-PbSn$_{40}$). The phase distribution of the lead concentration in the roof runoff was dominated by the particulate phase (almost 97 % at the beginning of the rain event).

Figure 67: Photo from the antimony-free solder sealing material used to seal the chimneys on the roof.

Table 32. Total lead concentration in rain water and in roof runoff

Rain event	Pb_{RW} (µg/l)	Pb_{1SBF} (µg/l)	Pb_{2SBF} (µg/l)	Pb_{RRWBF} (µg/l)
1	< 5.0	< 5.0	< 5.0	< 5.0
2	16.3	84.0	34.0	9.0
3	< 5.0	< 5.0	< 5.0	< 5.0
4	< 5.0	< 5.0	< 5.0	< 5.0
5	< 5.0	< 5.0	< 5.0	< 5.0
6	< 5.0	6.1	< 5.0	< 5.0
7	< 5.0	< 5.0	< 5.0	< 5.0
8	< 5.0	< 5.0	11.4	< 5.0
9	< 5.0	< 5.0	< 5.0	< 5.0
10	< 5.0	< 5.0	< 5.0	< 5.0
11	< 5.0	< 5.0	8.1	< 5.0
12	< 5.0	< 5.0	< 5.0	< 5.0
13	< 5.0	8.6	< 5.0	< 5.0
14	< 5.0	< 5.0	< 5.0	< 5.0
15	< 5.0	14.4	16.6	8.5

6.3.2 Performance of the retention facility

The retention capability of the clinoptilolite barrier material concerning zinc concentration in the roof runoff is presented in Figure 68. The performance of the barrier material at the beginning of the rain event was 92 % regarding zinc elimination (Fig. 68(a)). Later on, during the remaining roof runoff, representing the main volume of the precipitation event, it was 97 % (Fig. 68(b)). Although clinoptilolite had showed an advanced performance at the beginning of the rain event, low zinc concentrations were detected in the runoff after the passage through the barrier material during the 1st, 3rd, 4th, 6th, 8th, 10th and the 15th rain event. The dry weather period between the rain events resulted in liquid misdistributions and channelling in the body of the barrier material (unsaturated barrier material); the rain intensity at the beginning of the rain event and the phase distribution of the zinc concentration in the roof runoff at the beginning of the rain event could be assumed to be the reasons for the presence of low zinc concentrations in the runoff in the outflow of the retention facility.
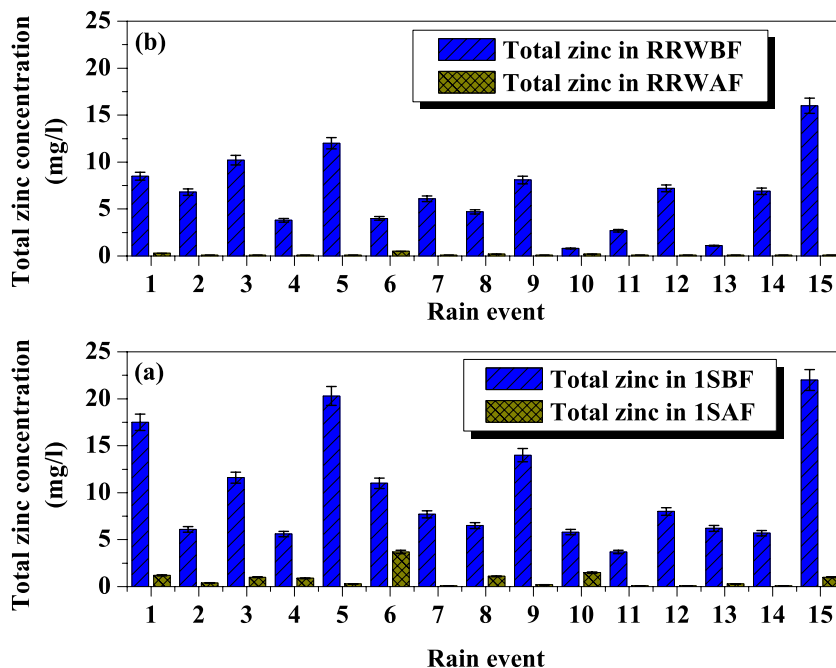
Figure 68: Performance of the clinoptilolite barrier material concerning zinc elimination at (a) the beginning of the rain event and (b) the rest of the rain event.

From the clinoptilolite selectivity's series obtained through the equilibrium experiments and the fixed bed experiments (see paragraph 5.1.2.2 and 5.2.6) one would expect that the

performance of the clinoptilolite barrier material regarding lead elimination would at least be better than that for the zinc elimination. As can be seen in Figure 69 the retention performance of the clinoptilolite barrier material regarding lead elimination from the roof runoff was unsatisfactory. The following reasons could explain that performance: (a) the phase distribution of lead concentration in the roof runoff was dominated by the particulate phase up to 97 % while zinc appeared mostly in the dissolved phase; (b) the difference in concentration between zinc and lead affects by one order of magnitude; (c) unsaturated barrier material conditions caused by the antecedent dry period (down flow modus); and (d) the rain intensity.
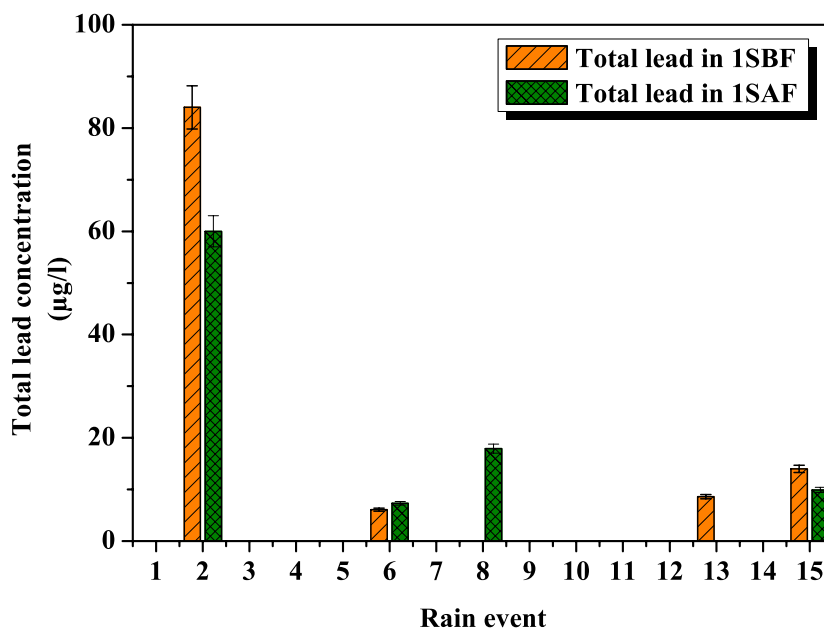
Figure 69: Performance of the clinoptilolite barrier material concerning lead elimination at the beginning of the rain event.

6.3.3 Conclusions

The results obtained can be summarised as follows:

- The cover material of the roof and the drainage system were responsible for the high zinc and lead concentrations in the roof runoff

- The phase distribution of the zinc concentration in the roof runoff was dominated by the dissolved phase and it varied between 93 and 98 %. Thus the zinc was almost completely bioavailable.

- The phase distribution of the lead concentration in the roof runoff was dominated by the particulate phase up to 97 % resulting in an unsatisfactory retention performance of the clinoptilolite barrier material.

- High concentrations of zinc were observed at the beginning of every rain event. The concentration of zinc remained as high as 6.6 mg/l throughout the rain event. Therefore it is important to treat the entire runoff from rain event.

- The clinoptilolite barrier material reduced the zinc concentration from the roof runoff by a factor up to 97 %.

From these results it becomes obvious that on site infiltration using clinoptilolite as an artificial barrier material may be the advanced way of managing roof runoff situations in urban areas provided the hydrological and geological conditions allow infiltration.

6.4 Full scale application

Twenty rain events were sampled from the copper roof of the Academy of Fine Arts in Munich, during the period March 2004 – February 2005. One hundred and one samples were analysed from each rain event of the four monitored retention facilities:

o One from the rainwater before it comes in contact with the roof

o Twelve from the roof runoff before it enters the infiltration facility

o Twelve from the runoff after passing the barrier material

o One from the percolation water.

6.4.1 Quality of the roof runoff

The measured roof runoff volume, obtained through the flow meter recordings in the sampling period (March 2004 – February 2005), was almost 313 m^3 at the west site (468 m^2 roof surface), 147 m^3 at the east site (468 m^2 roof surface), 105 m^3 at the south east site (412 m^2 roof surface) and 179 m^3 at the south west site (412 m^2 roof surface). The runoff volume, calculated by multiplying the rain height, obtained from the weather station of the Ludwig-Maximilian-University of Munich in the same sampling period, with a theoretical flat roof surface of 500 m^2 , was almost 177 m^3 (see Table 33).

It can be seen that the sampling roof at the west site generated more runoff than the other ones because the roof is facing into the prevailing wind (west facing) and also experiences less evaporation than those facing south or east. Similar observations have been reported by *Ragab et al.,* (2003). Orientation, inclination and height of the roof have a significant impact on the generated runoff volume (Maksimovic 1996; Hollis and Ovenden 1988; Davies and Hollis 1981). This means that the application of rain data in roof runoff models, which do not take into account the influence of aspect, slope and height of the roof, includes a high risk and probably can lead to wrong estimations, e.g. in risk assessments or maintenance of retention facilities.

Table 33. Measured roof runoff and rainfall in the period March 2004 – February 2005

| Month | Runoff volume (m³) - MID | | | | Weather station | |
	West site	East site	South east site	South west site	Rain height (mm)	Calculated runoff volume (m³)
March	6.572	11.174	8.916	18.149	13.12	6.560
April	30.208	9.743	7.355	17.182	21.66	10.830
May	40.837	12.325	8.920	16.597	26.14	13.070
June	14.043	21.377	13.004	19.609	46.70	23.350
July	49.280	24.717	18.177	19.125	80.83	40.415
August	32.279	13.613	11.044	12.907	44.36	22.180
September	28.629	11.790	8.577	14.584	28.67	14.335
October	29.770	18.591	10.980	13.836	50.68	25.340
November	20.736	5.423	4.656	12.248	12.85	6.425
December	21.815	3.150	2.703	7.695	10.14	5.070
January	17.961	3.506	3.961	12.500	14.55	7.275
February	20.653	11.454	6.280	14.185	18.07	9.035

In the rain water the pH varied from 6.8 to 8.0; and the mean value was 7.3. The mean pH value of the roof runoff of the four retention facilities was between 6.5 and 7.6. The pH is of major interest in the roof runoff due to its impact on the bioavailability of copper.

With respect to suspended particles, the mean concentration in the roof runoff was almost 3.0 mg/l. The orographic position and the height of the roof were responsible for the low concentrations of the suspended particles obtained.

As was expected different amounts of copper were washed off the roof surface during all sampled rain events. In the rainwater the copper concentration, stemming from the brake pad material, varied between 16.0 and 230 µg/l; and the mean value was 70.7 µg/l. After contact

with the roof material the concentration of copper in the roof runoff increased significantly. At the west site the total copper concentration in the roof runoff varied between 390 and 6,980 µg/l. At the east site the total copper concentration was between 1,010 and 11,100 µg/l, at the south east between 400 and 4,300 µg/l and at the south west site between 200 and 5,910 µg/l.

It can be seen that a marked fluctuation in copper concentration in the roof runoff was typical during every precipitation event. To evaluate the effect of those fluctuations on the performance of the retention facilities and receiving water bodies the use of the event mean concentration (EMC) is introduced. The EMC represents a flow weighted average concentration computed as the total pollutant mass divided by the total runoff volume, for an event of duration t_r (Charbenau and Barretti., 1998; Sansalone and Buchberger., 1997).

$$EMC = \frac{M}{V} = \frac{\int_0^{t_r} C_t Q_t dt}{\int_0^{t_r} Q_t dt} \cong \frac{\sum C_t Q_t \Delta t}{\sum Q_t \Delta t} \tag{1}$$

where EMC is the event mean concentration (mg/l); M is the total mass of pollutant over entire event duration (g); V is the total volume of the flow over the entire event duration (m^3); t is the time (min); C_t is the time variable concentration (mg/l); Q_t is the time variable flow (m^3/min); and Δt is the discrete time interval (min). The EMC is computed for the entire runoff duration. A partial event mean concentration (PEMC) can be defined as

$$PEMC = \frac{m(t)}{u(t)} = \frac{\int_0^t C_t Q_t dt}{\int_0^t Q_t dt} = \frac{\sum C_t Q_t \Delta t}{\sum Q_t \Delta t} \tag{2}$$

where m(t) is the pollutant mass transported at the time t (g); u(t) is the flow volume at the time t (m^3). From equation (1) and (2) it follows that M=m(t_r), V=u(t_r); and PEMC(t_r)=EMC. The dimensionless normalised mass and flow volumes are needed from the urban storm runoff. Equations (3) and (4) represent the first flush phenomenon:

$$L_p = \frac{m(t_r)}{M} \tag{3}$$

$$F = \frac{u(t_r)}{V} \tag{4}$$

where L_p is the dimensionless cumulative pollutant mass and F is the dimensionless cumulative runoff volume. A first flush exists at time t if the dimensionless cumulative pollutant mass L_p exceeds the dimensionless cumulative runoff volume F at all instances during the rain events. A 45° line, when plotting L_p against F, indicates that the pollutants are

uniformly distributed throughout the rain event. If the data from a particular precipitation event lie above the 45° line, a first flush is suggested and PEMC(t_r)≥EMC. Conversely, dilution occurs when the data lie below the 45° line, meaning that a first flush fails to occur (Geiger et al., 1987; Gupta and Saul., 1996; Ashley et al., 1992). Every L_p curve can be fitted with F by a power function (Saget et al., 1996; Bertrand et al., 1998).

$$L_p = F^b \qquad\qquad (5)$$

where b represents the first flush coefficient. The value of the first flush coefficient computed by the linear regression of equation (6).

$$\ln(L_p) = b \ln(F) \qquad\qquad (6)$$

where b indicates the gap between the L_p curve and the bisector. In order to sort out the curves *Saget et al.*, (1996) defined six areas (see Table 34).

Table 34. Definition of the L_p curve area according the value of the first flush coefficient (Saget et al., 1996)

Area	Values of the parameter		Deviation from the diagonal
1	0<b≤0.185		strong deviation above the diagonal
2	0.185<b≤0.862	positive	moderate deviation above the diagonal
3	0.862<b≤1.000		little deviation above the diagonal
4	1.000<b≤1.159		little deviation below the diagonal
5	1.159<b≤5.395	negative	moderate deviation below the diagonal
6	5.395<b<+∞		strong deviation below the diagonal

Saget et al., (1996) suggested a very strict definition of the phenomenon; a first flush occurs when at least 80 % of the pollution load is transferred in the first 30 % of the runoff volume. *Vorreiter and Hickey* (1994) have defined the phenomenon in terms of the pollution load in the first 25 % of the event volume.

The first flush phenomenon with respect to copper concentration in roof runoff was studied by plotting the cumulative copper mass against the cumulative runoff volume as shown in Figure 70. At the west and east site some of the cumulative copper mass curves lay above the 45° line, suggesting the presence of the first flush phenomenon. However, first flush phenomenon events such as *Saget et al.*, (1996) proposed were not observed. *Wanielista and Yousef* (1993) suggested that a first flush phenomenon occurs when 50 % of the pollutant mass is transported in the first 25 % of the total rain volume. In our case this profile was observed once at the
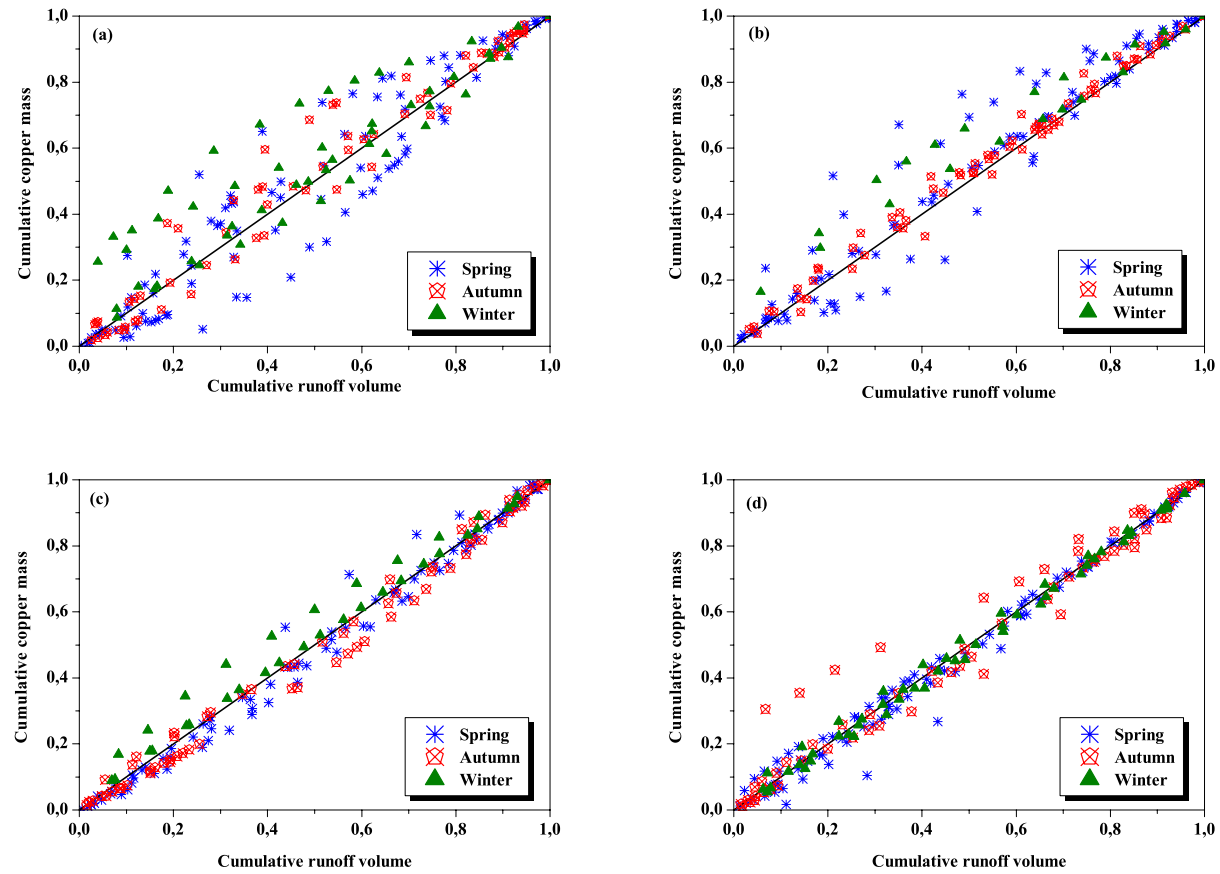
Figure 70: Cumulative mass and volume curves for copper in the roof runoff at the (a) west site, (b) east site, (c) south east site, and (d) south west site.

west site and once at the east site in spring. By contrast, at the south east and south west site almost no curve was above the 45° line, suggesting the absence of the first flush phenomenon.

The copper load in the first flush may be predicted using the relationships between rainfall intensity, rain event duration and the antecedent dry weather period (Gupta and Saul 1996). To identify the influence of rain intensity and the antecedent dry weather period on the first flush phenomenon observed at the west site, the first flush coefficient (*b*) was plotted against the flow rate of the roof runoff and against the dry weather period, respectively (Fig. 71).
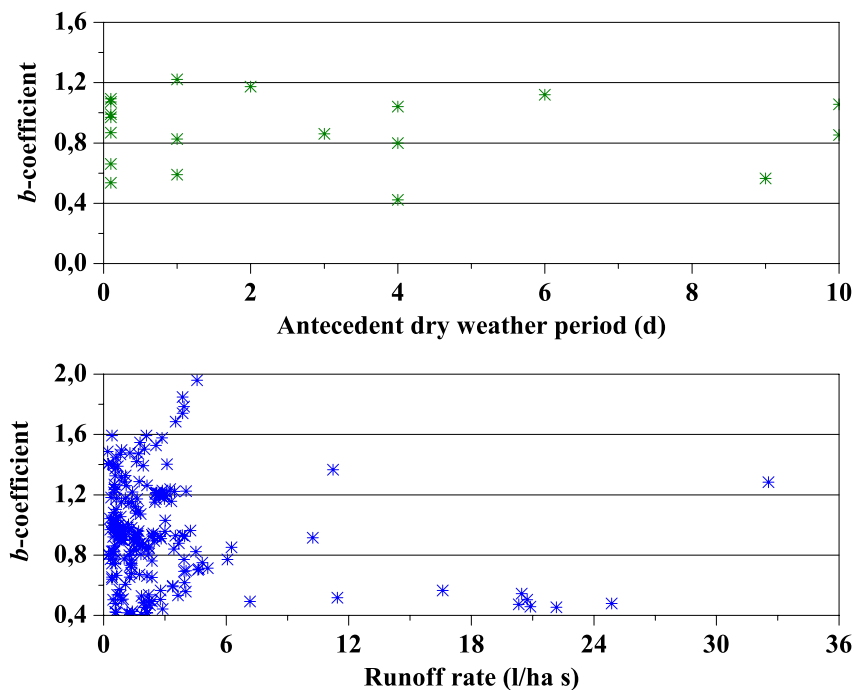
Figure 71: Relationship between the first flush coefficient, the runoff rate and the dry weather period at the west site.

It can be seen that there is a correlation between runoff rates with values higher than 6 l/ha s and the presence of the first flush phenomenon regarding copper load in the runoff at the west site. No correlation was found between the first flush and the antecedent dry weather period at the west site. The same results were obtained at the east site.

As is shown in Figure 72 there is a linear correlation between the washed copper mass of the roof surface during the sampled rain event and the roof runoff volume of the sampled rain event. In Table 35 are presented the results of the analysis of variance. The copper runoff rates obtained in the one year sampling period were 1.44 g/m^2y for the west site, 0.95 g/m^2y for the east site, 0.63 g/m^2y for the south east site and 0.69 g/m^2y for the south west site,

respectively. Copper runoff rates between 0.6 and 1.7 g/m^2y were reported for two year field exposure research from *Wallinder and Leygraf* (2001). A field exposure program performed by *Cramer and Mc Donald* (1990) at test sites of varying SO_2 concentration in the United States reported runoff rates of 1.2 – 2.7 g/m^2y for copper. It is evident that the copper runoff rate was significantly influenced by the precipitation volume hitting the roof surface. Thus roof surfaces with aspects towards the wind direction generate higher copper runoff rates. According to *Wallinder et al.*, (2000) runoff rates are higher for low inclinations from the horizontal and when the wind direction is against the exposed surface.

Table 35. Analysis of variance for the linear regression between the washed copper mass of the roof surface during a rain event and the runoff volume of the rain event

Roof site	Source	Degrees of freedom	Sum of squares	Mean square	F statistic	p-value
West site	Regression	1	46.24825	46.24825		
	Residual error	20	14.33213	0.71661	64.53784	0.0001
	Total	21	60.58038			
East site	Regression	1	52.97918	52.97918		
	Residual error	17	13.62392	0.80141	66.10772	0.0001
	Total	18	66.60309			
South east site	Regression	1	20.40152	20.40152		
	Residual error	17	1.66441	0.09791	208.378	0.0001
	Total	18	22.06593			
South west site	Regression	1	12.2204	12.2204		
	Residual error	20	1.21946	0.06097	200.423	0.0001
	Total	21	13.43985			
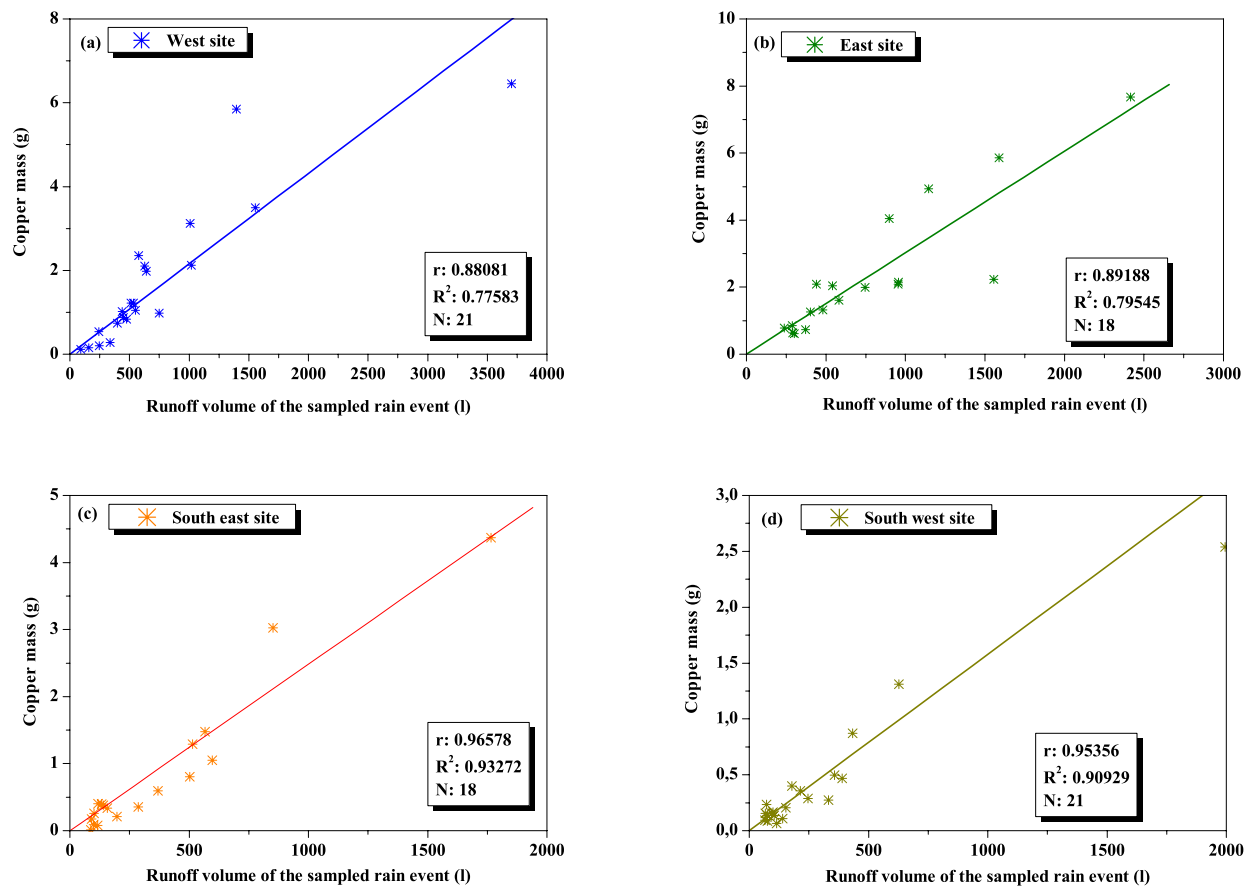
Figure 72: Linear correlation between the washed copper mass of the roof surface during a rain event and the runoff volume of the rain event at the (a) west site, (b) east site, (c) south east site, and (d) south west site.

To identify the influence of rain intensity on the copper runoff rate, the washed copper mass of the roof surface during a rain event was plotted against the mean runoff rate of the rain event (Fig. 73). The data showed a clear relationship between the rain intensity and the amount of the released copper. Rain events with high mean precipitation rates showed high runoff rates and vice versa. This means that the volume and the rate of precipitation have a significant influence on the magnitude of the copper runoff rate.

The phase distribution of copper concentration in roof runoff was dominated by the dissolved phase around 80 % during spring, 78 % in autumn and almost 96 % in winter. *Karmen et al.*, (2002) demonstrated that nearly all copper in runoff water sampled directly after its release from the roof was bioavailable and toxic towards the green algae *Raphidocelis subcapitata*. The majority of copper (60 -100 %) in runoff water was present in its most bioavailable form, the free hydrated copper ion.
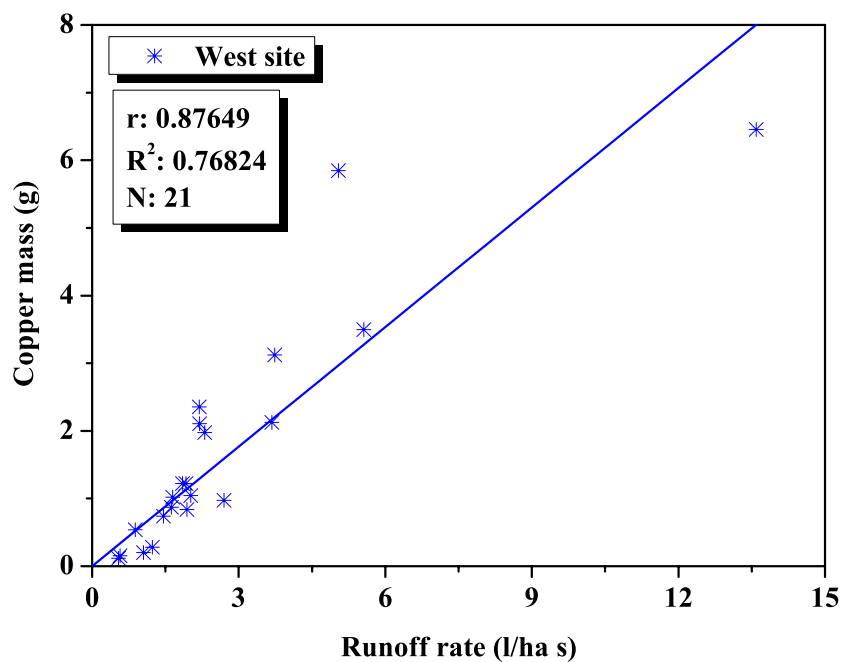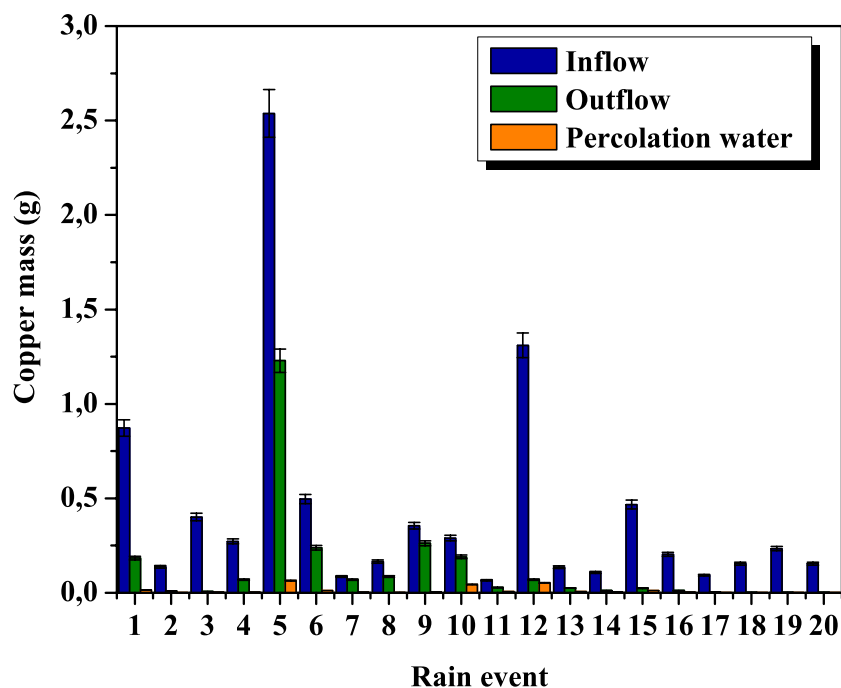

Figure 73: Influence of runoff rate of a rain event on the amount of washed copper mass.

6.4.2 Performance of the clinoptilolite retention facility

The performance of the clinoptilolite retention facility (RF IV) at the south west site regarding copper elimination is demonstrated in Figure 74. The unsatisfactory performance of the

clinoptilolite barrier material during the first ten rain events (1st period) was due to a construction failure. During heavy rain events part of the roof runoff passed by the barrier material through the emergency overflow pipe, contaminating the treated outflow (see Fig. 24). In this period, the copper runoff concentrations after the clinoptilolite bed varied between 18.4 and 2,400 µg/l; the mean concentration was 514 µg /l. After the repair of the construction failure (next ten rain events-2nd period) the copper concentration in the runoff after passing the barrier material lay between 38.0 and 980 µg/l; the mean concentration was158 µg/l.

The copper concentration in percolation water varied between 19.0 and 84 µg/l, and the mean copper concentration was 47 µg/l. It is obvious that the application of the special infiltration ditch seems to be necessary to achieve copper concentrations in percolation water lower than 50 µg/l (BBodSchV. − 12.07.1999-BGBl. I, S. 1554).

Figure 74: Performance of the clinoptilolite retention facility regarding copper elimination.

To identify the influence of the construction failure on the performance of the clinoptilolite retention facility, regarding copper elimination, a mass balance of copper, for the system Inflow-Outflow-Percolation water, was plotted for the two monitored periods (Fig. 75). It is evident that the clinoptilolite barrier material was able to reduce the copper from the roof runoff, during the 1st period (construction failure) by a factor up to 58 % and during the 2nd

115

period by a factor up to 94%. Finally the clinoptilolite retention facility (RF IV) was able to reduce the copper from the roof runoff, during both periods, by a factor up to 97%.
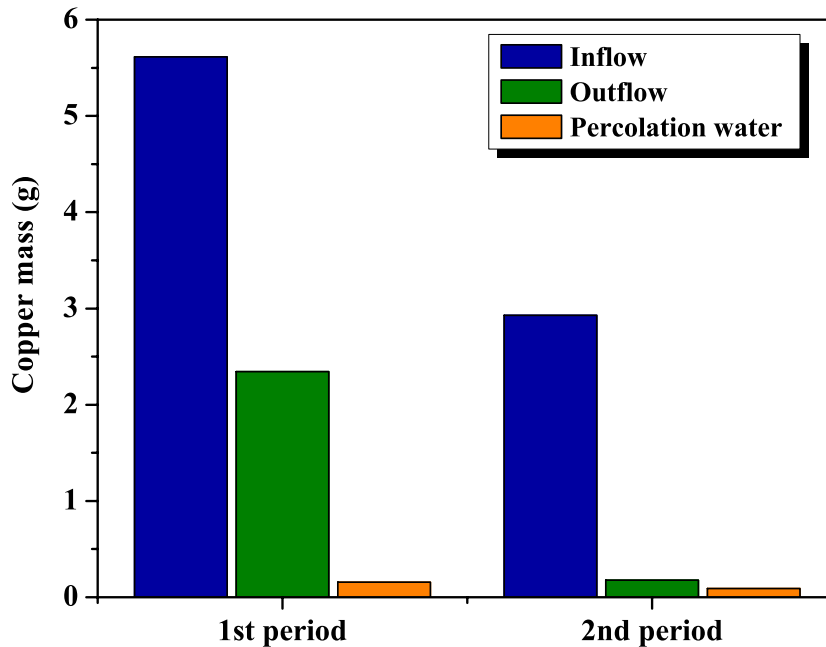
Figure 75: Copper mass balance for the clinoptilolite retention facility (RF IV).

6.4.3 Conclusions

The results obtained can be summarised as follows:

- The cover material of the roof and the drainage system were responsible for the high copper concentrations in the roof runoff

- There was a significant impact of the orientation of the roof on the runoff volume in an urban environment. Roofs facing into the prevailing wind receive higher rainfall

- The amount and the rate of the precipitation were the most important parameters for the magnitude of the copper runoff rate

- The phase distribution of the copper concentration in the roof runoff was dominated by the dissolved phase

- A first flush phenomenon regarding copper concentration in the roof runoff was observed only in some rain events at the west and east site

- No correlation was found between the first flush and the antecedent dry weather period

- The clinoptilolite retention facility was able to reduce the copper from the roof runoff by a factor up to 97 %.

Regarding these results it becomes obvious that on site infiltration using clinoptilolite as an artificial barrier material is the advanced way of managing roof runoff situations in urban areas provided the hydrological and geological conditions allow infiltration.

7. Conclusions

From the experimental and theoretical research results presented in this study the following conclusions were drawn:

Lab scale experiments

(1)   The chemical conditioning of clinoptilolite with a sodium chloride solution almost doubles the effective ion exchange capacity of the material and give values of the order of 0.12 mmol/g for Zn^{2+}, 0.09 mmol/g for Cu^{2+} and 0.2 mmol/g for Pb^{2+}.

(2)   The clogging of the pores of the natural material resulted in smaller ion exchange capacity and in slower ion exchange rates. Removal of the fine fraction prior to application of clinoptilolite is advisable.

(3)   The selectivity series deduced from the equilibrium isotherms and ion exchange kinetic experiments was $Pb^{2+} > Zn^{2+} > Cu^{2+}$.

(4)   At low metal concentrations the factor that controlled the ion exchange behaviour of clinoptilolite and thus the ion exchange rate, was the surface charge.

(5)   The zeta potential of the modified clinoptilolite, and therefore the surface charge, was strongly affected by the pH of the metal solution.

(6)   The removal efficiency of clinoptilolite was strongly affected by the pH of the metal solution.

(7)   The pseudo-second-order chemical reaction model can predict the sorption reaction of Zn^{2+}, Cu^{2+} and Pb^{2+} on the modified clinoptilolite.

(8)   The chemical conditioning of clinoptilolite strongly affects its physical properties such as pore surface area, pore size and surface charge, and thus can exert a significant influence on the operating ion exchange capacity of the material.

(9)   The operating ion exchange capacity of the fixed clinoptilolite bed is strongly dependent of the pH of the metal solution and is favoured by high pH values.

(10)   Down flow operation suffers from channelling of the flow, especially in low volumetric flow rates. Therefore the optimum removal efficiency of an ion exchange clinoptilolite bed can be attained only in up flow modus.

(11)   The operating ion exchange capacity is favoured by lower volumetric flow rates and it was increased by a factor of up to 14 by lowering the flow rate from 8.5 to 1.7 BV/h for the metal studied.

(12)   The removal efficiency of the fixed clinoptilolite bed is favoured by low metal concentrations and the increase of the operating ion exchange capacity was proportional to the concentration of the metal studied.

(13)   The removal efficiency is favourable for lead and unfavourable for copper and zinc.

(14)   Regeneration in discontinuous mode is more effective than in continuous mode.

Pilot plant (Zinc metal roof)

(15)   The cover material of the roof and the drainage system were responsible for the high zinc and lead concentrations in the roof runoff.

(16)   The phase distribution of the zinc concentration in the roof runoff was dominated by the dissolved phase and it varied between 93 and 98 %. Thus the zinc was almost completely bioavailable.

(17)   The phase distribution of the lead concentration in the roof runoff was dominated by the particulate phase up to 97 % resulting in an unsatisfactory retention performance of the clinoptilolite barrier material.

(18)   High concentrations of zinc were observed at the beginning of every rain event. The concentration of zinc remained as high as 6.6 mg/l throughout the rain event. Therefore it is important to treat the entire runoff from rain event.

(19)   The clinoptilolite barrier material reduced the zinc concentration from the roof runoff by a factor up to 97 %.

Full scale application (Copper metal roof)

(20)   The cover material of the roof and the drainage system were responsible for the high copper concentrations in the roof runoff.

(21)   There was a significant impact of the orientation of the roof on the runoff volume in an urban environment. Roofs facing the prevailing wind direction receive higher rainfall.

(22)   The amount and the rate of the precipitation were the most important parameters for the magnitude of the copper runoff rate.

(23) The phase distribution of the copper concentration in the roof runoff was dominated by the dissolved phase.

(24) A first flush phenomenon regarding copper concentration in the roof runoff was observed only in some rain events at the west and east site.

(25) No correlation was found between the first flush and the antecedent dry weather period.

(26) The clinoptilolite retention facility was able to reduce the copper from the roof runoff by a factor up to 97 %.

Regarding these results it can be concluded that the application of clinoptilolite as a barrier material for on site infiltration of runoff from metal roofs, such as zinc and copper, includes low risk for ground and the groundwater pollution and appears to be the advanced way of managing roof runoff situations in urban areas provided the hydrological and geological conditions allow infiltration.

8. References

Allen, H. E., Cho, S. H., & Neubecker, T. A. (1983). Ion-Exchange and Hydrolysis of Type-a Zeolite in Natural-Waters. *Water Research, 17*(12), 1871-1879.

Allen, T. (1997). *Particle size measurement* (Fifth ed. Vol. 2). London: Chapman & Hall.

Altin, O., Ozbelge, H. O., & Dogu, T. (1998). Use of general purpose adsorption isotherms for heavy metal clay mineral interactions. *Journal of Colloid and Interface Science, 198*(1), 130-140.

Arroyave, C., Lopez, FR.A., and Morcillo, M. (1995). The early atmospheric corrosion stages of carbon steel in acidic fogs. *Corrosion Science, 37*(11), 1751-1761.

Ashley, R. M., Wotherspoon, D. J. J., Coghlan, B. P., & Mcgregor, I. (1992). The Erosion and Movement of Sediments and Associated Pollutants in Combined Sewers. *Water Science and Technology, 25*(8), 101-114.

Athanasiadis, K., Hellmreich, B. and Wilderer, P.A. (2003). *Entfernung von Zink aus Dachabläufen eines Zinkdachs durch Klinoptilolith*. Garching.

Athanasiadis, K., Helmreich, B., & Wilderer, P. A. (2005). Elimination of zinc from roof runoff through geotextile and clinoptilolite filters. *Acta Hydrochimica Et Hydrobiologica, 32*(6), 419-428.

DWA-A 138. (2005). Planung, Bau und Betrieb von Anlagen zur Versickerung von Niederschlagswasser. *DWA Deutsche Vereinigung für wasserwirtschaft, Abwasser und Abfall e.V.*; Hennef.

Balci, S. (2004). Nature of ammonium ion adsorption by sepiolite: analysis of equilibrium data with several isotherms. *Water Research, 38*(5), 1129-1138.

Barrer, R. M., FRS. (1978). *Zeolites and clay minerals as sorbents and molecular sieves*: Academic press Inc., New York.

Beattie, J. K., Djerdjev, A. M., & Gibb, S. E. (2003). Electroacoustic and dielectric response of suspensions of zeolites A and Y. *New Journal of Chemistry, 27*(10), 1433-1439.

Bektas, N., Agim, B. A., & Kara, S. (2004). Kinetic and equilibrium studies in removing lead ions from aqueous solutions by natural sepiolite. *Journal of Hazardous Materials, 112*(1-2), 115-122.

Bektas, N., & Kara, S. (2004). Removal of lead from aqueous solutions by natural clinoptilolite: equilibrium and kinetic studies. *Separation and Purification Technology, 39*(3), 189-200.

Beler-Baykal, B., Bayram, S., Akkaymak, E., & Cinar, S. (2004). Removal of ammonium from human urine through ion exchange with clinoptilolite and its recovery for further reuse. *Water Science and Technology, 50*(6), 149-156.

Bertrand-Krajewski, J. L., Chebbo, G., & Saget, A. (1998). Distribution of pollutant mass vs volume in stormwater discharges and the first flush phenomenon. *Water Research, 32*(8), 2341-2356.

Boller, M. A. (1997). Tracking heavy metals reveals sustainability deficits of urban drainage systems. *Water Science and Technology, 35*(9), 77-87.

Boller, M. A., and Steiner, M. (2002). Diffuse emission and control of copper in urban surface runoff. *Water Science and Technology, 46*(6-7), 173-181.

Breck, D. W. (1974). *Zeolite molecular sieves, Structure, Chemistry and Use*. New York: John Wiley & Sons.

Carland, R. M., & Aplan, F. F. (1995). Improving the ion-exchange capacity and elution of Cu+2 from natural sedimentary zeolites. *Minerals and Metallurgical Processing, 12*(4), 210-218.

Charbeneau, R. J., & Barrett, M. E. (1998). Evaluation of methods for estimating stormwater pollutant loads. *Water Environment Research, 70*(7), 1295-1302.

Chebbo, G., & Gromaire, M. C. (2004). The experimental urban catchment 'Le Marais' in Paris: what lessons can be learned from it? *Journal of Hydrology, 299*(3-4), 312-323.

Coker, E. N., Roelofsen, D. P., Barrer, R. M., Jansen, J. C., & van Bekkum, H. (1998). Sorption of bulky aromatic molecules into zeolite NaX. *Microporous and Mesoporous Materials, 22*(1-3), 261-268.

Cook, T. E., Cilley, W. A., Savitsky, A. C., & Wiers, B. H. (1982). Zeolite-a Hydrolysis and Degradation. *Environmental Science & Technology, 16*(6), 344-350.

Crittenden, J. C., & Weber, W. J. (1978a). Predictive Model for Design of Fixed-Bed Adsorbers - Parameter-Estimation and Model Development. *Journal of the Environmental Engineering Division-Asce, 104*(2), 185-197.

Crittenden, J. C., & Weber, W. J. (1978b). Predictive Model for Design of Fixed-Bed Adsorbers - Single-Component Model Verification. *Journal of the Environmental Engineering Division-Asce, 104*(3), 433-443.

Cronstedt, A. F. (1756). *Akad. Handl. Stockholm*(18), 120-130.

Cruceanu, M., Grecu, M., Popa, A., Popovici, E., Alexandroaei, M., Vasile, A., et al. (1985). Rheology of Detergent Pastes Containing Synthetic Zeolites. *Revista De Chimie, 36*(4), 310-317.

Curkovic, L., CerjanStefanovic, S., & Filipan, T. (1997). Metal ion exchange by natural and modified zeolites. *Water Research, 31*(6), 1379-1382.

Damour, A. (1840). *Ann. Mines, 17*, 191.

Daub, J., Forster, J., Herrmann, R., Robien, A., & Striebel, T. (1994). Chemodynamics of Trace Pollutants During Snowmelt on Roof and Street Surfaces. *Water Science and Technology, 30*(1), 73-85.

Dauber L., Z. J., Novak B. and Zürcher F. (1979). Pollutants in stormwater from a highway(in German). *Stuttgarter Berichte zur Siedlungswasserwirtschaft, 64*, 41-57.

Davis, A. P., and Burns, M. (1999). Evaluation of lead concentration in runoff from painted structures. *Water Research, 33*(13), 2949-2958.

Davis, A. P., Shokouhian, M. and Ni, S. (2001). Loading estimates of lead, copper, cadmium and zinc in urban runoff from specific sources. *Chemosphere, 44*, 997-1009.

Deville, H. d. S. C. (1862). *Compt. Rend., 54*, 324.

Dierkes, C. (1999). *Verhalten von Schwermetallen in Regenabfuss von Verkehrsflächen bei der Versickerung über poröse Deckbeläge.* GH Essen, Essen.

Dierkes, C., Benze, W., and Wells, J. (2002). *Sustainable Urban Drainage and Pollutant Source Control by Infiltration.* Paper presented at the 6th Regional Conference of Urban Stormwater, Orange.

Dormoy, T., Tisserand, B., and Herremans, L. (1999). Impact of the volume of rain water on the operating constraints for a treatment plan. *Water Science and Technology, 39*(2), 145-150.

Feliu, S., Morcillo, M., and Feliu, S.Jr. (1993). The prediction of atmospheric corrosion from meteorological and pollution parameters.-I. Annual corrosion. *Corrosion Science, 34*(3), 403-414.

Feng, D., Aldrich, C., & Tan, H. (2000). Removal of heavy metal ions by carrier magnetic separation of adsorptive particulates. *Hydrometallurgy, 56*(3), 359-368.

Fletcher, P., & Townsend, R. P. (1982). Transition-Metal Ion-Exchange in Mixed Ammonium-Sodium X-Zeolites and Y-Zeolites. *Journal of Chromatography, 238*(1), 59-68.

Fletcher, P., & Townsend, R. P. (1983). Ion-Exchange of Amminated Palladium and Platinum in Synthetic Sodium Zeolites. *Zeolites, 3*(2), 129-133.

Fletcher, P., & Townsend, R. P. (1985). Ion-Exchange in Zeolites - the Exchange of Cadmium and Calcium in Sodium-X Using Different Anionic Backgrounds. *Journal of the Chemical Society-Faraday Transactions I, 81*, 1731-1744.

Förster, J. (1996). Patterns of roof runoff contamination and their potential implications on practice and regulation of treatment and local infiltration. *Water Science and Technology, 33*(6), 39-48.

Förster, J. (1999). Variability of roof runoff quality. *Water Science and Technology, 39*(5), 137-144.

Geiger, W. (1987). *Flushing effects in combined sewer systems.* Paper presented at the 4th International Conference on Urban Storm Drainage, Lausanne, Switzerland.

Good, J. C. (1993). Roof Runoff as a Diffuse Source of Metals and Aquatic Toxity in Storm Water. *Water Science and Technology, 28*(3-5), 317-321.

Granaud, S., Mouchel, J.M., Chebbo, G. and Thevenot, D.R. (1999). Heavy metal concentrations in dry and wet atmospheric deposits in Paris district: comparison with urban runoff. *The Science of Total Environment, 235*(1), 235-245.

Grandjean, F. (1909). *Compt. Rend., 149*, 866-868.

Grim, M. (1968). *Clay Mineralogy*. New York: Mc Graw-Hill Inc.

Gromaire, M. C., Garnaud, S., Saad, M., & Chebbo, G. (2001). Contribution of different sources to the pollution of wet weather flows in combined sewers. *Water Research, 35*(2), 521-533.

Gromaire-Mertz, M. C., Garnaud, S., Gonzalez, A., & Chebbo, G. (1999). Characterisation of urban runoff pollution in Paris. *Water Science and Technology, 39*(2), 1-8.

Guangsheng, Z., Xingzheng, L., Guangju, L., and Quanchang, Z. (1988). *Removal of copper from electroplating effluents using clinoptilolite.* Paper presented at the Occurence, properties and utilization of natural zeolites, Budapest.

Gudowicz, T. H. (1985). Zeolites as Detergent Builders - a Market Update. *Abstracts of Papers of the American Chemical Society, 190*(SEP), 7-Cmc.

Gupta, K., & Saul, A. J. (1996). Specific relationships for the first flush load in combined sewer flows. *Water Research, 30*(5), 1244-1252.

Hamadi, N. K., Chen, X. D., Farid, M. M., & Lu, M. G. Q. (2001). Adsorption kinetics for the removal of chromium(VI) from aqueous solution by adsorbents derived from used tyres and sawdust. *Chemical Engineering Journal, 84*(2), 95-105.

Harland, C. E. (1994). *Ion exchange: Theory and Practice*. Cambridge.

Harrison M., a. W. J. (1985). The chemical composition of highway drainage I-III. *The Science of Total Environment, 43*(1/2), 63-102.

He, W., Wallinder, I. O., & Leygraf, C. (2001). A laboratory study of copper and zinc runoff during first flush and steady-state conditions. *Corrosion Science, 43*(1), 127-146.

Heijerick, D. G., Jansen, C.R., Karlen, C., Odnevall Wallinder, I., and Leygraf, C. (2002). Bioavailability of zinc in runoff water from roofing materials. *Chemosphere, 47*(1), 1073-1080.

Helfferich, F. (1995). *Ion Exchange*. New York.

Herrmann, R., Daub, J., Forster, J., & Striebel, T. (1994). Chemodynamics of Trace Pollutants During Roof and Street Runoff. *Water Science and Technology, 29*(1-2), 73-82.

Herrmann R., D. J., Förster J. and Striebel T. (1994). Chemodynamics of trace pollutants during street runoff. *Water Science and Technology, 29*(9), 73-82.

Ho, Y. S., & McKay, G. (1998). Kinetic models for the sorption of dye from aqueous solution by wood. *Process Safety and Environmental Protection, 76*(B2), 183-191.

Ho, Y. S., & McKay, G. (1999). Pseudo-second order model for sorption processes. *Process Biochemistry, 34*(5), 451-465.

Ho, Y. S., Ng, J. C. Y., & McKay, G. (2001). Removal of lead(II) from effluents by sorption on peat using second-order kinetics. *Separation Science and Technology, 36*(2), 241-261.

Hopkins, B., & Argue, J. R. (1994). Constructed Source Wetland Concepts Applied to Urban Landscapes. *Water Science and Technology, 29*(4), 133-140.

Inglezakis, V. J., Diamandis, N. A., Loizidou, M. D., & Grigoropoulou, H. P. (1999). Effect of pore clogging on kinetics of lead uptake by clinoptilolite. *Journal of Colloid and Interface Science, 215*(1), 54-57.

Inglezakis, V. J., & Grigoropoulou, H. (2004). Effects of operating conditions on the removal of heavy metals by zeolite in fixed bed reactors. *Journal of Hazardous Materials, 112*(1-2), 37-43.

Inglezakis, V. J., & Grigoropoulou, H. P. (2003). Modeling of ion exchange of Pb2+ in fixed beds of clinoptilolite. *Microporous and Mesoporous Materials, 61*(1-3), 273-282.

Inglezakis, V. J., Hadjiandreou, K. J., Loizidou, M. D., & Grigoropoulou, H. P. (2001). Pretreatment of natural clinoptilolite in a laboratory-scale ion exchange packed bed. *Water Research, 35*(9), 2161-2166.

Inglezakis, V. J., Lemonidou, M., & Grigoropoulou, H. P. (2001). Liquid holdup and flow dispersion in zeolite packed beds. *Chemical Engineering Science, 56*(17), 5049-5057.

Inglezakis, V. J., Loizidou, M. D., & Grigoropoulou, H. P. (2002). Equilibrium and kinetic ion exchange studies of Pb2+, Cr3+, Fe3+ and Cu2+ on natural clinoptilolite. *Water Research, 36*(11), 2784-2792.

Inglezakis, V. J., Loizidou, M. M., & Grigoropoulou, H. P. (2004). Ion exchange studies on natural and modified zeolites and the concept of exchange site accessibility. *Journal of Colloid and Interface Science, 275*(2), 570-576.

Iwata, S., Tabuchi, T., and Warkentin, P.B. (1995). *Soil-Water Interactions*. New York: Dekker.

Karlen, C., Wallinder, I. O., Heijerick, D., & Leygraf, C. (2002). Runoff rates, chemical speciation and bioavailability of copper released from naturally patinated copper. *Environmental Pollution, 120*(3), 691-700.

Kinniburgh, D. G. (1986). General-Purpose Adsorption-Isotherms. *Environmental Science & Technology, 20*(9), 895-904.

Kinniburgh, D. G., Barker, J. A., & Whitfield, M. (1983). A Comparison of Some Simple Adsorption-Isotherms for Describing Divalent-Cation Adsorption by Ferrihydrite. *Journal of Colloid and Interface Science, 95*(2), 370-384.

Korenromp, R. H. J., and Hollander, J.C.Th. (1999). *Diffusive emissions of zinc due to atmospheric corrosion of zinc and zinc coated (galvanised) materials* (No. 29824). Apeldoorn, Nederland: TNO Institute of Environmental Sciences, Energy Research and Process Innovation.

Kraepiel, A. M. L., Keller, K., & Morel, F. M. M. (1998). On the acid-base chemistry of permanently charged minerals. *Environmental Science & Technology, 32*(19), 2829-2838.

Krejci V., S. W. a. G. W. (1990). *Ziele und Aufgaben der Siedlungsentwässerung*. Zurich.

Langella, A., Pansini, M., Cappelletti, P., Gerraro, B., Gennaro, M., Collela, C. (2000). NH^{4+}, Cu^{2+}, Zn^{2+}, Cd^{2+} and Pb^{2+} exchange for Na^+ in a sedimentary clinoptilolite, North Sardinia, Italy. *Microporous and Mesoporous Material, 37*(1), 337-343.

Lehmann, B. (1995). *Freiwitterungsverhalten von Dächern mit Metalldeckung, Untersuchung zur Zinkabgabe von Dachdeckungen mit Titanzink.*, Universität von Hannover.

Leschber, R., Pernak, K.D. and Zimmermann, U. (1991). Untersuchung des Verhaltens anorganischer und organischer Stoffe bei Konzentrierter Regenwasserversickerung. *Stadtentwässerung und Gewässerschutz, 4*, 169-188.

Leyva-Ramos, R., Aguilar-Armenta, G., Gonzalez-Gutierrez, L. V., Guerrero-Coronado, R. M., & Mendoza-Barron, J. (2004). Ammonia exchange on clinoptilolite from mineral deposits located in Mexico. *Journal of Chemical Technology and Biotechnology, 79*(6), 651-657.

Lide, D. R. (1998-1999). *Handbook of Chemistry and Physics* (79 ed.): The Chemical Rubber CO.

Lindström, R., Svensson, J.E., and Johansson, L.G. (2002). The influence of salt deposits on the atmospheric corrosion of zinc. The important role of the sodium ion. *Journal of the Electrochemical Society, 149*(2), B57-B64.

Lobnig, R., Sinclair, J.D., Unger, M., and Stratmann, M. (2003). Mechanism of atmospheric corrosion of copper in the presence of ammonium sulfate particles. *Journal of the Electrochemical Society, 150*(6), A835-A849.

Loizidou, M., Haralambous, K.J., Loukatos, A., and Dimitrakopoulou, D. (1992). Natural zeolites and their ion exchange behavior towards chromium. *Journal of Environmental Science and Health, Part A., 27*(7), 1759-1769.

Malliou, E., Malamis, M., and Sakelaridis, P.O. (1992). Lead and cadmium removal by ion exchange. *Water Science and Technology, 25*(1), 133-138.

Marsalek, J., and Marsalek, P.M. (1997). Characteristics of sediments from a stormwater management pond. *Water Science and Technology, 36*(8-9), 117-122.

Mason, Y., Ammann, A. A., Ulrich, A., & Sigg, L. (1999). Behavior of heavy metals, nutrients, and major components during roof runoff infiltration. *Environmental Science & Technology, 33*(10), 1588-1597.

McBain, J. W. (1932). *The sorption of gases and vapors by solids*. London: Rutledge and Sons.

Michaels, A. S. (1952). Simplified Method of Interpreting Kinetic Data in Fixed-Bed Ion Exchange. *Industrial and Engineering Chemistry, 44*(8), 1922-1930.

Milan, Z., Sanchez, E., Weiland, P., deLasPozas, C., Borja, R., Mayari, R., et al. (1997). Ammonia removal from anaerobically treated piggery manure by ion exchange in columns packed with homoionic zeolite. *Chemical Engineering Journal, 66*(1), 65-71.

Misaelides, P., Godelitsas, A., Filippidis, A., Charistos, D., & Anousis, I. (1995). Thorium and uranium uptake by natural zeolitic materials. *Science of the Total Environment, 173*(1-6), 237-246.

Mondale, K. D., Carland, R. M., & Aplan, F. F. (1995). The Comparative Ion-Exchange Capacities of Natural Sedimentary and Synthetic Zeolites. *Minerals Engineering, 8*(4-5), 535-548.

Namasivayam, C., & Senthilkumar, S. (1999). Adsorption of copper(II) by "waste" Fe(III)/Cr(III) hydroxide from aqueous solution and radiator manufacturing industry wastewater. *Separation Science and Technology, 34*(2), 201-217.

Nederlof, M. M., Vanriemsdijk, W. H., & Koopal, L. K. (1990). Determination of Adsorption Affinity Distributions - a General Framework for Methods Related to Local Isotherm Approximations. *Journal of Colloid and Interface Science, 135*(2), 410-426.

Negrel, P., & Roy, S. (1998). Chemistry of rainwater in the Massif Central (France): a strontium isotope and major element study. *Applied Geochemistry, 13*(8), 941-952.

Ouki, S. K., & Kavannagh, M. (1997). Performance of natural zeolites for the treatment of mixed metal-contaminated effluents. *Waste Management & Research, 15*(4), 383-394.

Ouki, S. K., & Kavannagh, M. (1999). Treatment of metals-contaminated wastewaters by use of natural zeolites. *Water Science and Technology, 39*(10-11), 115-122.

Pabalan, R. T. (1994). Thermodynamics of Ion-Exchange between Clinoptilolite and Aqueous-Solutions of Na+/K+ and Na+/Ca2+. *Geochimica Et Cosmochimica Acta, 58*(21), 4573-4590.

Panayotova, M. I. (2001). Kinetics and thermodynamics of copper ions removal from wastewater by use of zeolite. *Waste Management, 21*(7), 671-676.

Peric, J., Trgo, M., & Medvidovic, N. V. (2004). Removal of zinc, copper and lead by natural zeolite - a comparison of adsorption isotherms. *Water Research, 38*(7), 1893-1899.

Persson, D., and Kucera, V. (2001). Release of metals from buildings, constructions and products during atmospheric exposure in stockholm. *Water, Air and Soil Pollution: Focus, 1*, 133-150.

Pratt, C. J., Harrison, J.J. and Adams, J.R.W. (1984). *Storm runoff simulation in runoff quality investigations*. Gothenburg: Chalmers University of Technology.

Reimann, C., DeCaritat, P., Halleraker, J. H., Volden, T., Ayras, M., Niskavaara, H., et al. (1997). Rainwater composition in eight arctic catchments in northern Europe (Finland, Norway and Russia). *Atmospheric Environment, 31*(2), 159-170.

Reiss, D., Rihm, B., Thoni, C., & Faller, M. (2004). Mapping stock at risk and release of zinc and copper in Switzerland - Dose response functions for runoff rates derived from corrosion rate data. *Water Air and Soil Pollution, 159*(1), 101-113.

Rocher, V., Azimi, S., Gasperi, J., Beuvin, L., Muller, M., Moilleron, R., et al. (2004). Hydrocarbons and metals in atmospheric deposition and roof runoff in central Paris. *Water Air and Soil Pollution, 159*(1), 67-86.

Saget, A., Chebbo, G., & BertrandKrajewski, J. L. (1996). The first flush in sewer systems. *Water Science and Technology, 33*(9), 101-108.

Sansalone, J. J., & Buchberger, S. G. (1997). Partitioning and first flush of metals in urban roadway storm water. *Journal of Environmental Engineering-Asce, 123*(2), 134-143.

Sarioglu, M. (2005). Removal of ammonium from municipal wastewater using natural Turkish (Dogantepe) zeolite. *Separation and Purification Technology, 41*(1), 1-11.

Shinoda, T. (1990). *Drainage systems and runoff reduction.* Paper presented at the Fiffth Internationall conference on urban storm drainage, Osaka.

Sposito, G., Holtzclaw, K. M., Charlet, L., Jouany, C., & Page, A. L. (1983). Sodium Calcium and Sodium Magnesium Exchange on Wyoming Bentonite in Perchlorate and Chloride Background Ionic Media. *Soil Science Society of America Journal, 47*(1), 51-56.

Sposito, G., Holtzclaw, K. M., Jouany, C., & Charlet, L. (1983). Cation Selectivity in Sodium - Calcium, Sodium - Magnesium, and Calcium - Magnesium Exchange on Wyoming Bentonite at 298-K. *Soil Science Society of America Journal, 47*(5), 917-921.

Sposito, G., Jouany, C., Holtzclaw, K. M., & Levesque, C. S. (1983). Calcium-Magnesium Exchange on Wyoming Bentonite in the Presence of Adsorbed Sodium. *Soil Science Society of America Journal, 47*(6), 1081-1085.

Stumm, W., and Morgan, J.J. (1970). *Aquatic Chemistry*. New York: Wiley.

Taylor, A. M., & Roy, R. (1965). Zeolite Studies .V. Dehydration Behavior of Na-P Zeolites and Some Ion-Exchanged Derivatives. *Journal of the Chemical Society*(JUL), 4028-&.

Theng, B. K. G. (1971). Adsorption of Molybdate by Some Crystalline and Amorphous Soil Clays. *New Zealand Journal of Science, 14*(4), 1040-&.

Thompson, H. S. a. R., J. (1850). *Agr. Soc. Engl., 11*, 68.

Top, A., & Ulku, S. (2004). Silver, zinc, and copper exchange in a Na-clinoptilolite and resulting effect on antibacterial activity. *Applied Clay Science, 27*(1-2), 13-19.

Tsitsishvili, G. V., Andronikashvili, T.G., Kirov, G.M., and Filizova, L.D. (1992). *Natural Zeolites*. Chichester, UK: Ellis Horwood Limited.

Van Hooff, J. H. C., and Roolefson, J.W. (1991). *Introduction to Zeolite Science and Practice: Technics of Zeolite Characterization, Studies in Surface Science and Catalysis*. Amsterdam: Elsevier.

Vansant, E. F. (1990). *Pore size engineering in zeolites*. Baffins Lane, Chichester, England: John Wiley & Sons Ltd.

Verbiest, P., Waeterschoot, H., Racek, R., and Leclercq, M. (1997). Zinc and the environment. *Protective Coatings Europe, 9*(1), 47-57.

W.L. McCabe, J. C. S. a. P. H. (1993). *Unit operations in chemical engineering* (Vol. 5th edition): McGrawHill, International editions.

Wallinder, I. O., He, W., and Leygraf, C. (2001). A comparison between corrosion rates and runoff rates from new and aged copper and zinc as roofing material. *Water, Air and Soil Pollution: Focus, 1*, 67-82.

Wallinder, I. O., & Leygraf, C. (1997). A study of copper runoff in an urban atmosphere. *Corrosion Science, 39*(12), 2039-2052.

Wallinder, I. O., & Leygraf, C. (2001). Seasonal variations in corrosion rate and runoff rate of copper roofs in an urban and a rural atmospheric environment. *Corrosion Science, 43*(12), 2379-2396.

Wallinder, I. O., Verbiest, P., He, W., & Leygraf, C. (2000). Effects of exposure direction and inclination on the runoff rates of zinc and copper roofs. *Corrosion Science, 42*(8), 1471-1487.

Wanielista, M. P., and Yousef, Y.A. (1993). *Storm water management*. NY, USA: John Wiley and Sons, Inc.

Weigel, O., and Steinhoff, E. (1925). *Z. Cristallogr., 61*, 125-154.

Wilderer, P. A., and Wilderer, M. C. (2005). *On the Roles Engineers May Play in the Attempt to Meet Basic Demands of Man and Nature*. Weinheim: WILEY-VCH Verlag GmbH & Co. KGaA.

Yong, N. R., Mohammed, O. M. A., and Warkentin, P. B. (1992). *Principals of contaminant transport in soils*. London: Elsevier.

Zobrist, J., Muller, S. R., Ammann, A., Bucheli, T. D., Mottier, V., Ochs, M., et al. (2000). Quality of roof runoff for groundwater infiltration. *Water Research, 34*(5), 1455-1462.

9. List of symbols and abbreviations

K_e	Equilibrium constant
C_{A_e}	Equilibrium metal concentration in the solution
C_{B_e}	Equilibrium metal concentration on modified clinoptilolite
X_{A_e}	Fractional conversion of metal at equilibrium
C_{A_i}	Initial metal concentration in the solution
C_{B_i}	Initial metal concentration on the modified clinoptilolite
1SAF	Content of the first bottle after the filter
1SBF	Content of the first bottle before the filter
1SBF	Content of the second bottle before the filter
2SAF	Content of the second bottle after the filter
ANOVA	Analysis of variance
b	First flush coefficient
BauGB	Baugesetzbuch
BV	Bed volume
C_0	Influent cation concentration
C_A	Ion metal concentration in the solution
C_B	Ion metal concentration on the modified clinoptilolite
C_e	Equilibrium metal concentration
CEC	Cationic exchange capacity
C_i	Initial metal concentration
CSS	Combined sewer system
C_t	Effluent cation concentration
Cu_{total}	Total copper
D-R	Dubinin-Radushkevich isotherm

DWA	German Association for Water, Wastewater and Waste
EC	Electric conductivity
EEA	European Environment Agency
EMC	Event mean concentration
F	Dimensionless cumulative runoff volume
h	Initial metal sorption rate
HEU	Heulandite group of minerals
K	Surface adsorption equilibrium constant
K_1	First-order rate constant
K_2	First order rate constant
K_r	Overall rate constant
L	Langmuir isotherm
L-F	Langmuir-Freundlich isotherm
L_p	Dimensionless cumulative pollutant mass
M	Maximum ion exchange capacity
m(t)	Pollutant mass transported at time t
MID	Magnetic induction device
n	Ions sorbed per gram of clinoptilolite
NE	North-East
NLLS	Non linear least squares
NW	North-West
PAH	Polycyclic Aromatic Hydrocarbons
Pb_{total}	Total lead
PEMC	Partial event mean concentration
q	Amount of metal adsorbed at any time
q_e	Amount of metal adsorbed at equilibrium per unit of clinoptilolite
RF I	Retention facility I

RF II	Retention Facility II
RF III	Retention facility III
RF IV	Retention Facility IV
R-P	Redlich-Petersen isotherm
RRWAF	Remaining rainwater after the filter
RRWBF	Remaining rain water before the filter
RW	Rainwater
SE	South-East
SW	South-West
t	time
T	Toth isotherm
u(t)	Flow volume at time t
U(t)	Fractional attainment of equilibrium
UTD-1	Framework structure of clinoptilolite
V	Total volume of the flow over the entire event duration
V/V	Volume per volume
W/W	Weight per weight
WHG	German Federal Water Act
X_A	Fractional conversion of metal
XRD	X-Ray diffraction
Zn_{total}	Total zinc
ZSM-5	Framework structure of clinoptilolite
β	Degree of heterogeneity
η	Metal uptake degree